

24 weeks long-term efficacy and tolerability of a skin care regimen with Thiamidol in patients with moderate to severe facial hyperpigmentation

Roggenkamp D¹, Fürstenau M², Kausch M², Sammain A¹, Kolbe L²

¹International Medical Management Eucerin, Beiersdorf AG, Hamburg, Germany | ²Research & Development, Beiersdorf AG, Hamburg, Germany

INTRODUCTION & OBJECTIVES

Hyperpigmentation is a frequent cosmetic condition characterized by dark spots on sun-exposed areas due to increased melanogenesis [1]. Tyrosinase inhibitors are in the focus of the research for the treatment of hyperpigmentation [2]. The purification of soluble variants of human tyrosinase allowed the identification of Thiamidol (isobutylamido-thiazolyl-resorcinol) as its most potent inhibitor out of 50,000 screened compounds [3].

The objective of this study was the vehicle-controlled investigation of the long-term efficacy and tolerability of a skin care regimen with Thiamidol in patients with moderate to severe facial hyperpigmentation for 24 weeks.

MATERIAL & METHODS

We report about a 24 weeks, monocentric, randomized, vehicle-controlled, double-blinded clinical trial to assess the efficacy and tolerability of a skin care regimen containing Thiamidol in 48 female subjects (36–64 yrs, phototypes III–V) suffering from moderate to severe facial hyperpigmentation.

Subjects allocated to the verum group (n=23) applied a Dual Serum containing Thiamidol twice a day (morning and evening) followed by Day Care with Thiamidol and SPF 30 in the morning and Night Care with Thiamidol in the evening. The vehicle group (n=25) applied the same skin care routine using vehicle formulations leaving out Thiamidol. Consequently, the vehicle Day Care had a SPF 30.

The primary outcome was a change in MASI Score and standardized clinical photography (VISIA CR). Secondary outcome included the tolerability of the skin care regimen as assessed by experts and panelists. Furthermore, subjects were asked to give their feedback on how the skin care regimen impacted their skin condition (self-grading on a 10-step scale and self-assessment) and their quality of life using a 7-point scale (1 no discomfort, 7 discomfort always) in a quality of life questionnaire with

10 questions (Table 1). All parameters were assessed at baseline and every four weeks within the total study duration of 24 weeks.

Table 1: Questions in quality of life questionnaire

Considering the previous week, how did you feel about:	
Q1:	the appearance of your melasma
Q2:	the frustration linked to your melasma
Q3:	the discomfort linked to your melasma
Q4:	the feeling of depression linked to your melasma
Q5:	the effect of melasma on your interactions with others (family/ friends)
Q6:	the effect of melasma on your wish to be in someone's company
Q7:	the discomfort of your melasma to express your feelings
Q8:	your skin coloration in giving you the impression of not being attractive
Q9:	your skin coloration in giving you the impression of being less lively and efficient
Q10:	your skin coloration in altering your feeling of freedom

RESULTS

Treatment efficacy in subjects using the verum formulations containing Thiamidol proved to be significantly superior compared to baseline and to vehicle formulations at end of study/every time point as measured by primary outcome, the MASI Score and assessed via clinical photography (Figures 1 and 2).

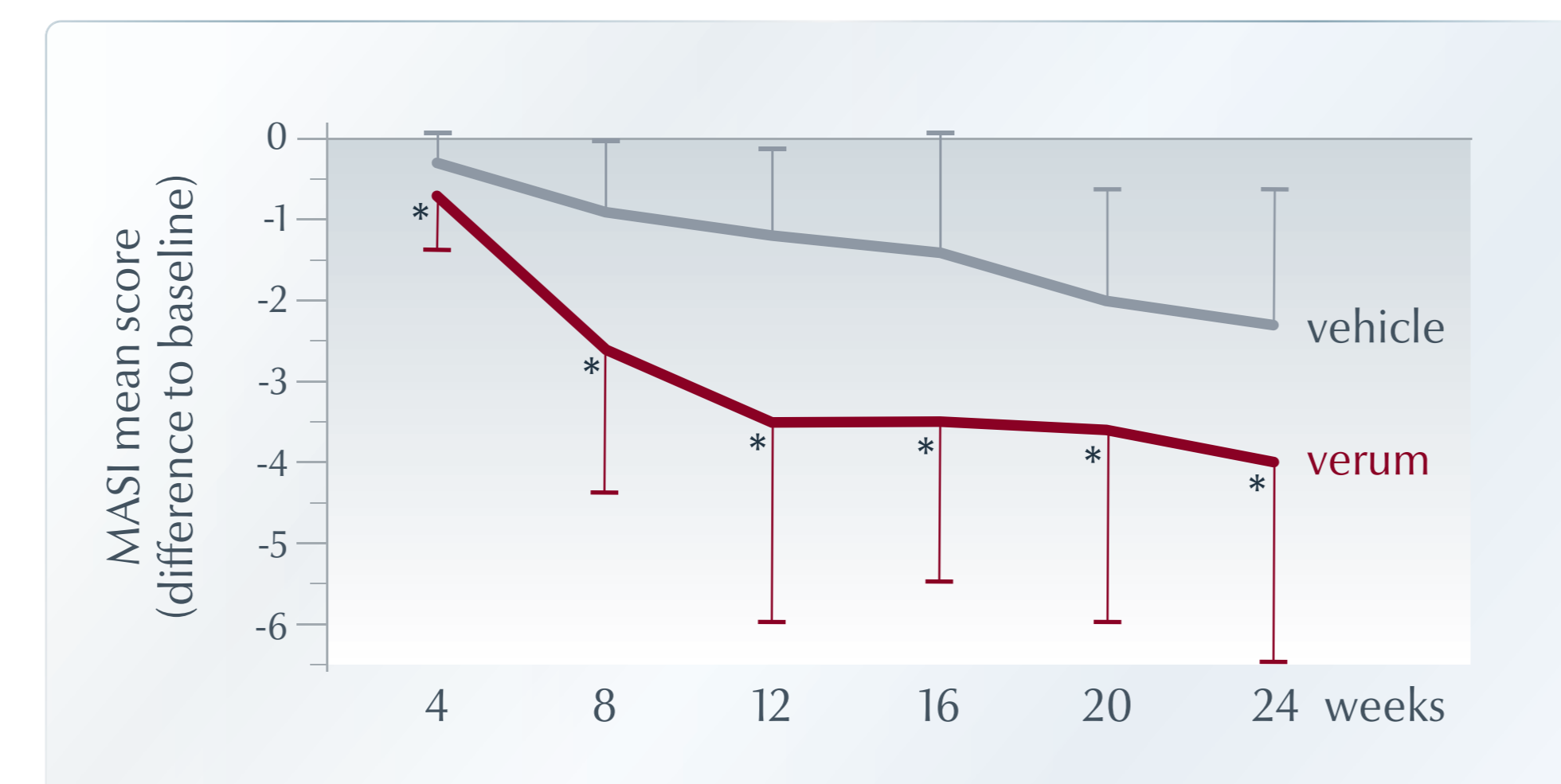


Figure 1: MASI score (difference to baseline) in verum and vehicle group over 6 months (24 weeks). * Significant improvement compared to baseline and vehicle.

Secondary outcomes regarding overall efficacy of the skin care regimen containing Thiamidol as assessed by self-grading of overall intensity of hyperpigmentation by subjects, were significantly improved compared to baseline at each point of time / at end of study (Figure 3).



Figure 2: Clinical photography

Subjects confirmed the efficacy and tolerability of the skin care regimen containing Thiamidol in a self-assessment questionnaire (Figure 4). This was accompanied by a significant improvement of their quality of life (Figure 5). The skin care regimen containing Thiamidol was very well tolerated over the entire study period of 24 weeks.

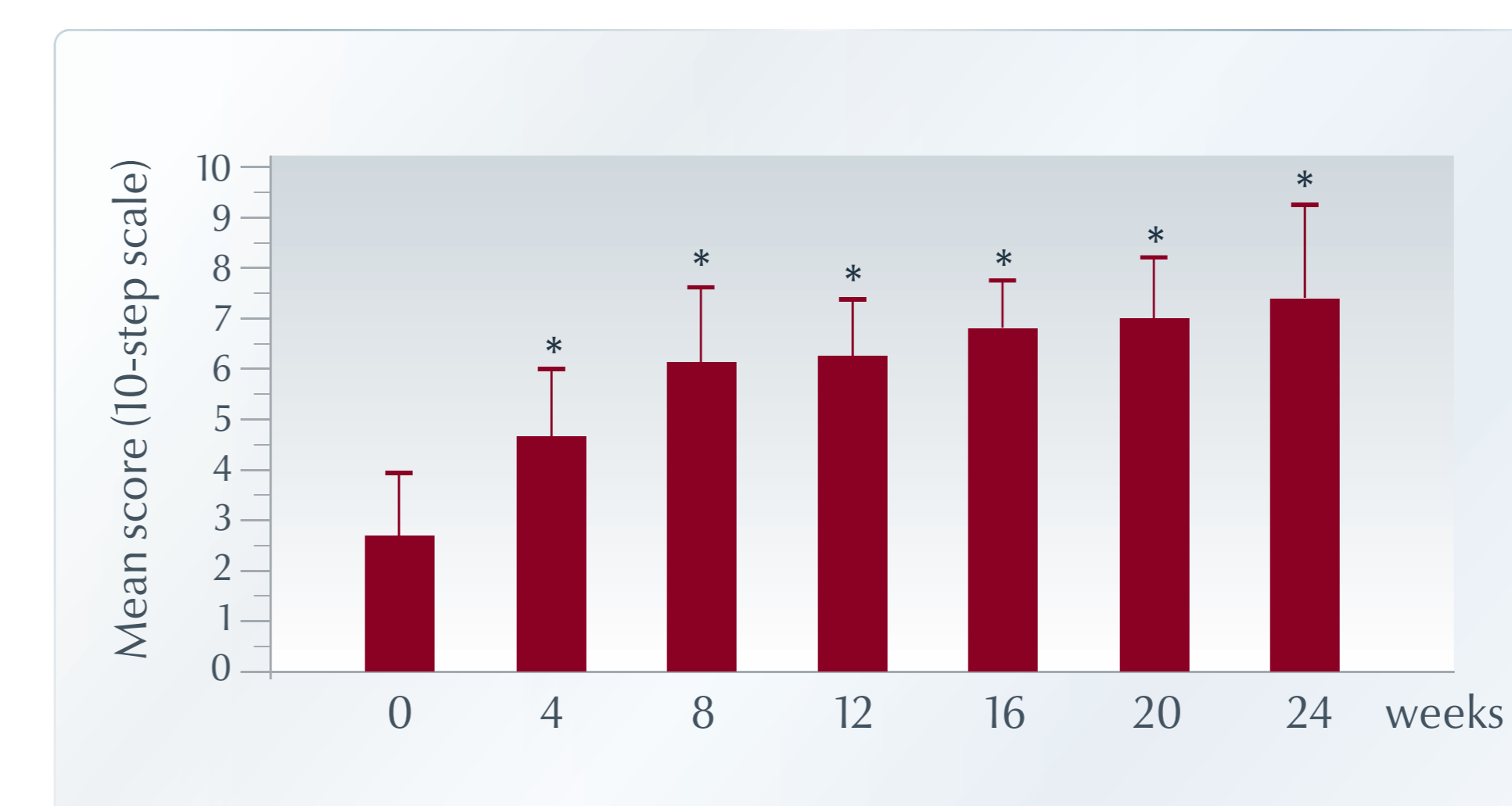


Figure 3: Improvement of overall intensity of hyperpigmentation. Self-grading on a 10-step scale* Significant improvement compared to baseline.

Patients confirm that the skin care regimen...

- 91%** diminishes hyperpigmentation
- 87%** provides me with a more even skin tone
- 96%** gives a radiant complexion
- 91%** reduces the area of my hyperpigmentation
- 83%** brightens without side effects
- 91%** has good skin compatibility
- 91%** I would like to continue using the skin care regimen
- 91%** I would recommend the skin care regimen to friends/family

Figure 4: Self-assessment of subjects after 24 weeks

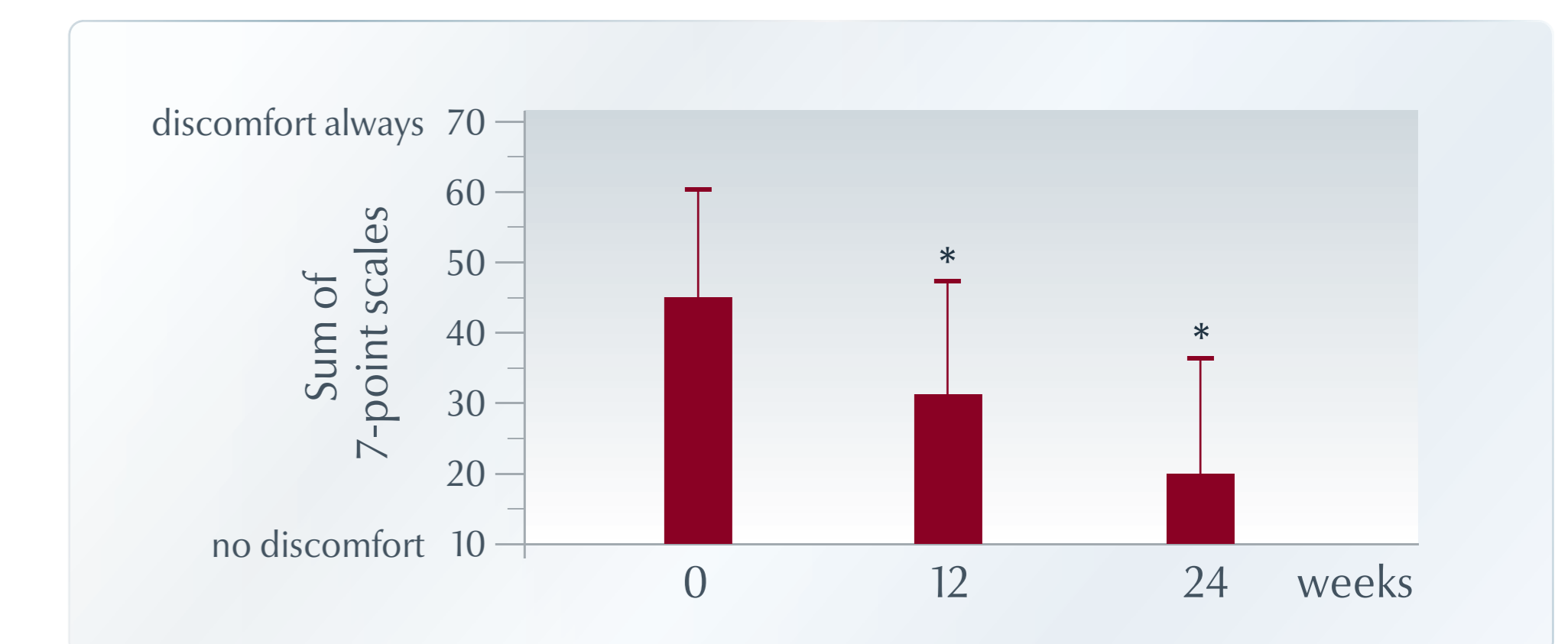


Figure 5: Quality of life questionnaire (Table 1). Subjects were asked to fill a 7-point scale (sum of 10 questions) to give their feedback on how the skin care regimen impacted their quality of life. A decrease in mean scores shows improvement in quality of life. * Significant improvement compared to baseline.

CONCLUSION

The skin care regimen containing Thiamidol was very well tolerated and superior compared to baseline and to its vehicle formulations over the entire study period of 24 weeks.

The subjects confirmed the very good efficacy and tolerability and reported a significant improvement of their quality of life after using the skin care regimen with Thiamidol.

References: [1] Kang, W.H., Yoon, K.H., Lee, E.S. et al. Melasma: histopathological characteristics in 56 Korean patients. *Br. J. Dermatol.* 146, 228–237 (2002) | [2] Gillbro, J.M. and Olsson, M.J. The melanogenesis and mechanisms of skinlightening agents—existing and new approaches. *Int. J. Cosmet. Sci.* 33, 210–221 (2011) | [3] Mann, T., Gerwat, W., Batzer, J. et al. Inhibition of human tyrosinase requires molecular motifs distinctively different from mushroom tyrosinase. *J. Invest. Dermatol.* 138, 1601–1608 (2018a)

A skin care regimen with Thiamidol effectively reduces post-inflammatory hyperpigmentation in patients with resolved acne

Roggenkamp D¹, Neufang G¹, Pillay A², Zoric I³, Kausch M³, Dlova NC⁴

¹ International Medical Management, Beiersdorf AG, Hamburg, ² Pharmacy Brands Team, Beiersdorf South Africa, Durban, ³ Research & Development, Beiersdorf AG, Hamburg, ⁴ Dermatology, School of Clinical Medicine, Durban

INTRODUCTION

Post-inflammatory hyperpigmentation (PIH) is an acquired hypermelanosis induced by cutaneous inflammation or skin injury and occurs more frequently in Fitzpatrick photo skin types IV-VI. The most common causes of PIH in skin of color patients are acne vulgaris, atopic dermatitis and pseudofolliculitis barbae. Acne is by far the most common skin condition seen in black patients seeking skin treatment, both in private and state facilities. Post-inflammatory hyperpigmentation and scarring are a major concern for black patients, resulting in impaired quality of life [1].

The aim of this study was to investigate the efficacy and tolerability of a skin care regimen with the new tyrosinase inhibitor Thiamidol (Isobutylamido Thiozoyl Resorcinol) in South African black patients with PIH after resolution of acne [2,3].

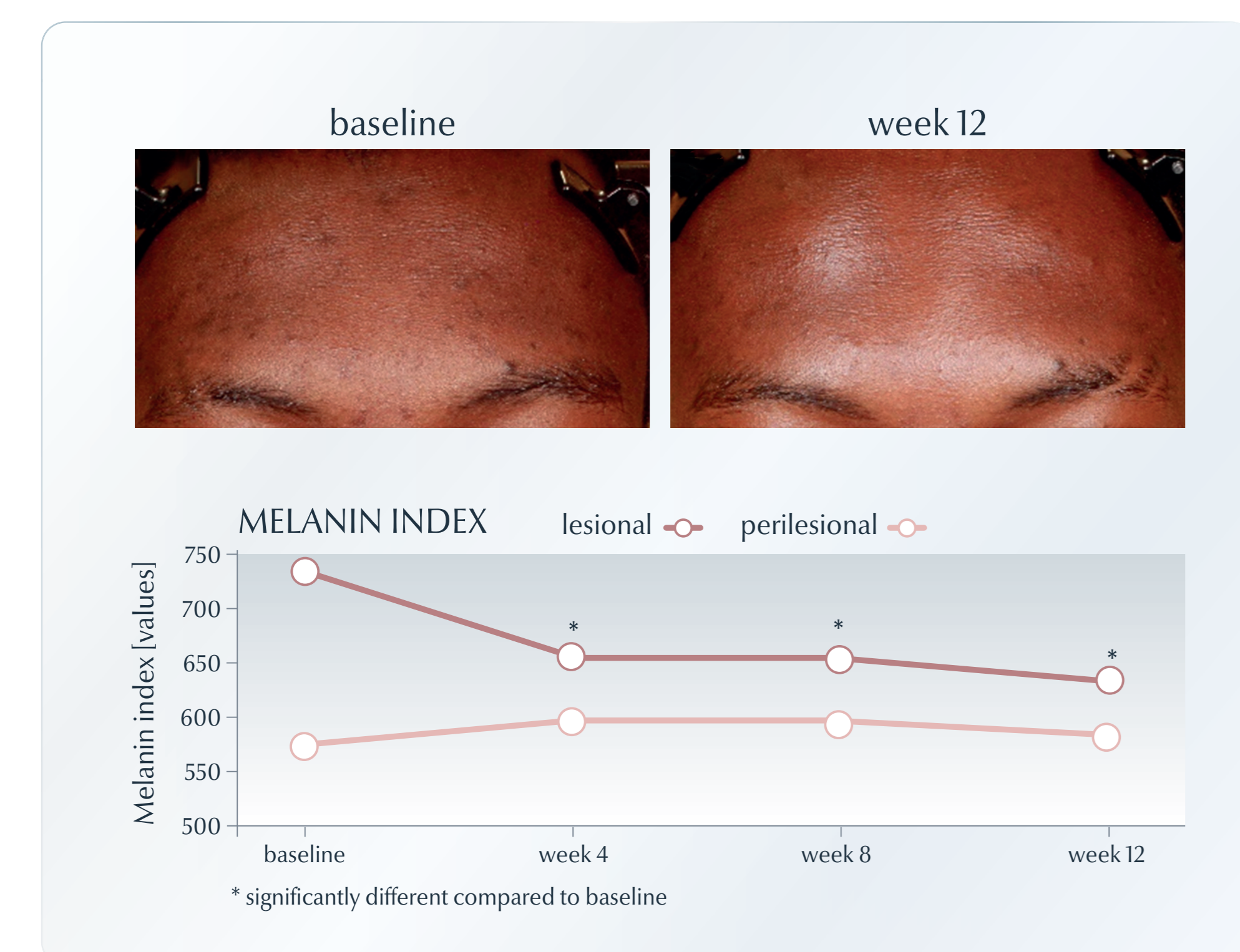


Figure 1. Clinical photography and melanin index. Patients with acne-induced post-inflammatory hyperpigmentation applied a day care SPF30, night care and serum, all containing Thiamidol, for 12 weeks on the whole face. Melanin index was measured on dark acne marks (lesional) and the surrounding non-affected skin (perilesional).

MATERIAL & METHODS

A total of 29 South African black patients of African descent (25 female, 4 male; aged 18-45; Fitzpatrick skin types V-VI) with acne-related PIH were recruited; patients with active acne were excluded. Patients were instructed to apply the skin care regimen with Thiamidol (serum and day care SPF 30 in the morning, night care in the evening) on the whole face once a day for 12 weeks. Patients' self-assessment, clinical assessment by an experienced dermatologist, mexameter measurement and clinical photography were performed at baseline and after four, eight and 12 weeks.

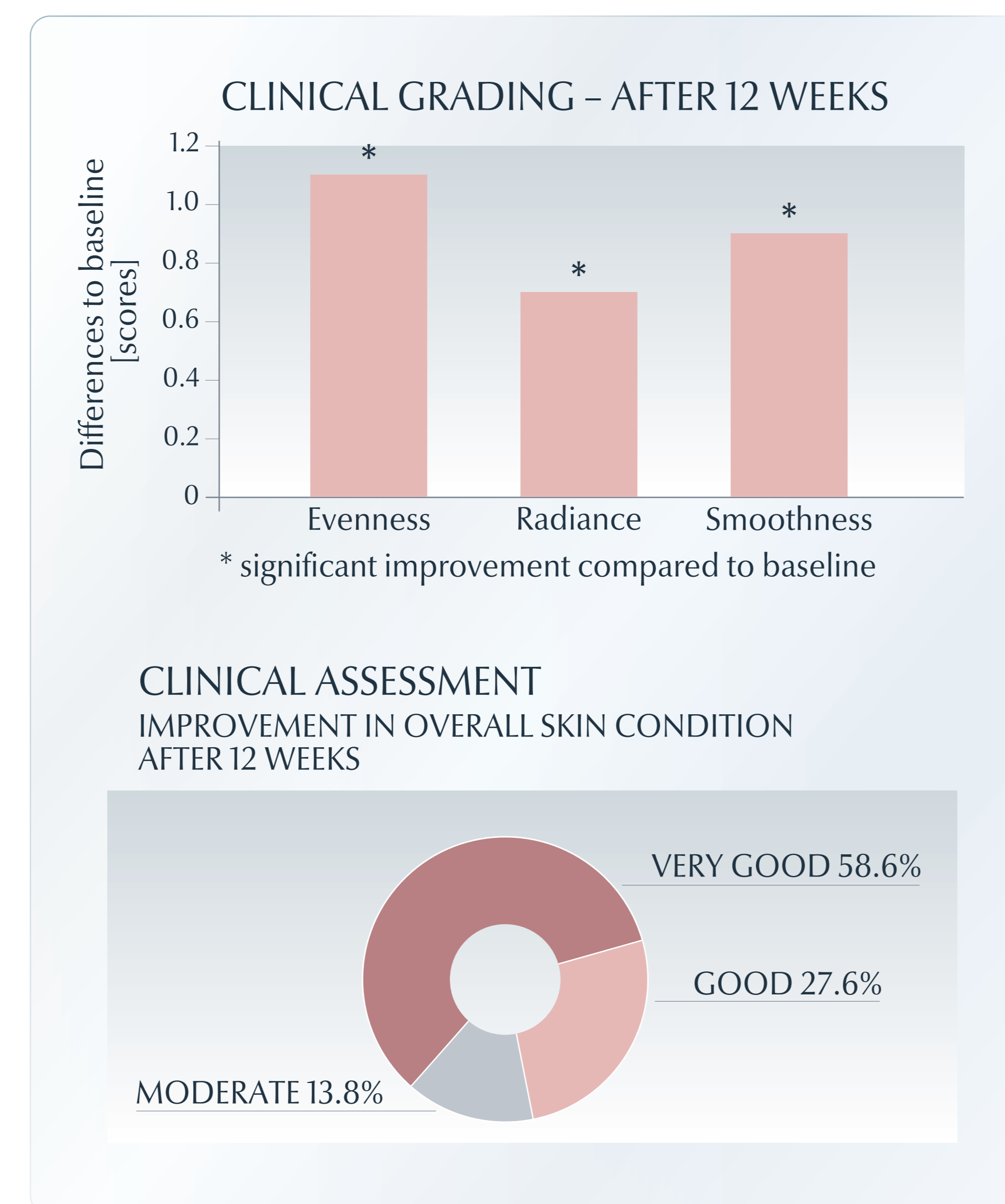


Figure 2. Clinical grading of skin tone evenness, radiance and smoothness as well as clinical assessment of improvement in overall skin condition. Patients with acne-induced post-inflammatory hyperpigmentation applied a day care SPF30, night care and serum, all containing Thiamidol, for 12 weeks on the whole face. Clinical grading was conducted on a 5-step scale.

RESULTS

Clinical grading demonstrated a significant improvement in skin evenness in 90% of patients after 12 weeks. Furthermore, skin radiance and smoothness improved significantly in clinical grading after the study period (Figure 2). Patients assessed a continuous improvement in skin evenness, glow (radiance) and smoothness over 12 weeks and 100% of patients stated that their dark spots (PIH) were less pronounced after 12 weeks (Figure 3). Mexameter measurements confirmed a significant reduction in the intensity of pigment spots (PIH), which was also demonstrated via clinical photography. The melanin index of the perilesional skin did not change significantly during the study period (Figure 1). In 93% of all patients, the overall skin tolerability of the skin care regimen with Thiamidol was rated as very good (Figure 4).

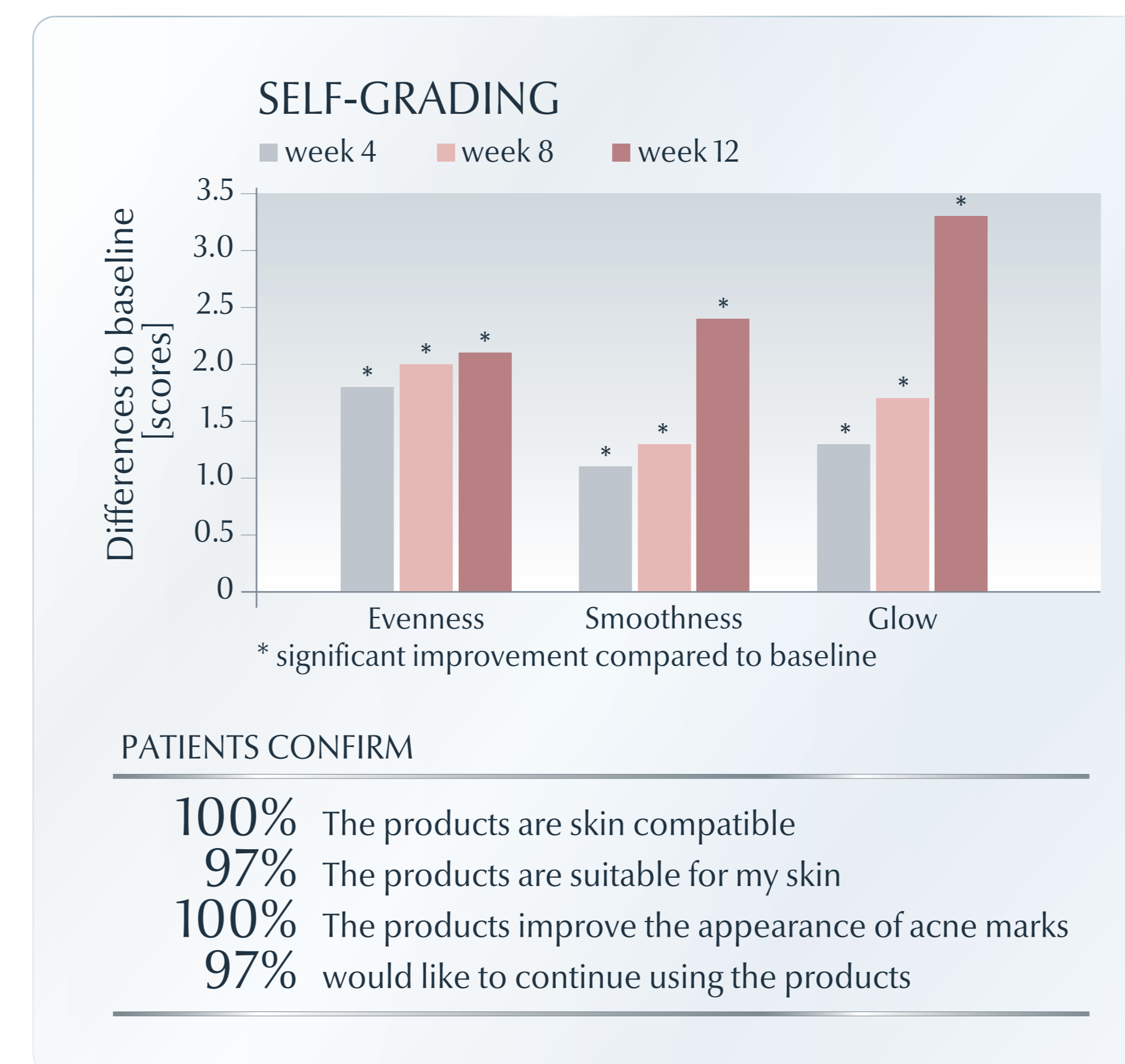


Figure 3. Self-grading of skin tone evenness, glow and smoothness as well as patients' self-assessment. Patients with acne-induced post-inflammatory hyperpigmentation applied a day care SPF30, night care and serum, all containing Thiamidol, for 12 weeks on the whole face. Self-grading was conducted on a 10-step scale.

CONCLUSION

The results of this study clearly demonstrate the efficacy and tolerability of a skin care regimen with Thiamidol in patients with acne-induced PIH.

[1] Erica C. Davis and Valerie D. Callender. Postinflammatory Hyperpigmentation. A Review of the Epidemiology, Clinical Features, and Treatment Options in Skin of Color. *J of Clinical and Aesthetic Dermatology*. 2010 Jul;3(7):20-31

[2] Mann et al., Inhibition of Human Tyrosinase Requires Molecular Motifs Distinctly Different from Mushroom Tyrosinase. *J Invest Dermatol*. (2018) 138:1601-1608.

[3] Arrowitz et al., Effective tyrosinase inhibition by Thiamidol results in significant improvement of mild to moderate melasma. *Journal Invest. Dermatol*. (2019) 139(8):1691-1698

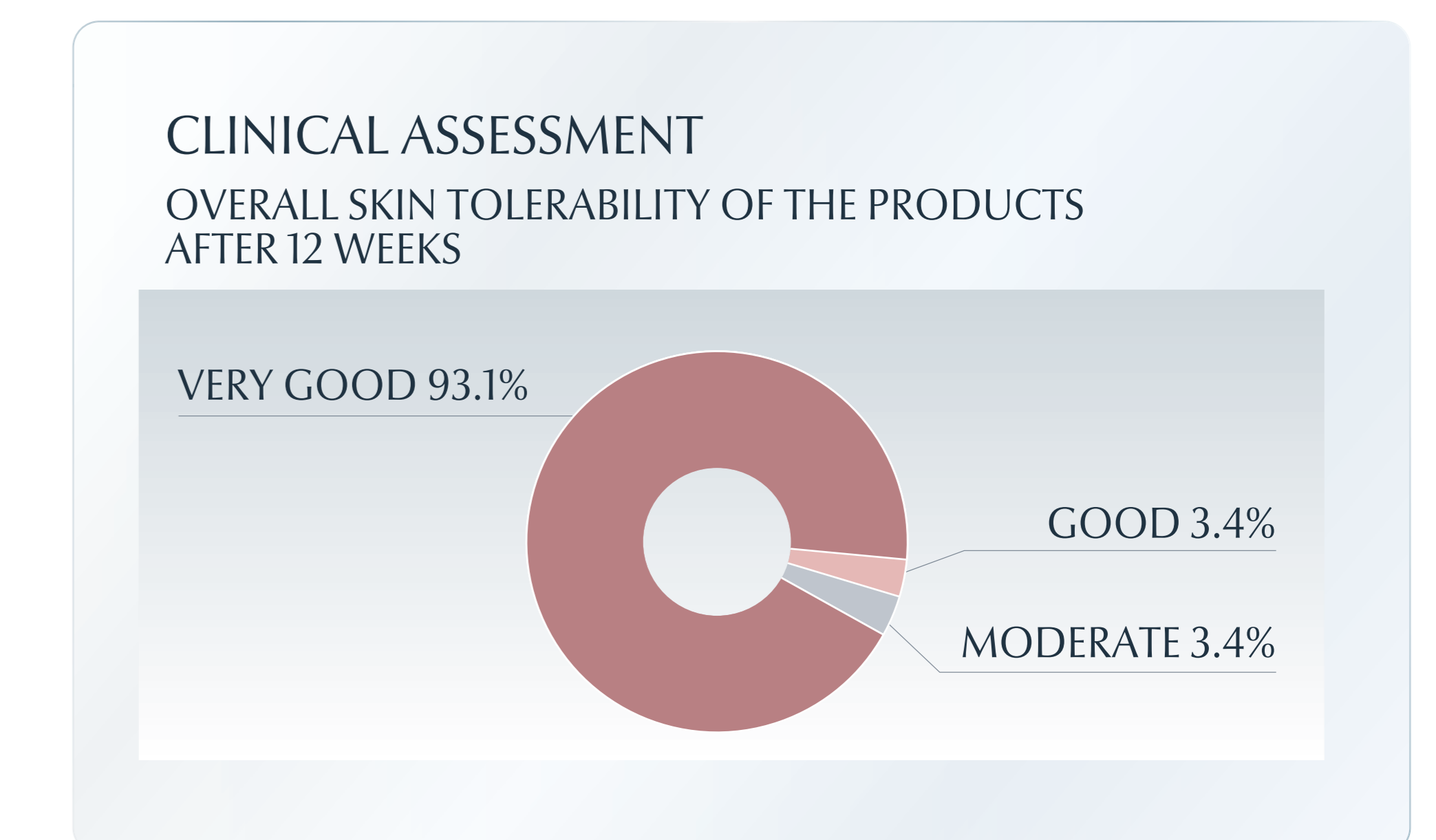


Figure 4. Clinical assessment of overall skin tolerability. Patients with acne-induced post-inflammatory hyperpigmentation applied a day care SPF30, night care and serum, all containing Thiamidol, for 12 weeks on the whole face.

ORIGINAL ARTICLE

Efficacy and safety of a novel triple combination cream compared to Kligman's trio for melasma: A 24-week double-blind prospective randomized controlled trial

Clémence Bertold¹  | Eric Fontas² | Tanya Singh¹  | Nadia Gastaut³ |
Sandra Ruitort³ | Sylvia Wehrlen Pugliese³ | Thierry Passeron^{1,4} 

¹Department of Dermatology, CHU Nice, Université Côte d'Azur, Nice, France

²Department of Clinical Research, Cimiez Hospital, CHU Nice, Université Côte d'Azur, Nice, France

³Pharmacy Department, CHU Nice, Université Côte d'Azur, Nice, France

⁴INSERM U1065, Centre Méditerranéen de Médecine Moléculaire, Université Côte d'Azur, Nice, France

Correspondence

Thierry Passeron, Department of Dermatology, CHU Nice, 151 Route de Saint-Antoine, Nice 06200, France.
Email: passeron@unice.fr

Abstract

Background: Kligman's trio (KT), combining hydroquinone, retinoic acid and corticosteroid, is considered as the gold standard treatment of melasma. Its efficacy has never been matched before, but it is tempered by frequent adverse effects.

Objective: To assess the efficacy and tolerance of a New Trio (NT) combination with isobutylamido-thiazolyl-resorcinol, retinoic acid and corticosteroid compared to KT.

Methods: We conducted a 24-week monocentric trial, randomized, double-blind, controlled versus KT, with 40 melasma patients. NT and KT were applied for 12 weeks and associated with the same sunscreen applied for 24 weeks. The primary endpoint was the modified Melasma Area Severity Index (mMASI) at 12 weeks. Patient quality of life was investigated using MelasQoL.

Results: After 12 weeks, KT and NT groups both demonstrated a significant improvement in mMASI, respectively -2.84 (SE 0.69, $p < 0.0002$) and -4.33 (SE 0.71, $p < 0.0001$). The mean difference between the two groups was -1.49 (IC 95% -3.52 to 0.54 , $p = 0.14$). MelasQoL improvement was -6.66 (SE 3.29, $p = 0.0515$) with KT and -12.57 (SE 3.29, $p = 0.0006$) with NT.

Conclusion: The NT combination appears to be an effective treatment option for treating melasma and could be considered as a well-tolerated alternative to KT.

INTRODUCTION

Melasma is a common skin disorder affecting up to 30% of the female population.¹ The clinical pattern is characterized by an acquired hyperpigmentation of the face, with symmetric disposition, linked to an accumulation of melanin. The pathogenesis of melasma is complex.² Affecting pregnant women in 20% of cases, melasma is sometimes considered as a consequence of hormonal stimulation on a predisposed background.³ Apart from pregnancy, other risk factors are Fitzpatrick skin type from III to V, female sex, genetic predisposition, exposure to ultraviolet and visible light and exogenous sexual hormone stimuli with oral contraceptive or hormone

replacement therapy.⁴ More recently, melasma has been described as a photoaging skin disorder, with a central role of the dermal compartment (altered basal membrane, solar elastosis, increased vascularization with secreted factors produced by endothelial cells, fibroblasts and sebocytes).⁵⁻⁷

Melasma has been demonstrated to negatively impact the quality of life of affected individuals.⁸ Treatment options include topical depigmenting creams and cosmetic interventions such as peeling combined with broad-spectrum sunscreen protecting against UVB, long-wave UVA and high-energy visible light.^{9,10} Triple combination cream, first described by Kligman in 1975,¹¹ is considered as the gold standard treatment of melasma. It combines 5% hydroquinone,

Clinicaltrials.gov listing: NCT 05119413.

This is an open access article under the terms of the [Creative Commons Attribution-NonCommercial](https://creativecommons.org/licenses/by-nc/4.0/) License, which permits use, distribution and reproduction in any medium, provided the original work is properly cited and is not used for commercial purposes.

© 2023 The Authors. *Journal of the European Academy of Dermatology and Venereology* published by John Wiley & Sons Ltd on behalf of European Academy of Dermatology and Venereology.

tretinoin (retinoic acid) and corticosteroid. The efficacy of Kligman's Trio (KT) combination has never been matched to date.¹² This topical approach is however associated with irritating adverse effects, for example erythema, desquamation and burning sensation. Hydroquinone and tretinoin are suspected to be responsible for irritating adverse effects. Exogenous ochronosis is a blue-black hyperpigmentation resulting from the long-term use of hydroquinone. It is more frequently reported with high concentrations of hydroquinone and in patients with dark skin types.¹³ Irritation and potential risk of exogenous ochronosis limit the use of Kligman's trio for melasma treatment. The use of hydroquinone as cosmetic agent has moreover been banished in Europe due to concerns regarding a potential drug-induced carcinogenesis.¹⁴ Inconsistent efficacy and adverse effects of the available treatment options make melasma a therapeutic challenge.

Isobutylamido-thiazolyl-resorcinol is an inhibitor of human tyrosinase that demonstrated superior melanogenesis inhibition compared to hydroquinone *in vitro*.¹⁵ Isobutylamido-thiazolyl-resorcinol has been tested as a depigmenting agent clinically in comparative studies against hydroquinone 2% and 4%.^{16,17} However, in these protocols, it was applied twice a day while hydroquinone was applied only once. We hypothesized that replacing 5% hydroquinone with isobutylamido-thiazolyl-resorcinol in the depigmentation preparation would improve efficacy and tolerance.

We therefore conducted a prospective interventional study to assess the efficacy and tolerance of a new combination composed of isobutylamido-thiazolyl-resorcinol, tretinoin and corticosteroid compared with reference treatment described by Kligman, both applied once a day and associated with the same photoprotection.

MATERIALS AND METHODS

Design

We conducted a prospective, randomized, double-blind, controlled study in the department of dermatology of the university hospital of Nice, France, between November 2021 and September 2022. The study was approved by the Ethics Committee Sud-Méditerranée I; #21 11 (EudraCT: 2020-006107-42) and registered at Clinicaltrial.gov (NCT05119413).

Population

Patients aged ≥ 18 years old with melasma clinically diagnosed under Wood's light examination were included. The study excluded patients with another pigmentation disorder on the face, having received any depigmenting cosmetic, systemic corticosteroid, inhaled corticosteroid, topical corticosteroid on the face or the eyes, topical hydroquinone or retinoic acid on the face within 1 month prior to inclusion, patients using non steroid anti-inflammatory for more than 10 days monthly, patients refusing to be taken in photograph,

pregnant and breastfeeding women or planning to have a child during the 24 weeks of the study.

Intervention

Subjects were randomized to receive a NT combining 0.1% isobutylamido-thiazolyl-resorcinol (Thiamidol; Eucerin®), 0.1% retinoic acid and 0.1% dexamethasone acetate, or to receive KT combining 5% hydroquinone, 0.1% retinoic acid and 0.1% dexamethasone acetate. Patients applied the preparation all over the face but sparing the eye area, once daily in the evening for 12 weeks. Subjects in both arms were given the same amount of topical cream, in identical packaging. Both treatments had identical appearance and were prepared at the central pharmacy of the hospital. The same SPF50+ topical sunscreens were given to all the patients at baseline to be applied until W24. Centralized block (aleatory size) randomization with a 1:1 ratio was conducted by the Department of Clinical Research and Innovation (DRCI) of Nice University Hospital. Lists were created using Nquery© Advisor v 7.0. software.

Data collection

Study data were recorded in an electronic case report form (e-CRF) designed and implemented by the Data Manager of the DRCI using RedCAP® software.

Evaluation

The primary endpoint was the change in mMASI score between baseline and Week 12, defined as Δ mMASI = W12 mMASI – baseline mMASI. mMASI is a validated score for assessing the melasma extent.¹⁸ It was assessed at baseline, Week 12 and Week 24 by the same trained dermatologist blinded to the treatment received. Standardized pictures were taken with the Color Face system® (Newtone®) at baseline, Week 12 and Week 24.

The quality of life was assessed at baseline, Week 12 and Week 24 using MelasQoL score.⁸ The other secondary endpoints were the change in mMASI score between Week 12 and Week 24. The type of adverse events (AE), their duration and their severity, graded accordingly to the Common Terminology Criteria for Adverse Events (CTCAE), were noted. Visual analogic scales (VAS) were used by subjects to rate the severity between 0 (no symptom) and 100 (major severity symptom) of AE of special interest (erythema, skin dryness sensation, irritation and desquamation).

Sample size

The efficacy of a combination associating isobutylamido-thiazolyl-resorcinol, retinoic acid and dexamethasone has never been evaluated prospectively. We estimated that a

population of 20 patients in each group should allow performing statistical analyses adequately. This sample size was suitable with the recruitment capacities of our centre allowing, around 150 patients matching selection criteria per year.

Statistical analyses

Analysis of the primary objective was performed on the modified intention-to-treat (ITT_m) principle. All subjects who underwent randomization and applied the topical treatment at least once were included in the analysis. Missing data for the analysis of the primary endpoint were imputed according to the last-observation-carried-forward (LOCF) procedure. In the absence of mMASI assessment at W12, the missing data were replaced by the baseline values traducing no improvement with the treatment.

Modified Melasma Area Severity Index change from baseline at W12 and W24 was compared between the study arms using an ANCOVA model with the treatment group as the variable of interest and the mMASI baseline score as covariate. MelasQoL evolution between the groups was studied in the same way. The severity of symptoms of special interest (erythema, skin dryness sensation, irritation and desquamation) was compared between the groups with the Wilcoxon rank sum test. Weight of sunscreen used, and duration of AE were compared using Student *t*-tests. All tests were two-sided, and *p* values <0.05 were considered statistically significant. We used SAS Enterprise Guide software version 7.1 (SAS institute, Inc.) for statistical analyses.

RESULTS

Demography

Forty-eight patients were screened, and 40 were included and underwent randomization. Thirty-nine patients were analysed (19 in the NT arm and 20 in the KT arm) as one patient randomized in NT arm was having a concomitant pigmentation disorder and was excluded before he applied any treatment. Three patients discontinued due to patient decision in KT arm, and two patients discontinued due to patient decision in the NT arm (Figure 1). Eighteen patients in each group applied the treatment for the full 12 first weeks. The demographic and clinical characteristics of the patients are summarized in Table 1. The mean age was 47.6 years old in the KT group and 41.2 in the NT group. Almost all the subjects were female in each group. No subjects had a skin phototype I or VI. Most of them had a skin phototype III or IV. Melasma was mostly classified epidermal using Wood's lamp. The mean duration of melasma was 9.3 years in the KT group and 8.4 years in the NT group. Prior to inclusion in the study, 19 patients in the KT group (95%) and 17 patients (89.5%) in the NT group had previously been treated. The treatments tried before were triple combination cream, depigmenting cosmetics, laser and oral tranexamic acid.

mMASI evolution

The mean mMASI at baseline was 7.54 ± 4.24 in the NT arm and 6.08 ± 3.31 in the KT arm. The mean mMASI at

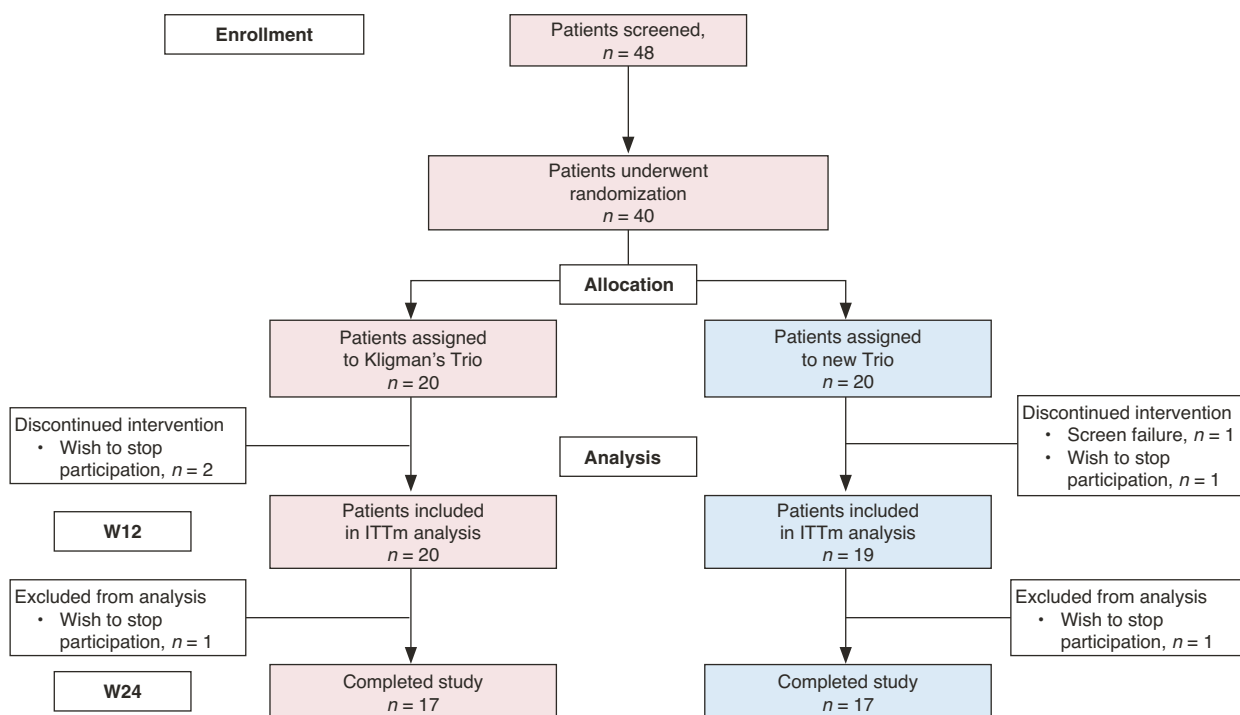


FIGURE 1 Study flowchart.

TABLE 1 Demographic and clinical baseline characteristics.

	Kligman's Trio (<i>n</i> = 20)		New Trio (<i>n</i> = 19)	
	<i>n</i>	%	<i>n</i>	%
Age (years), Mean (\pm SD)	20	47.6 (8.1)	19	41.2 (5.5)
Sex				
Male	1	5.0	1	5.3
Female	19	95.0	18	94.7
Phototype				
I	0	0.0	0	0.0
II	2	10.0	1	5.3
III	8	40.0	11	57.9
IV	7	35.0	7	36.8
V	3	15.0	0	0.0
VI	0	0.0	0	0.0
Ethnicity				
Caucasian	10	50	13	68.4
African	9	45	6	31.6
Asian	1	5	0	0
Melasma type				
Epidermal	16	80.0	16	84.2
Dermal	1	5.0	2	10.5
Mixed	3	15.0	1	5.3
Melasma localization				
Centrofacial	10	50	15	79.0
Mandibular	9	45	9	47.4
Malar	18	90	17	89.5
Melasma duration (years) Mean (\pm SD)	18	9.3 (6.0)	19	8.4 (5.2)

W12 was 2.93 ± 4.09 in the NT arm with a mean improvement (adjusted improvement, ANCOVA model) in mMASI after 12 weeks of treatment compared with baseline of 63% ($-4.33; \pm 0.71, p < 0.0001$). The mean mMASI at W12 was 3.51 ± 3.57 in the KT arm with an adjusted mean improvement in mMASI after 12 weeks of treatment compared with baseline of 39% ($-2.84; \pm 0.69, p = 0.0002$). The adjusted mean difference in the variation of the mMASI between the groups was -1.49 (IC 95% -3.52 to $0.54, p = 0.14$). The mean mMASI at W24 was 4.40 ± 4.35 in the NT group and 3.64 ± 2.76 in the KT group, showing a relapse in both arm of treatment when treatment was not applied anymore despite the continuous application of sunscreen (Figures 2 and 3).

Quantity of topical sunscreen applied

Subjects included in the trial applied in average 88.2g, and 96.9g of sunscreen at W12 for NT and KT, respectively ($p = 0.5322$). Between W12 and W24, the patients applied an

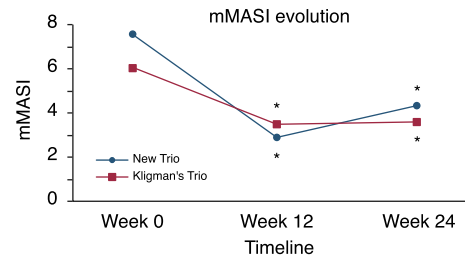


FIGURE 2 Evolution of the modified Melasma Area Severity Index (mMASI) score. Ordinate represents the mean mMASI score of the subjects of each treatment arm in points. mMASI values range from 0 to 24. *The improvement is significant ($p < 0.05$).

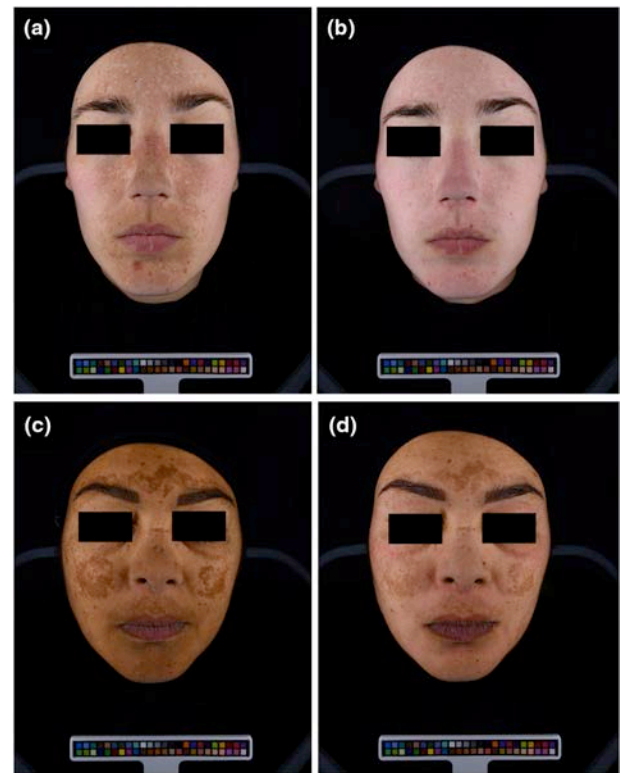


FIGURE 3 Clinical examples of evolutions of melasma under treatment. (a) At baseline. (b) After 12 weeks of treatment with the New Trio. (c) At baseline. (d) After 12 weeks of treatment with Kligman's Trio.

average of 86.1 g and 108.8g in NT and KT groups, respectively ($p = 0.0671$).

Quality of life

The adjusted mean improvement in the MelasQoL score at W12 compared with baseline was -12.57 (SE 3.29; IC 95% -19.28 to $-5.86, p = 0.0006$) in the NT group and -6.66 (SE 3.29; IC 95% -13.37 to $0.05, p = 0.0515$) in the KT group. After 24 weeks, the mean improvement in the MelasQoL score was -6.95 (SE 3.65; IC 95% -14.41 to $0.51, p = 0.0665$) in the NT group and -3.67 (SE 3.65; IC 95% -11.13 to $3.78, p = 0.3218$) in the KT group (Figure 4).

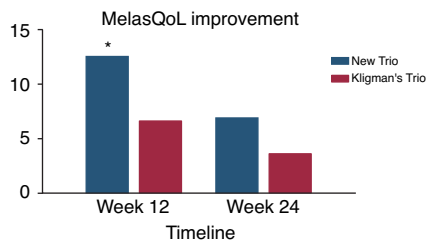


FIGURE 4 Improvement of the melasQoL score. Ordinate represents the mean melasQoL score improvement of the subjects of each treatment arm in points. melasQoL values range from 0 to 70. *The improvement is significant ($p < 0.05$).

Adverse events and tolerance

A total of 97 AE were reported. Three AE were medically significant (grade 3 according to CTCAE) but not related to the treatment (1 renal colic, 1 breast cancer, 1 abdominal pain). AE retained related to the treatment were acne, hypertrichosis, erythema, desquamation and irritation. A total of 36 and 38 AE related to the treatment were respectively reported in NT and KT groups. Acne and hypertrichosis were considered related to corticosteroid and were all transient. One case of contact dermatitis, related to the topical sunscreen, has been declared in the NT group.

Erythema was reported by 11 subjects (57.9%) in NT arm and 15 subjects in KT arm (75%). Desquamation was reported by three subjects in NT arm (21.1%) and six subjects in KT arm (30%). Irritation was reported by 13 subjects in NT arm (68.4%) and 13 subjects in KT arm (65%). Those irritative adverse effects were graded 1 or 2 only, accordingly to CTCAE, and led mostly to no action or a transient spacing of the applications in both groups. One subject in each treatment arm temporarily stopped the study due to a related AE (irritation for one patient in NT arm and irritation and desquamation for one patient in KT arm). The only AE leading to a permanent interruption of the study were grade 2 desquamation and irritation, reported by the same patient in the KT arm.

Severity of the symptoms, erythema, dryness sensation, irritation and desquamation were self-assessed by patients with VAS. Mean severity of erythema was 49.33 (IC 95% 34.1–64.56) in NT arm and 49.11 (IC 95% 30.30–67.92) in KT arm. Mean severity of dryness sensation was 34.21 (IC 95% 25.15–59.18) in NT arm and 44.89 (IC 95% 26.06–63.72) in KT arm. Mean severity of irritation was 56.56 (IC 95% 41.69–71.42) in NT arm and 47.94 (IC 95% 30.35–65.54) in KT arm. Mean severity of desquamation was 26.06 (IC 95% 11.65–40.46) in NT arm and 37.22 (IC 95% 18.95–55.49) in KT arm.

DISCUSSION

The NT combining isobutylamido-thiazolyl-resorcinol, retinoic acid and corticosteroid used with daily sun protection, demonstrated potent efficacy to treat melasma

with a mMASI reduction at week 12 of 63% compared to 39% with Kligman's Trio, considered as the gold standard since 1974. Despite a mean improvement of 4.33 points for NT compared to 2.84 for KT, the difference between the two groups, which is clinically relevant, does not reach the statistical significance ($p = 0.14$). This could be explained by the high outcome variability in the two groups. Interestingly, the higher improvement rate in patients treated with the NT was corroborated by a greater quality of life improvement compared to patients treated with the KT combination. Importantly, the greater improvement in the NT group cannot be explained by a more rigorous use of sunscreen. Indeed, there was no statistical differences between the two groups at W12, and a numerical greater consumption of sunscreen in KT group (96.9 g) compared to NT group (88.2 g).

Tolerance was globally good, and no major adverse event related to NT or KT was reported throughout the study period. Only one patient (in KT group) had to stop permanently the treatment due to a related AE. Some subjects reported transient acne and hypertrichosis, probably caused by the corticosteroid present in both combinations. Irritation was reported equally in both treatment arm and could be related to retinoic acid, as the risk of irritative adverse effects can significantly increase with local tretinoin cream.¹⁹ We therefore suggest a decrease of retinoic acid concentration for patients complaining about irritation. Patients in KT arm reported a higher, although non-significant, severity of desquamation when graded with visual analogical scale. This low severity of AE in NT arm, combined with a higher decrease in mMASI, could explain that MelasQoL improvement was higher and only significant for patient in NT arm ($p = 0.0006$).

Both groups showed a partial but limited relapse during the 12 weeks follow-up despite the use of a potent UVA and UVB sunscreen. The absence of protection against visible light^{20,21} and the relatively limited duration of treatment (12 weeks) may explain the relapses in both groups. The use of a sunscreen not covering the visible light was decided to better assess a potential rebound after the discontinuation of the depigmenting formulations. Interestingly, no rebound and worsening of the mMASI compared to baseline was observed in any of the two groups.

The main limitations of this study are its monocentric design and the inclusion of patients having mostly a European ancestry with the three only patients with skin type V were randomized in the KT group. We could hypothesize that this imbalance in skin type V between the two groups may have disadvantaged the KT group. However, those three patients had similar decrease in mMASI score compared to the rest of the KT group. Melasma is known to be even more challenging to treat in Asian and African population because they report more skin irritation, and they are prone to develop hyperpigmentation secondary to hydroquinone use.^{22,23} We may thus hypothesize that the NT without hydroquinone could be even more beneficial for these populations. Unfortunately, the relative low number of skin type V and

VI patients and the lack of Asian ancestry patients (except one) in our study prevent drawing conclusions in these populations. Additional studies including more diverse populations and skin types are warranted to define the positioning of this new depigmenting combination. We decided to use the original Kligman's formula as the comparator for this study. However, since its first description, many physicians are using in their current practice the modified Kligman formula (tretinoin 0.05% + hydroquinone 4% + 0.01% fluocinolone acetonide), which usually provides better tolerance. We decided to keep the original formula for this study, as it contains higher concentration of hydroquinone and tretinoin and, thus, is potentially the most effective one. It is thus very interesting to note that the NT is, at least, as effective than the most potent Kligman trio.

Together, these data attest that the NT combination demonstrated efficacy and significant improvement in the quality of life in treating melasma patients. This new approach could be considered as an alternative to the Kligman's Trio.

ACKNOWLEDGEMENT

We would like to thank all the patients who participated to this clinical trial.

FUNDING INFORMATION

None.

CONFLICT OF INTEREST STATEMENT

TP has received grants and/or honoraria from Bioderma, Beiersdorf, Galderma, Hyphens, L'Oréal, Isis Pharma, Isdin, Mesoesthetics, Pierre Fabre, SUN Pharma, SVR and Symrise. CB, EF, TS, NG, SR and SWP report no conflict of interest.

DATA AVAILABILITY STATEMENT

Data are available for scientific purposes only upon reasonable request to fontas.e@chu-nice.fr.

ETHICS STATEMENT

Reviewed and approved by Sud-Méditerranée I; approval #21 11 (EudraCT 2020-006107-42).

ORCID

Clémence Bertold <https://orcid.org/0000-0002-1796-2076>

Tanya Singh <https://orcid.org/0000-0002-2062-7543>

Thierry Passeron <https://orcid.org/0000-0002-0797-6570>

REFERENCES

- Handel AC, Miot LD, Miot HA. Melasma: a clinical and epidemiological review. *An Bras Dermatol*. 2014;89(5):771–82. <https://doi.org/10.1590/abd1806-4841.20143063>
- Sheth VM, Pandya AG. Melasma: a comprehensive update: part I. *J Am Acad Dermatol*. 2011;65(4):689–97. <https://doi.org/10.1016/j.jaad.2010.12.046>
- Ortonne JP, Arellano I, Berneburg M, Cestari T, Chan H, Grimes P, et al. A global survey of the role of ultraviolet radiation and hormonal influences in the development of melasma. *J Eur Acad Dermatol Venereol*. 2009;23(11):1254–62. <https://doi.org/10.1111/j1468-3083.2009.03295>
- Handel AC, Lima PB, Tonolli VM, Miot LD, Miot HA. Risk factors for facial melasma in women: a case-control study. *Br J Dermatol*. 2014;171(3):588–94. <https://doi.org/10.1111/bjd.13059>
- Passeron T, Picardo M. Melasma, a photoaging disorder. *Pigment Cell Melanoma Res*. 2018;31(4):461–5. <https://doi.org/10.1111/pcmr.12684>
- Kwon SH, Na JI, Choi JY, Park KC. Melasma: updates and perspectives. *Exp Dermatol*. 2019;28(6):704–8. <https://doi.org/10.1111/exd.13844>
- Flori E, Mastrofrancesco A, Mosca S, Ottaviani M, Briganti S, Cardinali G, et al. Sebocytes contribute to melasma onset. *iScience*. 2022;25(3):103871. <https://doi.org/10.1016/j.isci.2022.103871>
- Balkrishnan R, McMichael AJ, Camacho FT, Saltzberg F, Housman TS, Grummer S, et al. Development and validation of a health-related quality of life instrument for women with melasma. *Br J Dermatol*. 2003;149(3):572–7. <https://doi.org/10.1046/j.1365-2133.2003.05419.x>
- Rendon M, Berneburg M, Arellano I, Picardo M. Treatment of melasma. *J Am Acad Dermatol*. 2006;54(5 Suppl 2):S272–81.
- Morgado-Carrasco D, Piquero-Casals J, Granger C, Trullàs C, Passeron T. Melasma: the need for tailored photoprotection to improve clinical outcomes. *Photodermatol Photoimmunol Photomed*. 2022;38(6):515–21. <https://doi.org/10.1111/phpp.12783>
- Kligman AM, Willis I. A new formula for depigmenting human skin. *Arch Dermatol*. 1975;111(1):40–8.
- Pennitz A, Kinberger M, Avila Valle G, Passeron T, Nast A, Werner RN. Self-applied topical interventions for melasma: a systematic review and meta-analysis of data from randomized, investigator-blinded clinical trials. *Br J Dermatol*. 2022;187(3):309–17. <https://doi.org/10.1111/bjd.21244>
- Olumide YM, Akinkugbe AO, Altraide D, Mohammed T, Ahamefule N, Ayanlowo S, et al. Complications of chronic use of skin lightening cosmetics. *Int J Dermatol*. 2008;47(4):344–53. <https://doi.org/10.1111/j.1365-4632.2008.02719.x>
- Westerhof W, Kooyers TJ. Hydroquinone and its analogues in dermatology – a potential health risk. *J Cosmet Dermatol*. 2005;4(2):55–9. <https://doi.org/10.1111/j.1473-2165.2005.40202.x>
- Mann T, Gerwat W, Batzer J, Eggers K, Scherner C, Wenck H, et al. Inhibition of human tyrosinase requires molecular motifs distinctively different from mushroom tyrosinase. *J Invest Dermatol*. 2018;138(7):1601–8. <https://doi.org/10.1016/j.jid.2018.01.019>
- Arrowitz C, Schoelermann AM, Mann T, Jiang LI, Weber T, Kolbe L. Effective tyrosinase inhibition by thiamidol results in significant improvement of mild to moderate melasma. *J Invest Dermatol*. 2019;139(8):1691–1698.e6. <https://doi.org/10.1016/j.jid.2019.02.013>
- Lima PB, Dias JAF, Cassiano DP, Esposito ACC, Miot LDB, Bagatin E, et al. Efficacy and safety of topical isobutylamido thiazolyl resorcinol (Thiamidol) vs. 4% hydroquinone cream for facial melasma: an evaluator-blinded, randomized controlled trial. *J Eur Acad Dermatol Venereol*. 2021;35(9):1881–7. <https://doi.org/10.1111/jdv.17344>
- Pandya AG, Hynan LS, Bhole R, Riley FC, Guevara IL, Grimes P, et al. Reliability assessment and validation of the Melasma Area and Severity Index (MASI) and a new modified MASI scoring method. *J Am Acad Dermatol*. 2011;64(78–83):78–83, 83.e1–2.
- Griffiths CE, Finkel LJ, Ditte CM, Hamilton TA, Ellis CN, Voorhees JJ. Topical tretinoin (retinoic acid) improves melasma. A vehicle-controlled, clinical trial. *Br J Dermatol*. 1993;129(4):415–21. <https://doi.org/10.1111/j.1365-2133.1993.tb03169.x>
- Mahmoud BH, Ruvolo E, Hensel CL, Liu Y, Owen MR, Kollias N, et al. Impact of long-wavelength UVA and visible light on melanocompetent skin. *J Invest Dermatol*. 2010;130(8):2092–7. <https://doi.org/10.1038/jid.2010.95>
- Boukari F, Jourdan E, Fontas E, Montaudié H, Castela E, Lacour JP, et al. Prevention of melasma relapses with sunscreen

- combining protection against UV and short wavelengths of visible light: a prospective randomized comparative trial. *J Am Acad Dermatol*. 2015;72(1):189–190.e1. <https://doi.org/10.1016/j.jaad.2014.08.023>
22. Vashi NA, Wirya SA, Inyang M, Kundu RV. Facial hyperpigmentation in skin of color: special considerations and treatment. *Am J Clin Dermatol*. 2017;18(2):215–30. <https://doi.org/10.1007/s40257-016-0239-8>
23. Davis EC, Callender VD. Postinflammatory hyperpigmentation: a review of the epidemiology, clinical features, and treatment options in skin of color. *J Clin Aesthet Dermatol*. 2010;3(7):20–31.

How to cite this article: Bertold C, Fontas E, Singh T, Gastaut N, Ruitort S, Wehrlen Pugliese S, et al. Efficacy and safety of a novel triple combination cream compared to Kligman's trio for melasma: A 24-week double-blind prospective randomized controlled trial. *J Eur Acad Dermatol Venereol*. 2023;00:1–7. <https://doi.org/10.1111/jdv.19455>

Ludger Kolbe · Jeannine Immeyer · Jan Batzer
Ursula Wensorra · Karen tom Dieck
Claudia Mundt · Rainer Wolber · Franz Stäb
Uwe Schönrock · Roger I. Ceilley · Horst Wenck

Anti-inflammatory efficacy of Licochalcone A: correlation of clinical potency and in vitro effects

Received: 4 January 2006 / Revised: 27 February 2006 / Accepted: 28 February 2006 / Published online: 22 March 2006
© Springer-Verlag 2006

Abstract Licochalcone A (LicA), a major phenolic constituent of the licorice species *Glycyrrhiza inflata*, has recently been reported to have anti-inflammatory as well as anti-microbial effects. These anti-inflammatory properties might be exploited for topical applications of LicA. We conducted prospective randomized vehicle-controlled clinical trials to assess the anti-irritative efficacy of cosmetic formulations containing LicA in a post-shaving skin irritation model and on UV-induced erythema formation. The clinical trials were accompanied by a series of in vitro experiments to characterize anti-inflammatory properties of LicA on several dermatologically relevant cell types. Topical LicA causes a highly significant reduction in erythema relative to the vehicle control in both the shave- and UV-induced erythema tests, demonstrating the anti-irritative properties of LicA. Furthermore, LicA is a potent inhibitor of pro-inflammatory in vitro responses, including *N*-formyl-MET-LEU-PHE (fMLP)- or zymosan-induced oxidative burst of granulocytes, UVB-induced PGE₂ release by keratinocytes, lipopolysaccharide (LPS)-induced PGE₂ release by adult dermal fibroblasts, fMLP-induced LTB₄ release by granulocytes, and LPS-induced IL-6/TNF- α secretion by monocyte-derived dendritic cells. The reported data suggest therapeutic skin care benefits from LicA when applied to sensitive or irritated skin.

Keywords Anti-inflammatory agents · Non-steroidal · Clinical trial · Dermatologic agents · Allergy and immunology · Licochalcone A

Abbreviations fMLP: *N*-formyl-MET-LEU-PHE · iDC: Immature dendritic cell · LicA: Licochalcone A · LPS: lipopolysaccharide · MTT: 3-[4,5-Dimethylthiazol-2-yl]-2,5-diphenyltetrazolium bromide

Introduction

As the outermost barrier of the body, the skin has to cope with a variety of environmental stress and physical insults, like mechanical stress or solar radiation. In sensitive skin, this often results in irritation with associated redness, itching or even pain. Cosmetic products with botanical ingredients are frequently used to soothe the early signs of skin irritation. Licochalcone A (LicA, CAS No. 58749-22-7, for chemical structure see Fig. 1), a reversely constructed chalcone or “retrochalcone” extracted from the licorice species *Glycyrrhiza inflata*, has drawn pharmacological attention in the recent past due to its anti-bacterial [6, 8, 9, 12, 15], anti-protozoan [3–5, 19], and anti-tumor properties [7, 16]. Besides these properties, suppressive effects of LicA on phorbol-ester-driven processes, like the mouse ear edema formation induced by arachidonic acid and TPA, have been described [13]. Furthermore, direct immunosuppressive effects of LicA on mitogen-induced T cell proliferation and IFN- γ production, as well as on LPS-induced cytokine production by monocytes, have been reported by Barfod et al. [2]. Thus, in the light of possible immunomodulating actions of LicA, we have initiated vehicle-controlled clinical studies to assess the topical anti-inflammatory potency of LicA in cosmetic formulations. The clinical studies were accompanied by a series of in vitro experiments to assess the effects of the LicA-rich licorice extract and synthetic LicA on several target cells involved in skin inflammation.

L. Kolbe (✉) · J. Immeyer · J. Batzer · U. Wensorra
K. tom Dieck · C. Mundt · R. Wolber · F. Stäb
U. Schönrock · H. Wenck
Beiersdorf AG, Research and Development, Unnastr. 48,
20245, Hamburg, Germany
E-mail: ludger.kolbe@beiersdorf.com
Tel.: +49-40-49092826
Fax: +49-40-49096770

R. I. Ceilley
Department of Dermatology, University of Iowa,
Iowa City, IA, USA

Materials and methods

Formulation of LicA for topical application and in vitro use

A LicA-rich licorice extract produced by aqueous extraction from *G. inflata* was purchased from Maruzen Chemicals Co, Osaka, Japan. The powdery extract had a content of 20% (w/v) LicA, and contained no other terpenes and flavonoids. Synthetic LicA with a purity of $\geq 96\%$ was purchased from Calbiochem-Novabiochem, Bad Soden, Germany. For some in vitro experiments glycyrrhizic acid was obtained from Sigma-Aldrich, Taufkirchen, Germany. Defined oil-in-water lotions containing either 0.025 or 0.05% of the LicA-rich licorice extract were used throughout the clinical studies. The emulsions consisted of water, glyceryl lanolate, triceteareth-4 phosphate, cyclomethicone, isopropyl palmitate, and carbomer. The same basal formulations were used for the verum and respective vehicle control. The LicA-rich extract and synthetic LicA for cell culture experiments were dissolved in DMSO to a 1% stock solution, and further diluted with cell culture medium to the final concentrations. Unless otherwise indicated, all in vitro concentrations given throughout this report reflect the final concentrations of the active compound (LicA) in cell culture medium.

Study population

A total of 57 healthy volunteers, ages 23–63 years, were enrolled in the studies: 45 of them took part in the razor test, and 12 in the UV-induced erythema test. The subjects were chosen according to the essential recommendations of the Helsinki Declaration (Edinburgh, Scotland, 2000) and following the basic ICH GCP Guidelines. They met defined eligibility and exclusion criteria, were informed about the study in writing and

orally before the start of the study, and signed a written Declaration of Consent.

Razor test

A controlled post-shave irritation model was used to assess the anti-irritant potential of cosmetic formulations containing LicA. The test was conducted on three test sites on the volar forearm. The sites were shaved without lubricant using a disposable razor and with a defined number of strokes for three consecutive days to induce erythema. The test formulation containing 0.025% of the LicA-rich extract and the respective vehicle were applied twice daily for 3 days, directly after shaving and at night. On day 4, skin redness was determined by spectrophotometry (see below) and by clinical grading.

Spectrophotometry of shaved skin

Skin redness of shaved skin sites was measured using a SpectroPen[®] reflectance spectrophotometer (Hach Lange GmbH, Düsseldorf, Germany). Skin redness was expressed as the difference between the *a* values (Lab color scale) of a shaved treated or untreated site, and an adjacent non-shaved untreated skin site. On each test site nine determinations of redness were performed and the mean was calculated.

UV-induced erythema test

Twelve volunteers with healthy skin (Fitzpatrick types II and III) were irradiated using a SU 5000 solar simulator (m.u.t. GmbH, Wedel, Germany) at increasing doses in 25% increments of UV light to determine their minimal erythema dose (MED) at latest 1 day before the start of the test. On the testing day, each volunteer was irradiated with 1.4 MED once for each product site. The test sites were randomized and allocated on the back. Immediately and 5 h after irradiation, the test sites were treated with either the test formulation containing 0.05% of the LicA-rich extract or the respective vehicle. After 5 and 24 h, the intensity of the UV-induced erythema was measured using hemoglobin reflectance spectroscopy (see below) and visual assessment.

Hemoglobin reflectance spectroscopy

For the measurement of the redness of the designated skin area, a Zeiss MCS UV-NIR reflectance spectrophotometer (Carl Zeiss, Jena, Germany) was used. The reflectance values were recorded as the areas under the curve (AUC) for hemoglobin peaks minus the AUC for an adjacent skin site, unexposed to the UV source. Each spot was measured three times and the mean of three measured values was calculated.

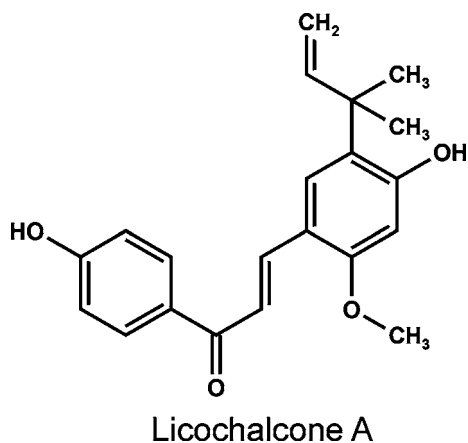


Fig. 1 Chemical structure of licochalcone A

Cell lines, primary isolates, and culture media

The EpiDerm™ skin model (EPI-200-HCF-PRF), a multi-layered highly differentiated in vitro model of human epidermis that consists of mitotically and metabolically active normal human epidermal keratinocytes (NHEK), was purchased from MatTek Corporation, Ashland, MA, USA. Adult human primary fibroblasts were isolated from skin biopsies or surgical material using dispase digestion. Adult human fibroblasts of three–five passages were used throughout all the experiments. Human granulocytes were prepared from fresh buffy coats by Ficoll density gradient centrifugation followed by hypo-osmotic treatment with distilled water to lyse erythrocytes. Monocytes were prepared from fresh buffy coats by Ficoll density gradient centrifugation followed by positive enrichment using anti-CD14-coupled magnetobeads (EasySep®, Stem Cell Technologies, Vancouver, BC, Canada). Differentiation of immature dendritic cells (iDC) from isolated monocytes was accomplished by culturing monocytes for 5 days in X-VIVO™ 15 medium (BioWhittaker, Walkersville, MD, USA) supplemented with 1,000 U/ml IL-4 (Strathmann Biotec, Hamburg, Germany), 800 U/ml GM-CSF (Immunex, Seattle, WA, USA), and 1.5% autologous serum. Phenotypes of differentiated iDC were controlled by flow cytometry.

3-[4,5-Dimethylthiazol-2-yl]-2,5-diphenyltetrazolium bromide (MTT) viability assay

Viability of human epidermal keratinocytes in the EpiDerm™ skin model inserts was assessed by means of an MTT assay. Briefly, culture inserts containing the EpiDerm™ skin model were rinsed carefully with PBS, transferred into the cavities of 24-well microplates containing 300 µl/well of fresh pre-warmed MM-Medium (EPI-100-MM-HCF-PRF, MatTek Inc.), and 0.4 mg/ml MTT (Sigma-Aldrich). After incubation for 3 h at 7% CO₂ and 37°C, the inserts were again carefully rinsed with PBS, excess buffer was aspirated, and the inserts were transferred into 24-well microplates containing 2 ml/well of 2-propanol. After additional incubation with gentle agitation for 2 h at ambient temperature (protected from light), the extinction of the dissolved blue formazan dye was photometrically measured at 550 nm.

Oxidative burst of fMLP- or zymosan-stimulated human granulocytes

Human granulocytes were incubated at a cell density of 5×10^6 cells/ml in a total volume of 250 µl with different concentrations of LicA or glycyrrhizic acid in lumina strips (Labsystems, Helsinki, Finland). Granulocytes were stimulated by the addition of fMLP (Sigma-Aldrich) at a final concentration of 10 µM, or zymosan (Sigma-Aldrich) at a final concentration of 80 µg/ml.

Oxidative burst was recorded during the first 6 min of stimulation in the case of fMLP, and during the first 30 min of stimulation in the case of zymosan, and quantified by the measurement of luminol-evoked chemiluminescence with a single photon camera (Hamamatsu Photonics GmbH, Germany). Total photon count within a period of 6 (fMLP reaction) or 30 min (Zymosan reaction) was calculated for every culture.

UVB-induced PGE₂ production by the EpiDerm™ skin models

Skin models were cultured in MM-HCF-PRF culture medium (MatTek Corp), containing either the LicA-rich extract from *G. inflata* at a final LicA concentration of 10 µg/ml, or the cyclooxygenase inhibitor diclofenac (Sigma-Aldrich) at a final concentration of 50 ng/ml, or pure medium without these compounds. The culture inserts, containing the multi-layered keratinocytes, were subsequently UV-irradiated at an intensity of 1×10^{-4} W/cm² for 15 min, resulting in an UVB dosage of 90 mJ/cm². An ORIEL UV-sun-simulator (Oriel Instruments, Stratford, CT, USA), giving a COLIPA compliant UV-spectrum was used as a source for UVB light. The culture medium was sampled for PGE₂ quantitation by ELISA 24 h after the first irradiation, and was replaced for a second time by 1 ml of fresh culture medium containing the same concentrations of LicA or diclofenac as before, followed by a second UV irradiation with 90 mJ UVB/cm². Viability of the keratinocytes was measured 24 h after the second irradiation by means of the MTT assay, as described above. A parallel set of identically treated cultures was incubated without UV irradiation.

LTB₄ production by fMLP-stimulated human granulocytes

Human granulocytes were incubated at a cell density of 5×10^6 cells/ml in a total volume of 200 µl with different concentrations of the LicA-rich extract from *G. inflata*, or synthetic LicA. Granulocytes were stimulated by the addition of fMLP at a final concentration of 10 µM, or were left unstimulated. After 2 h of stimulation culture supernatants were harvested for the quantitation of LTB₄ by ELISA (see below). Control cultures were set up in the presence of BAY×1005 (Bayer, Leverkusen, Germany) a specific inhibitor of 5-lipoxygenase-activating protein (FLAP) at a final concentration of 100 ng/ml.

PGE₂ production by LPS-stimulated adult dermal fibroblasts

Human adult fibroblasts were pre-cultured for 2 days at an initial cell density of 1×10^5 cells/ml in a total volume of

100 μ l until confluence. After pre-culture the medium was replaced by 200 μ l of fresh culture medium containing different concentrations of the LicA-rich extract from *G. inflata*, or synthetic LicA. Control cultures were set up in the presence of the cyclooxygenase inhibitor diclofenac at a final concentration of 50 ng/ml. Fibroblast cultures were subsequently stimulated by the addition of LPS (lipopolysaccharide from *Salmonella minnesota*, Sigma-Aldrich) at a final concentration of 25 ng/ml. Cell culture supernatants were sampled 24 h after stimulation for the quantitation of PGE₂ by ELISA.

Cytokine production by LPS-stimulated iDCs

After differentiation for 5 days, culture media of immature monocyte-derived human DC was supplemented with different concentrations of the LicA-rich extract from *G. inflata*. Control cultures were set up in the presence of dexamethasone (Sigma-Aldrich) at a final concentration of 100 ng/ml. DC cultures were subsequently stimulated by the addition of LPS (from *S. minnesota*) at a final concentration of 10 ng/ml. Additional control cultures were left unstimulated. Cell culture supernatants were sampled 24 h after stimulation for the quantitation of IL-6 and TNF- α by ELISA.

Quantitation of cytokines and prostanoids

Quantitation of PGE₂ and LTB₄ in culture supernatants was performed using commercially available ELISA kits (PGE₂-Kit, LTB₄-Kit, Cayman Chem., Ann Arbor, MI, USA) according to the manufacturers instructions. Commercially available ELISA kits (IL-6 Bio-Rad Multiplex, TNF- α Bio-Rad Multiplex, Bio-Rad, Munich, Germany) were also used for the quantitation of IL-6 and TNF- α in culture supernatants.

Statistical analysis

The normal distribution of clinical data was checked by means of the Shapiro–Wilk test. Means of parametric data showing normal distribution like reflectance data were analyzed using two-way ANOVA. For data not normally distributed, the Blom-transformed rank test was used. For non-parametric data Wilcoxon's signed rank test was used. Differences were regarded statistically significant at a $P < 0.05$ level.

Results

Anti-irritant efficacy of a LicA-rich licorice extract on human skin

The post-shave irritation test causes visible inflammation of skin sites that are repeatedly dry-shaved for three

consecutive days with a disposable razor. A shave test on 45 subjects was conducted to compare a LicA-containing oil-in-water lotion and the respective vehicle with regard to anti-irritative potency. The data from the razor test prove a substantial anti-irritative potency of the topically applied LicA-rich licorice extract. Figure 2 shows a statistically significant difference in the skin redness Δa values from 45 subjects (shaved site values minus adjacent unshaven site values) comparing the oil-in-water lotion containing LicA to its vehicle ($P < 0.0001$) and the untreated skin site ($P < 0.0001$). The vehicle-treated site was not significantly different from the untreated control site. Clinical assessments of erythema confirmed the instrumental results (data not shown).

Anti-irritative potency of the topical LicA-rich licorice extract was also observed in the UV-induced erythema test. When exposed to UV light at 1.4 MED, erythema of exposed skin occurs within several hours, peaking about 12 h after exposure. Erythema was evaluated instrumentally in 12 subjects by measuring the hemoglobin reflectance using a reflectance spectrometer. As shown in Fig. 3, a significantly reduced erythema was observed at the LicA-treated site, at 5 ($P < 0.05$) and 24 h ($P < 0.05$) after UV exposure, as compared with the vehicle-treated site. The results were confirmed by clinical erythema grading of the active compound- and vehicle-treated sites of the same subjects (data not shown).

Anti-inflammatory activity of the LicA-rich licorice extract and synthetic LicA in vitro

Inhibition of PGE₂ production by the LicA-rich extract can be demonstrated in an experimental model using LPS-stimulated adult human dermal fibroblasts. As shown in Fig. 4a, LPS-induced PGE₂ production by dermal fibroblasts is reduced by the extract as well as by synthetic LicA below the control level of non-stimulated fibroblasts. The inhibitory effect is dose dependent.

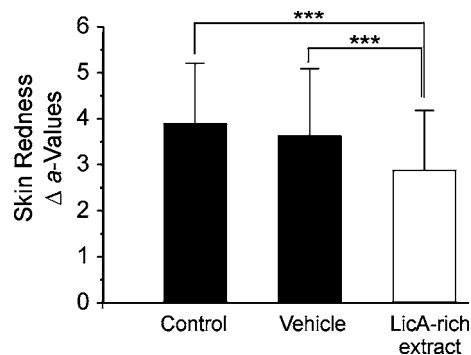


Fig. 2 Erythema (reflectance spectroscopy) of shaved sites on day 4. Quantification of skin redness (reflection Δa values) of shaven volar forearm test sites after shaving on three consecutive days. Sites were treated with either an oil-in-water lotion containing 0.025% licorice extract, the respective vehicle, or left untreated (Control). Bars representing group means \pm SD ($n = 45$). Statistics: two-way ANOVA; *** $P < 0.0001$

Diclofenac, a specific cyclooxygenase inhibitor, was used as a positive control. Inhibitory effects of LicA on LPS-induced PGE₂ production by dermal fibroblasts at a concentration of 1,000 ng/ml are close to positive control diclofenac at 50 ng/ml (Fig. 4a). Besides the PGE₂ production, the effect of the LicA-rich extract on the production of LTB₄, another pro-inflammatory eicosanoid, which is synthesized via the 5-lipoxygenase pathway, was assessed using fMLP-stimulated human granulocytes. Production of LTB₄ by human fMLP-stimulated granulocytes is inhibited by the LicA-rich extract as well as by synthetic LicA in a dose-dependent manner (Fig. 4b). The 5-lipoxygenase inhibitor BAY×1005 was used as a positive control. Inhibitory effects of LicA on fMLP-induced LTB₄ production by human granulocytes at a concentration around 1,000–2,000 ng/ml are close to positive control BAY×1005 at 100 ng/ml (Fig. 4b). The IC₅₀ values of the extract with regard to PGE₂ production by LPS-stimulated fibroblasts and LTB₄ production of fMLP-stimulated granulocytes are in the same order of magnitude.

We further analyzed the effects of the LicA-rich licorice extract on pro-inflammatory cytokine production by iDC stimulated with low concentrations of LPS (10 ng/ml). iDCs are the resident DC of peripheral tissues including the skin. As shown in Fig. 5, LPS-induced production of both pro-inflammatory cytokines, IL-6 and TNF- α , is suppressed in a dose-dependent manner by the LicA-rich extract. For both cytokines the production can be reduced by the extract up to the control level of non-stimulated DC, or even below. As a positive control dexamethasone was used at a concentration of 100 ng/ml. In the above experimental setting, LicA at a concentration of 150 ng/ml is equi-potent with 100 ng/ml dexamethasone in terms of inhibition of IL-6 production, and at 600 ng/ml in terms of TNF- α production.

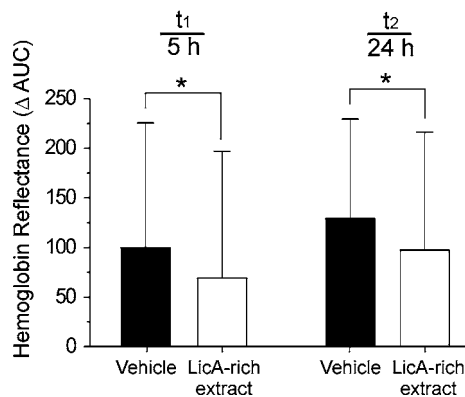


Fig. 3 UV-induced erythema, measured by hemoglobin reflectance spectroscopy. Quantification of hemoglobin reflectance (areas under the curve, Δ AUC) 5 h (t_1) and 24 h (t_2) after irradiation at test sites treated with either an oil-in-water lotion containing 0.05% licorice extract or the respective vehicle. Bars representing means \pm SD ($n=12$). Statistics: Blom-transformed rank test; * $P < 0.05$

The EpiDerm™ skin model was used to measure the inhibitory effect the LicA-rich extract on PGE₂ production after UV irradiation. As shown in Fig. 6a, the UV-induced PGE₂ production as well as the non-induced basal PGE₂ production by epidermal cells is significantly reduced in the presence 10 μ g/ml of the LicA-rich extract. As a positive control the specific

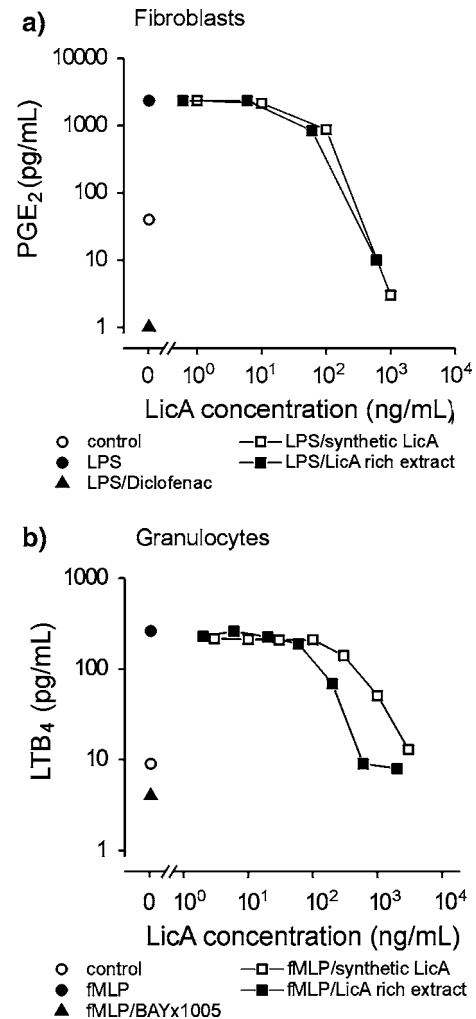


Fig. 4 Suppressive effects of LicA on prostanoid production by LPS-stimulated fibroblasts and fMLP-stimulated human granulocytes. Prostanoid concentrations in culture supernatants of LPS-stimulated human fibroblast (a) and fMLP-stimulated human granulocytes (b) were measured in the presence of different concentrations of the *G. inflata* extract (closed squares) and synthetic LicA (open squares). Extract concentrations are normalized to the real concentrations of LicA. In case of fibroblasts (a), control cultures without LicA were set up in the presence of LPS (closed circles), or LPS and diclofenac (50 ng/ml; closed triangles), or in the absence of LPS or diclofenac (open circles). In case of granulocytes (b), control cultures without LicA were set up in the presence of fMLP (closed circles), or fMLP and BAY×1005 (100 ng/ml; closed triangles), or in the absence of fMLP or BAY×1005 (open circles). Double logarithmic scale. Of six independent experiments each performed in duplicates, representative experiments are shown

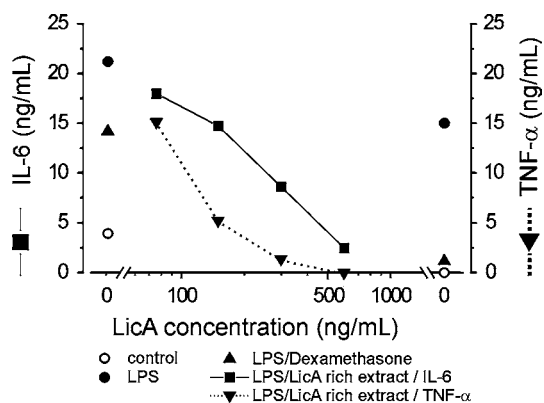


Fig. 5 Suppressive effects of LicA on IL-6 and TNF- α production by LPS-stimulated immature DC. Concentrations of IL-6 (closed squares) and TNF- α (closed triangles, down) were measured in culture supernatants of LPS-stimulated monocyte-derived DC in the presence of different concentrations of the *G. inflata* extract. Extract concentrations are normalized to the real concentrations of LicA. Control cultures without LicA were set up in the presence of LPS (closed circles), or LPS and dexamethasone (100 ng/ml; closed triangles, up), or in the absence of LPS or dexamethasone (open circles). Logarithmic scale for X-axis. Data representative of one out of five independent experiments for TNF-alpha and one out of three experiments for IL-6 measurement

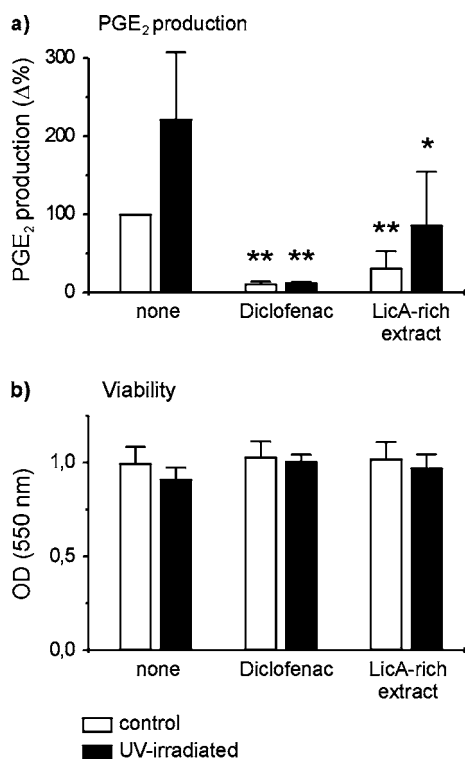


Fig. 6 Effects of LicA on PGE₂ production and viability of human keratinocytes. PGE₂ production (a) and viability (b) of human keratinocytes in the EpiDerm™ skin model without UV irradiation (open bars) or after UV irradiation (90 mJ UVB /cm²) (closed bars) were measured. Keratinocyte cultures were set up in the presence of the *G. inflata* extract corresponding to 10 μg/ml LicA, or 50 ng/ml diclofenac, or without the active compounds (none). Data represent means ± SD of three independent experiments. Statistics: two-sided *t* test for independent samples (active compound vs. none); **P* < 0.05; ***P* < 0.01

cyclooxygenase inhibitor diclofenac was used. At the given concentration of 10 μg/ml, the significant reduction of PGE₂ production by LicA does not reach the same level as seen in the presence of 50 ng/ml diclofenac. As measured by MTT turnover (Fig. 6b), the LicA-rich extract does not exert cytotoxic effects on cultured human epidermal cells at a concentration of 10 μg LicA/ml, neither after UV irradiation (90 mJ/cm²) nor on non-irradiated cells. Even with 100 μg LicA/ml still > 95% viability of keratinocytes was measured (data not shown), indicating a low in vitro toxicity of LicA.

Incubation of human granulocytes with the LicA showed a dose-dependent inhibition of the oxidative burst by LicA, whereas glycyrrhizic acid was only effective in the highest dose used in this assay. Therefore, LicA is more potent by a factor of > 100 than glycyrrhizic acid (Fig. 7).

Discussion

Several low molecular weight terpenoids and phenolic ingredients found in different species of licorice have been attributed pharmacological activities including anti-inflammatory, anti-virus, anti-bacterial, anti-protozoan, anti-ulcer, anti-carcinogenic activity (for

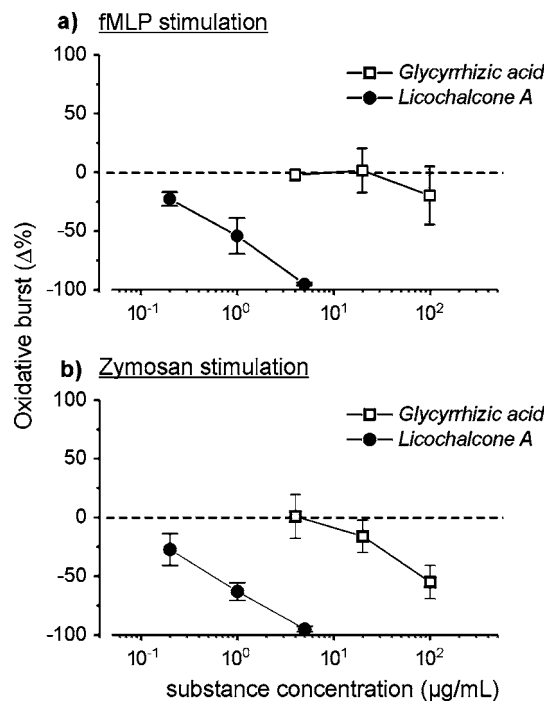


Fig. 7 Effects of licochalcone A and glycyrrhizic acid on granulocyte oxidative burst. Altered oxidative burst reactions (Δ%) of fMLP- (a) and zymosan-stimulated (b) human granulocytes in the presence of different concentrations of LicA (closed circles) and the glycyrrhizic acid (open squares). Concentrations are given as final concentration in the respective culture media. Logarithmic scale for X-axis. Mean ± SD of quadruplicate measurements is shown. Data representative of one out of three independent experiments

reviews see [1, 14, 16]). The focus of this report is on the anti-inflammatory potency of LicA, the characterizing phenolic constituent of *G. inflata* [10].

In order to assess its ability to reduce skin inflammation when topically applied, we provoked skin irritation in two controlled clinical tests, a post-shave irritation study, and a UV-induced erythema test. The post-shave irritation test causes visible inflammation of skin sites that are repeatedly dry-shaved with a disposable razor. In this model of skin irritation, the formulation containing 0.025% of the LicA-rich licorice extract, corresponding to a LicA concentration in the final formulation of about 50 µg/ml, had a highly significant erythema suppressive effect, as compared to the vehicle alone. Furthermore, when skin was treated with a LicA-containing formulation (0.05% of the LicA-rich licorice extract) immediately and 5 h after exposure to solar-simulated irradiation, the developing erythema was significantly diminished relative to the vehicle-treated site at 5 and at 24 h after irradiation. Although these two skin irritation models differ in the manner in which they elicit inflammation (barrier damage vs. penetrating UV radiation), the LicA-containing formulations were shown to be beneficial relative to the vehicle in both cases. Visible benefits to patients with erythematotelangiectatic rosacea and red facial skin not attributed to rosacea were also observed in another clinical study in which subjects used a regimen of skin care products containing LicA for 8 weeks [17].

In addition to the clinical efficacy of LicA, the in vitro data presented in this report clearly demonstrate that aqueous LicA-rich extracts of *G. inflata*, as well as synthetic LicA, are potent inhibitors of pro-inflammatory responses of a variety of dermatologically relevant cell types. Inhibition of pro-inflammatory responses in vitro by LicA can be demonstrated using fMLP- or zymosan-induced oxidative burst of granulocytes, UV-induced PGE₂ release by keratinocytes, LPS-induced PGE₂ release by adult dermal fibroblasts, fMLP-induced LTB₄ release by granulocytes, and LPS-induced IL-6/TNF- α release by iDC. Other investigators have reported inhibitory effects of LicA on mitogen-induced T cell proliferation and cytokine production [2], as well as the inhibition of phorbol ester-driven inflammatory responses [13]. Taken together, LicA must be considered a potent anti-inflammatory agent with a broad target spectrum.

LPS signaling in DC, mediated by the activation of NF κ B via Toll-like receptors [18], and fMLP signaling in granulocytes, requiring the activation of MAP kinases and PIP₃ via heterotrimeric G protein-coupled receptors [11], are non-overlapping sequences. Thus, an interference of LicA with upstream processes in the signal transduction cascade is rather unlikely. Given the broad range of anti-inflammatory actions of LicA described in this report and by others, an interference of LicA with downstream processes of gene regulation might be hypothesized.

Taken together, our studies demonstrate the anti-irritative potency of LicA in a topical formulation, which can be correlated with a substantial anti-inflammatory mode of action on a variety of dermatologically relevant cell types in vitro. Even though LicA's mode of action is still not resolved on a molecular level, the results suggest therapeutic skin care benefits from LicA when applied to sensitive or irritated skin.

References

- Armanini D, Fiore C, Mattarello MJ, Bielenberg J, Palermo M (2002) History of the endocrine effects of licorice. *Exp Clin Endocrinol Diabetes* 110:257–261
- Barfod L, Kemp K, Hansen M, Kharazmi A (2002) Chalcones from chinese liquorice inhibit proliferation of T cells and production of cytokines. *Int Immunopharmacol* 2:545–555
- Chen M, Christensen SB, Blom J, Lemmich E, Nadelmann L, Fich K, Theander TG, Kharazmi A (1993) Licochalcone A, a novel antiparasitic agent with potent activity against human pathogenic protozoan species of *Leishmania*. *Antimicrob Agents Chemother* 37:2550–2556
- Chen M, Theander TG, Christensen SB, Hviid L, Zhai L, Kharazmi A (1994) Licochalcone A, a new antimalarial agent, inhibits in vitro growth of the human malaria parasite *Plasmodium falciparum* and protects mice from *P. yoelii* infection. *Antimicrob Agents Chemother* 38:1470–1475
- Chen M, Zhai L, Christensen SB, Theander TG, Kharazmi A (2001) Inhibition of fumarate reductase in *Leishmania major* and *L. donovani* by chalcones. *Antimicrob Agents Chemother* 45:2023–2029
- Friis-Moller A, Chen M, Fuursted K, Christensen SB, Kharazmi A (2002) In vitro antimycobacterial and antilegionella activity of licochalcone A from chinese licorice roots. *Planta Med* 68:416–419
- Fu Y, Hsieh TC, Guo J, Kunicki J, Lee MY, Darzynkiewicz Z, Wu JM (2004) Licochalcone-A, a novel flavonoid isolated from licorice root (*Glycyrrhiza glabra*), causes G2 and late-G1 arrests in androgen-independent PC-3 prostate cancer cells. *Biochem Biophys Res Commun* 322:263–270
- Fukai T, Marumo A, Kaitou K, Kanda T, Terada S, Nomura T (2002) Anti-*Helicobacter pylori* flavonoids from licorice extract. *Life Sci* 71:1449–1463
- Haraguchi H, Tanimoto K, Tamura Y, Mizutani K, Kinoshita T (1998) Mode of antibacterial action of retrochalcones from *Glycyrrhiza inflata*. *Phytochemistry* 48:125–129
- Hayashi H, Hosono N, Kondo M, Hiraoka N, Ikeshiro Y, Shibano M, Kusano G, Yamamoto H, Tanaka T, Inoue K (2000) Phylogenetic relationship of six *Glycyrrhiza* species based on rbcL sequences and chemical constituents. *Biol Pharm Bull* 23:602–606
- Le Y, Murphy PM, Wang JM (2002) Formyl-peptide receptors revisited. *Trends Immunol* 23:541–548
- Nielsen SF, Boesen T, Larsen M, Schonning K, Kromann H (2004) Antibacterial chalcones—bioisosteric replacement of the 4'-hydroxy group. *Bioorg Med Chem* 12:3047–3054
- Shibata S (2000) A drug over the millennia: pharmacognosy, chemistry, and pharmacology of licorice. *Yakugaku Zasshi* 120:849–862
- Shibata S, Inoue H, Iwata S, Ma RD, Yu LJ, Ueyama H, Takayasu J, Hasegawa T, Tokuda H, Nishino A et al (1991) Inhibitory effects of licochalcone A isolated from *Glycyrrhiza inflata* root on inflammatory ear edema and tumour promotion in mice. *Planta Med* 57:221–224
- Tsukiyama R, Katsura H, Tokuriki N, Kobayashi M (2002) Antibacterial activity of licochalcone A against spore-forming bacteria. *Antimicrob Agents Chemother* 46:1226–1230

16. Wang ZY, Nixon DW (2001) Licorice and cancer. *Nutr Cancer* 39:1–11
17. Weber T, Schoelermann A, Buerger A, Rizer R (2005) Tolerance and efficacy of a skin care regimen containing licochalcone A with erythematous rosacea and facial redness. *J Am Acad Dermatol* 52:95
18. Yang RB, Mark MR, Gurney AL, Godowski PJ (1999) Signaling events induced by lipopolysaccharide-activated toll-like receptor 2. *J Immunol* 163:639–643
19. Ziegler HL, Hansen HS, Staerk D, Christensen SB, Hagerstrand H, Jaroszewski JW (2004) The antiparasitic compound licochalcone a is a potent echinocytogenic agent that modifies the erythrocyte membrane in the concentration range where antiplasmodial activity is observed. *Antimicrob Agents Chemother* 48:4067–4071

Efficacy of Thiamidol, Niacinamide, Tranexamic Acid, Cysteamine and Azelaic Acid on melanin production *in vitro*

Mann T¹, Welge V¹, Weise J¹, Roggenkamp D², Kolbe L¹, Beiersdorf AG, Hamburg, Germany | ¹Research & Development, ²International Medical Management Eucerin

INTRODUCTION & OBJECTIVES

Hyperpigmented skin spots and areas are a major cosmetic concern. Therefore, numerous strategies have been proposed to reduce unwanted melanin production in human skin. Inhibition of Tyrosinase, reduction of melanocytic activity and decreased reduction of melanosome transfer from melanocytes to keratinocytes are among the most prominent strategies. Various active ingredients have been developed for all these strategies and are available in topical products.

However, for some well-known ingredients, the mode of action is not known in detail and data on the mechanism is lacking. Therefore, we investigated the efficacy of the active ingredients Niacinamide, Tranexamic Acid, Cysteamine, Azelaic Acid and Thiamidol on melanin production *in vitro*.

MATERIAL & METHODS

The L-Dopa oxidase activity of human Tyrosinase was assayed by measuring the reaction product L-dopa quinone trapped by MBTH at 490 nm (1). Briefly, purified human Tyrosinase in 50 mM sodium phosphate buffer, pH 7.0, at a substrate (L-DOPA) concentration of 1 mM and various concentrations of inhibitors as noted. Data represent means \pm SD of at least 3 independent experiments.

MelanoDerm skin model tissues (MEL-300-A, MatTek-Corporation, Ashland, MA) were incubated with various inhibitors for 13 days to allow for melanin production. Each compound was tested, at least, at concentrations of 5 μ M and 15 μ M. Prior to melanin analysis, the grey value of photos of the skin models was determined by image analysis. Prevention of skin model darkening in comparison to untreated control models (0%) and control models snap frozen before incubation (100%) was calculated as a measure for the overall colour change. Subsequently, the melanin was dissolved and quantified measuring the integral of absorption between 380 nm and 440 [1].

The distribution of melanin in the skin models was visualised by histology. The visualisation of melanin production was performed by cryosectioning skin models and subsequently staining the sections with Fontana-Masson stain that leaves melanin black, nuclei red and cytoplasm pink. The staining protocol was as described by the manufacturer.

RESULTS

Isobutylamido Thiazolyl Resorcinol (Thiamidol) was identified as a potent inhibitor of human Tyrosinase (IC₅₀ \sim 1 μ M) while Azelaic Acid and Cysteamine only marginally inhibited human Tyrosinase (IC₅₀ >1000 μ M, Figure 1). Niacinamide and Tranexamic Acid did not inhibit human Tyrosinase which is in line with their proposed mechanisms, inhibition of melanosome transfer and reduction of melanocyte activity, respectively.

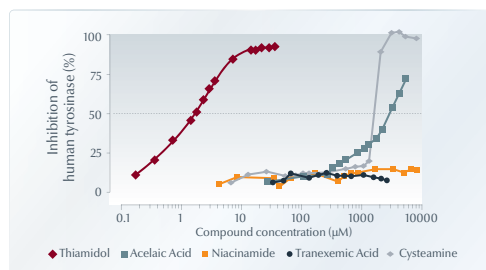


Figure 1: Inhibition of Tyrosinase activity by Thiamidol, Azelaic Acid, Niacinamide, Tranexamic Acid and Cysteamine. Thiamidol is by far the best inhibitor of human Tyrosinase with an IC₅₀ of \sim 1 μ M. Azelaic Acid and Cysteamine inhibit human Tyrosinase with a much higher IC₅₀ of around 3000 μ M and 1500 μ M, respectively. Niacinamide and Tranexamic Acid did not significantly inhibit Tyrosinase. Data of dose-response curves represent the means of at least 3 independent experiments.

The high potential of Thiamidol to inhibit melanin production was confirmed using MelanoDerm skin models (Figure 2). Unexpectedly, neither Niacinamide and Tranexamic Acid nor Cysteamine and Azelaic Acid showed any significant inhibition of melanin production at concentrations of 5 μ M and 15 μ M in the MelanoDerm assay.

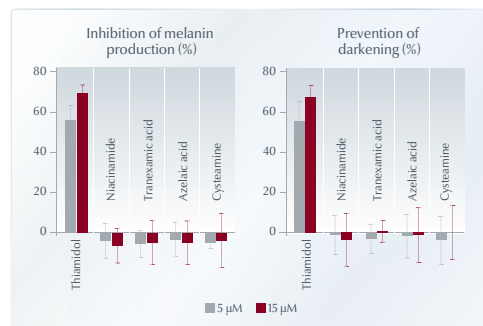


Figure 2: (A – left) Inhibition of melanin production in MelanoDerm skin models. In comparison to untreated control, Thiamidol inhibited melanin production by up to 70%. Neither at 5 μ M nor at 15 μ M, any of the other active ingredients inhibited melanin production. Data represent means \pm SD of 5 independent experiments.

(B – right) Prevention of skin model darkening. Prior to melanin analysis, the grey value of photos of the skin models was determined by image analysis. While Thiamidol dramatically prevented the darkening of the skin models, none of the other active ingredients was effective. Data represent means \pm SD of 5 independent experiments.

Niacinamide was additionally tested at a higher concentration of 50 μ M (Figure 3). Here, a slight inhibition of skin model darkening (10%) was observed but no Tyrosinase inhibition. This is in line with the proposed mode of action, inhibition of melanosome transfer from melanocytes to keratinocytes. However, much higher concentrations than 50 μ M would be needed to achieve significant efficacy.

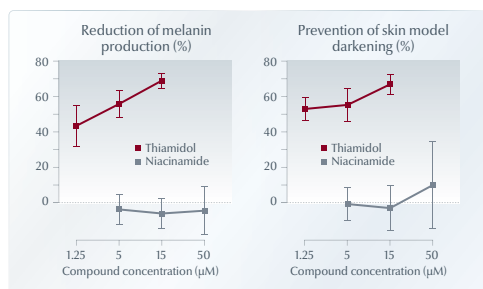


Figure 3: Melanin content and distribution in MelanoDerm skin models by Thiamidol and Niacinamide. Left: Inhibition of melanin production. Thiamidol shows dose-dependent inhibition of melanin production, reaching 70% inhibition in comparison to untreated control at 15 μ M. Niacinamide does not inhibit melanin production up to 50 μ M. Right: Prevention of skin model darkening. Colour measurements (grey value) in skin models showed more than 50% prevention of skin model darkening by Thiamidol already at 1.25 μ M. Niacinamide is not effective up to 15 μ M but shows a slight activity at 50 μ M.

HISTOLOGICAL EVALUATION OF MELANIN CONTENT AND DISTRIBUTION IN SKIN MODELS

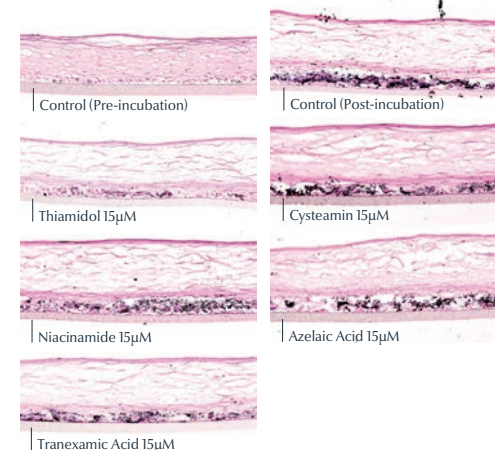


Figure 4: Melanin content and distribution in MelanoDerm skin models evaluated by Fontana-Masson stain. Control models show a significant increase in melanin content during the 2 weeks of incubation. While Thiamidol, clearly reduces melanin formation in skin models, none of the other compounds had any effect. Changes in melanin distribution were not observed.

Histological evaluation of MelanoDerm skin models treated with the ingredients confirmed that only Thiamidol significantly reduced melanin content (Figure 4).

CONCLUSION

Isobutylamido Thiazolyl Resorcinol showed a highly effective inhibition of human Tyrosinase enzyme activity and melanin production in skin models. Surprisingly, Niacinamide, Tranexamic Acid, Cysteamine, and Azelaic Acid did not show any efficacy on melanin production *in vitro*. This might point towards a more indirect *in vivo* mechanism of these substances via mediators of dermal cells like fibroblasts or endothelial cells etc., while Thiamidol directly inhibits the production of excessive melanin in melanocytes.

References: [1] Inhibition of Human Tyrosinase Requires Molecular Motifs Distinctively Different from Mushroom Tyrosinase. Mann T, Gerwat W, Batzer J, Eggers K, Schermer C, Wenck H, Stäb F, Hearing VJ, Röhme KH, Kolbe L. J Invest Dermatol. 2018 Jul;138(7):1601-1608.

Efficacy of skin care formulations with Thiamidol in reducing facial hyperpigmentation

Roggenkamp D¹, Riedel J², Muhr G-M², Warnke K², Kolbe L², Filbry A²

¹International Medical Management, Beiersdorf AG, Hamburg, Germany | ²Research & Development, Beiersdorf AG, Hamburg, Germany

INTRODUCTION

Hyperpigmentary disorders such as melasma, senile lentiginos and post-inflammatory hyperpigmentation are major cosmetic problems and can negatively impact quality of life of patients. Individuals with darker skin complexions tend to be affected with greater frequency and severity. Classical influencing factors are genetic dispositions, female sex hormones and sun exposure. There are numerous topical products on the market containing diverse active ingredients claiming to reduce melanin production and distribution. Many substances have been described in literature, however, most of them lack clinical efficacy and only a few of them are currently used in topical dermatological products [1].

In the present study, we investigated the clinical efficacy of two skin care formulations containing the new active ingredient Isobutylamido thiazolyl resorcinol (Thiamidol) in patients with facial hyperpigmentation [2].

MATERIALS AND METHODS

To evaluate the efficacy of the two skin care formulations with Thiamidol, a single-center, double-blind, randomized, controlled, split-face design clinical trial was conducted. 34 women (25-65 years of age, Fitzpatrick skin type I-IV) with mild to moderate hyperpigmentation on both sides of the face were enrolled. Subjects were assigned to treat the

left or the right side of the face with a serum containing Thiamidol. Additionally, subjects applied a day care with SPF 30 containing Thiamidol on the global face following serum treatment. Over the course of 12 weeks, subjects applied the products twice per day. Clinical evaluations were conducted at visit 1 (baseline), visit 2 (week 2), visit 3 (week 4), visit 4 (week 8) and visit 5 (week 12) and included clinical grading of efficacy parameters, subjective assessment (both assessments with 10-point modified Griffith's scales), chromameter (Chroma Meter CR-400) measurements and clinical photography (VISIA CR Photostation with a Canon Mark digital SLR camera).

RESULTS

Clinical photography demonstrated that the two skin care formulations with Thiamidol visibly reduced facial hyperpigmentation over the course of 12 weeks. The facial hyperpigmentation was lightened over the course of the study shown objectively via chromameter measurements.

Clinical grading of the efficacy parameters hyperpigmentation, smoothness and radiance, as well as self-grading of hyperpigmentation demonstrated an improvement over time and showed that application of the serum significantly enhanced the effect of the day care SPF30.

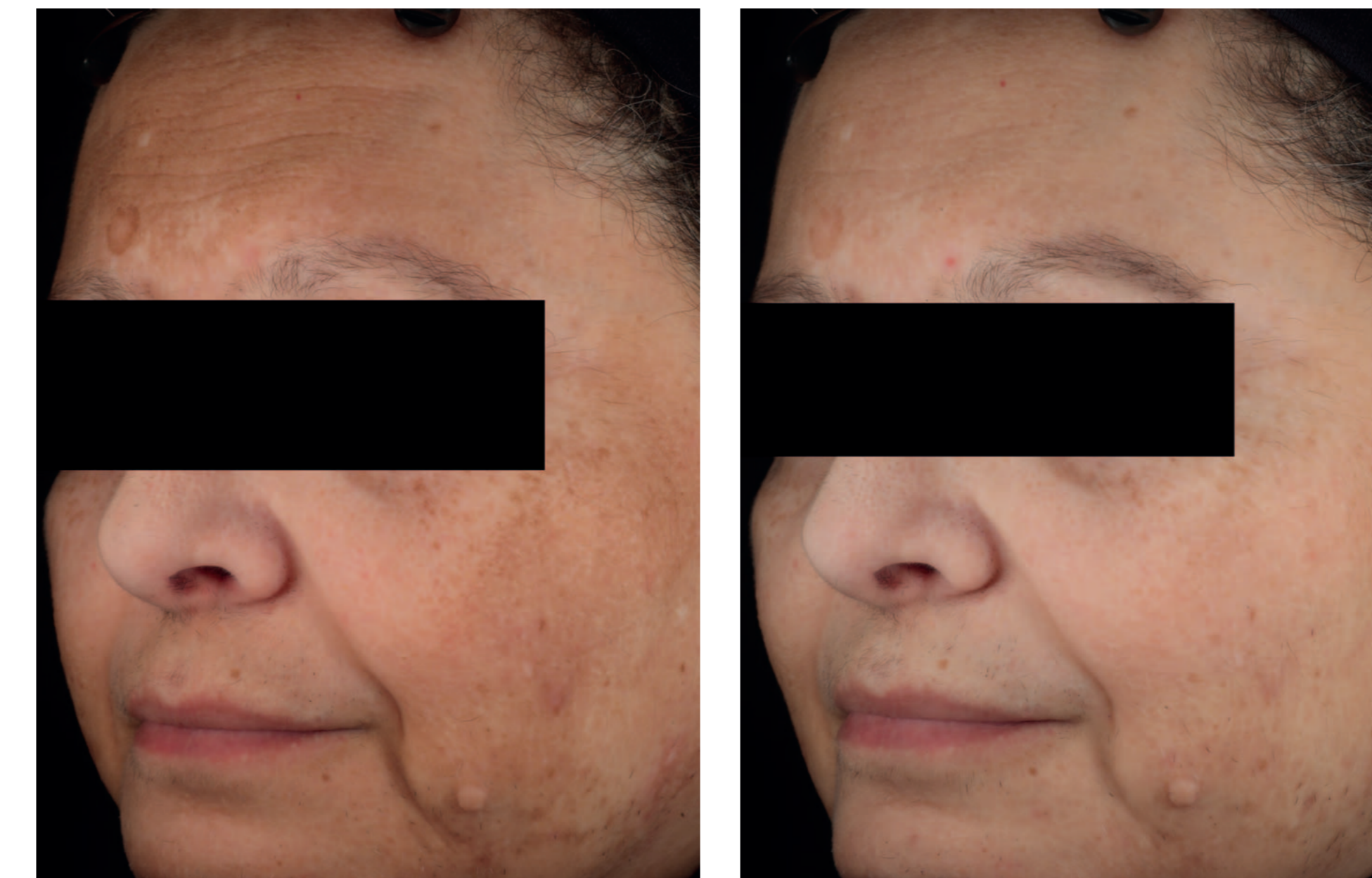


Figure 1: Clinical photography of a subject's side of the face treated with the combination of serum and day care SPF30, both containing Thiamidol, for 12 weeks.

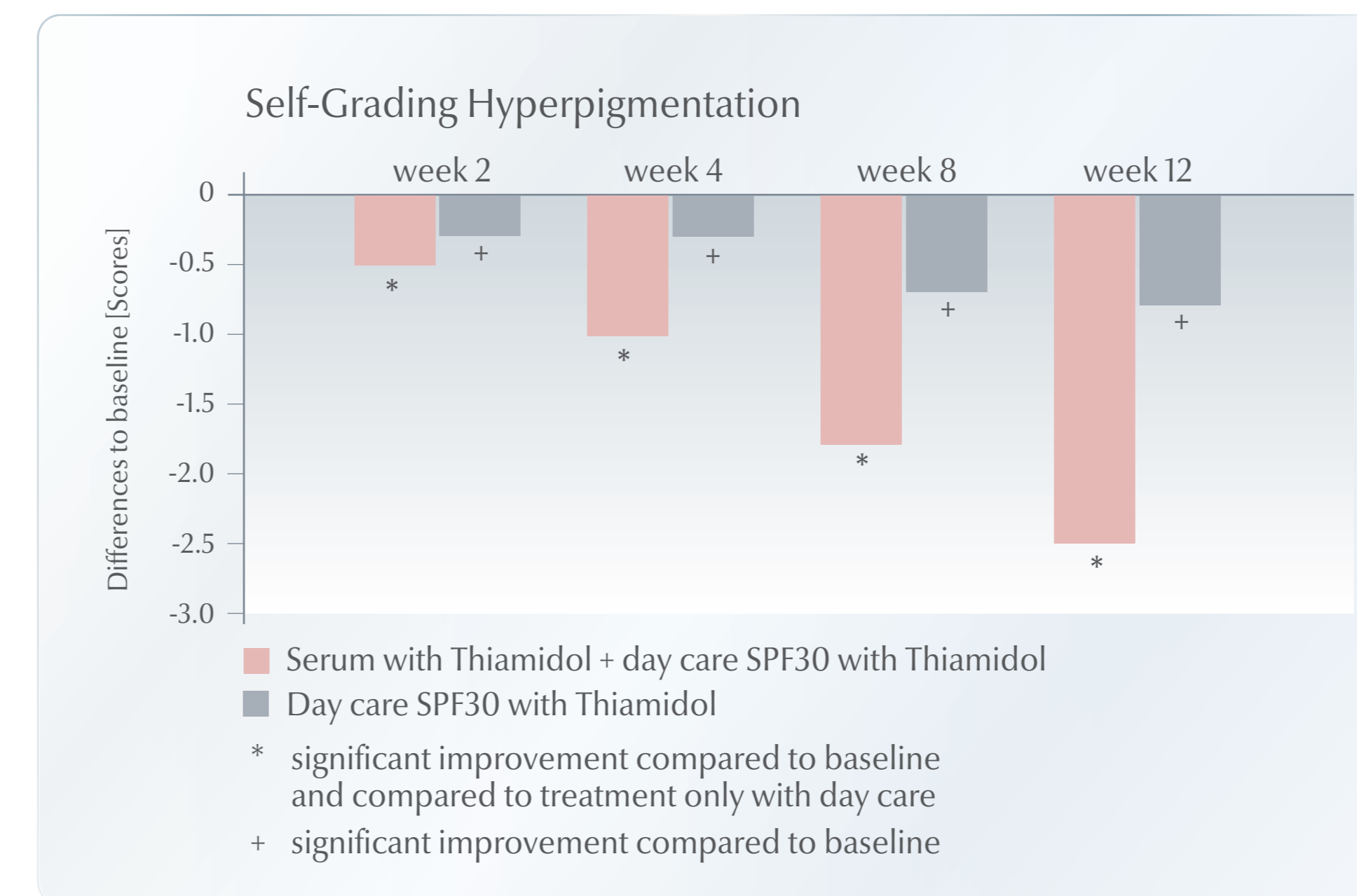


Figure 3: Self-grading of hyperpigmentation. Split-face application of either day care or combination of day care and serum (all containing Thiamidol) for 12 weeks.

CONCLUSION

The clinical study presented here demonstrates not only that the two skin care formulations with the new active ingredient Thiamidol are highly effective in the treatment of facial hyperpigmentation, but also that the combination of both products is even more effective.

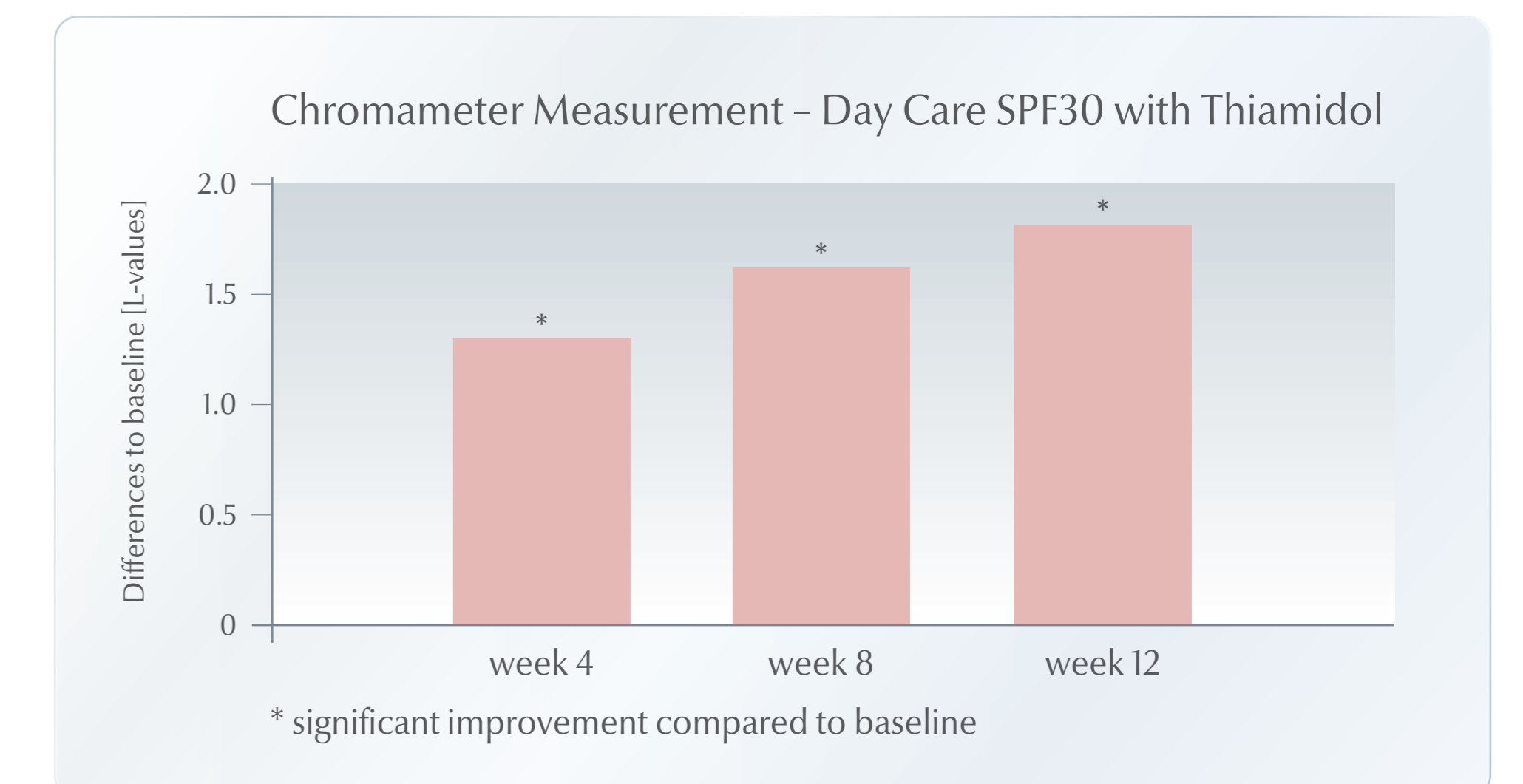


Figure 2: Chromameter measurements on subjects' side of the face treated with day care SPF30 with Thiamidol for 12 weeks.

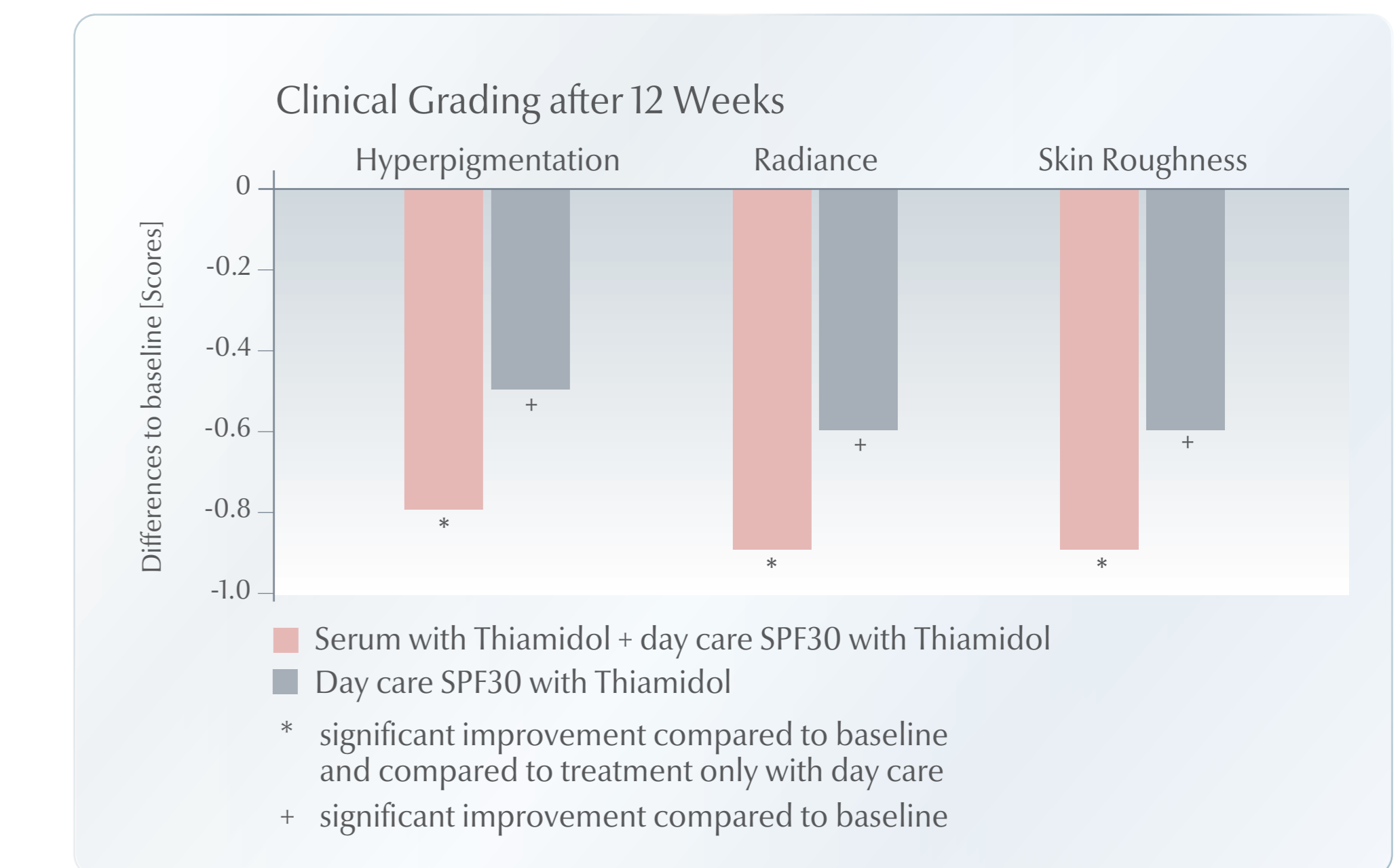


Figure 4: Clinical grading of efficacy parameters by investigator. Split-face application of either day care or combination of day care and serum (all containing Thiamidol) for 12 weeks.

References

- [1] Chang TS. An updated review of tyrosinase inhibitors. *Int J Mol Sci* 2009; 10:2440-75
- [2] Mann et al., Inhibition of human tyrosinase requires molecular motifs distinctively different from mushroom tyrosinase. *J Invest Dermatol.* (2018) 138: 1601-1608

Efficacy of skin care formulations with Thiamidol in reducing facial hyperpigmentation

Roggenkamp D¹, Riedel J², Muhr G-M², Warnke K², Kolbe L², Filbry A²

¹International Medical Management, Beiersdorf AG, Hamburg, Germany | ²Research & Development, Beiersdorf AG, Hamburg, Germany

INTRODUCTION

Hyperpigmentary disorders such as melasma, senile lentiginos and post-inflammatory hyperpigmentation are major cosmetic problems and can negatively impact quality of life of patients. Individuals with darker skin complexions tend to be affected with greater frequency and severity. Classical influencing factors are genetic dispositions, female sex hormones and sun exposure. There are numerous topical products on the market containing diverse active ingredients claiming to reduce melanin production and distribution. Many substances have been described in literature, however, most of them lack clinical efficacy and only a few of them are currently used in topical dermatological products [1].

In the present study, we investigated the clinical efficacy of two skin care formulations containing the new active ingredient Isobutylamido thiazolyl resorcinol (Thiamidol) in patients with facial hyperpigmentation [2].

MATERIALS AND METHODS

To evaluate the efficacy of the two skin care formulations with Thiamidol, a single-center, double-blind, randomized, controlled, split-face design clinical trial was conducted. 34 women (25-65 years of age, Fitzpatrick skin type I-IV) with mild to moderate hyperpigmentation on both sides of the face were enrolled. Subjects were assigned to treat the

left or the right side of the face with a serum containing Thiamidol. Additionally, subjects applied a day care with SPF 30 containing Thiamidol on the global face following serum treatment. Over the course of 12 weeks, subjects applied the products twice per day. Clinical evaluations were conducted at visit 1 (baseline), visit 2 (week 2), visit 3 (week 4), visit 4 (week 8) and visit 5 (week 12) and included clinical grading of efficacy parameters, subjective assessment (both assessments with 10-point modified Griffith's scales), chromameter (Chroma Meter CR-400) measurements and clinical photography (VISIA CR Photostation with a Canon Mark digital SLR camera).

RESULTS

Clinical photography demonstrated that the two skin care formulations with Thiamidol visibly reduced facial hyperpigmentation over the course of 12 weeks. The facial hyperpigmentation was lightened over the course of the study shown objectively via chromameter measurements.

Clinical grading of the efficacy parameters hyperpigmentation, smoothness and radiance, as well as self-grading of hyperpigmentation demonstrated an improvement over time and showed that application of the serum significantly enhanced the effect of the day care SPF30.

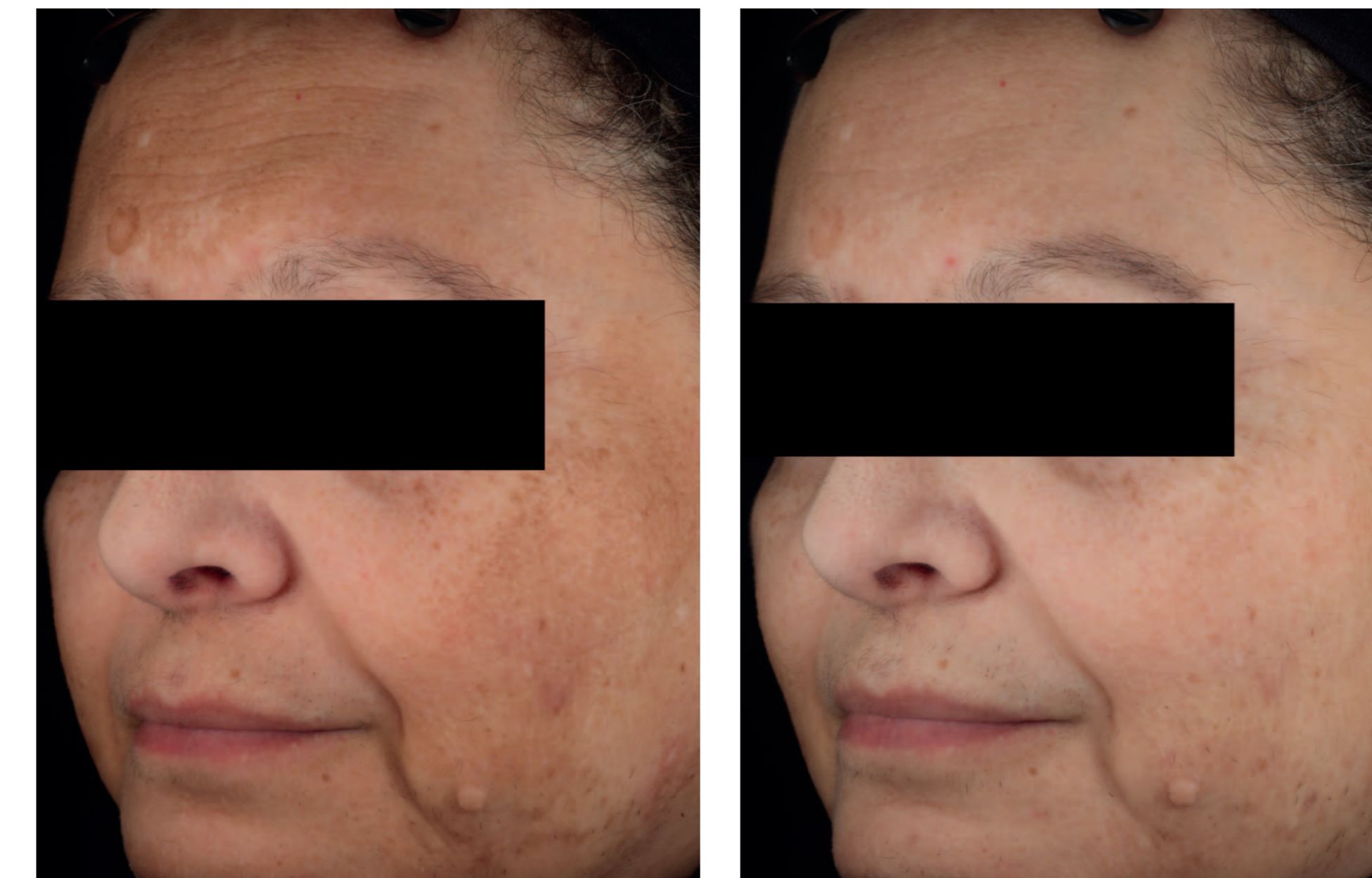


Figure 1: Clinical photography of a subject's side of the face treated with the combination of serum and day care SPF30, both containing Thiamidol, for 12 weeks.

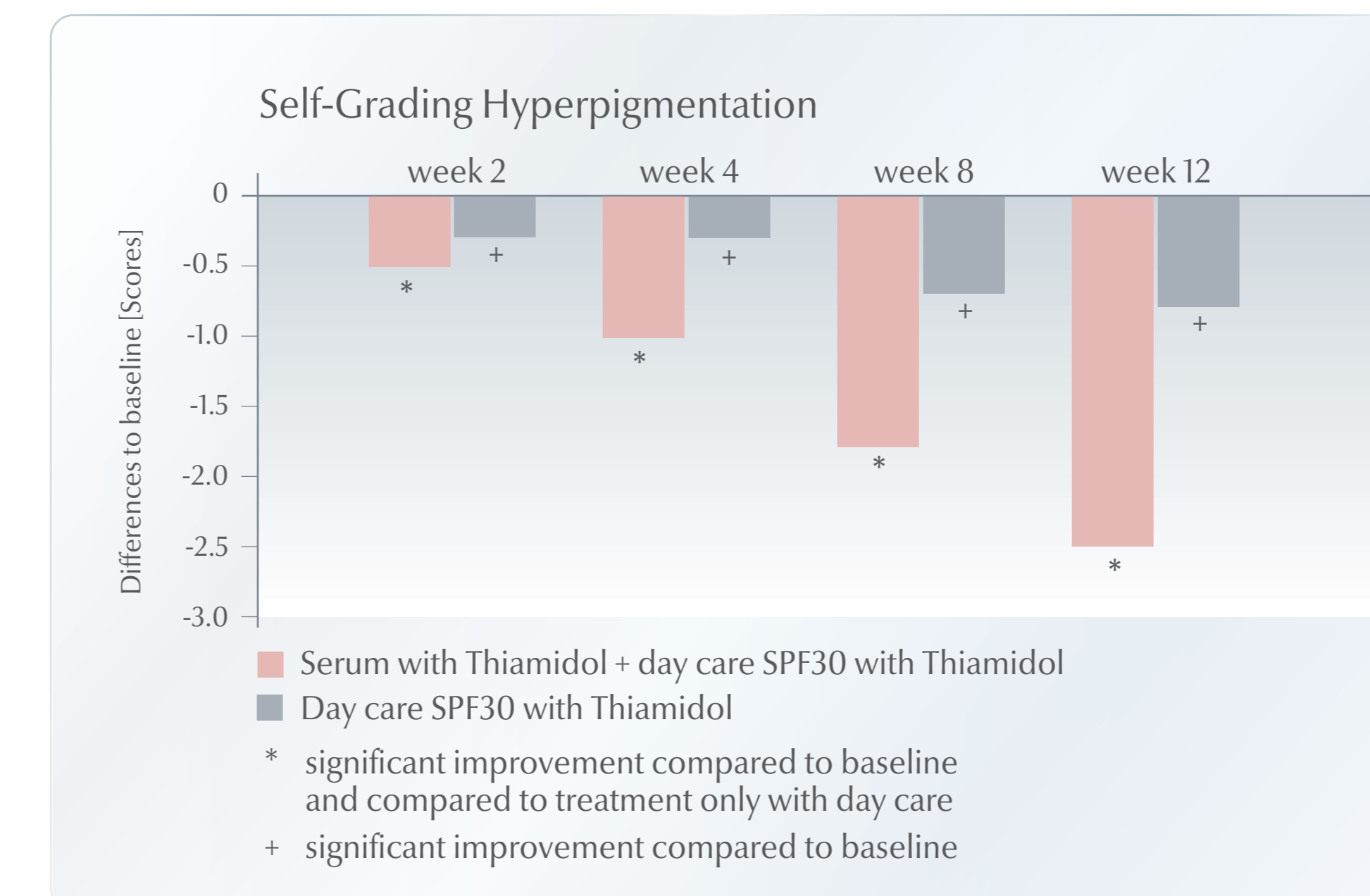


Figure 3: Self-grading of hyperpigmentation. Split-face application of either day care or combination of day care and serum (all containing Thiamidol) for 12 weeks.

CONCLUSION

The clinical study presented here demonstrates not only that the two skin care formulations with the new active ingredient Thiamidol are highly effective in the treatment of facial hyperpigmentation, but also that the combination of both products is even more effective.

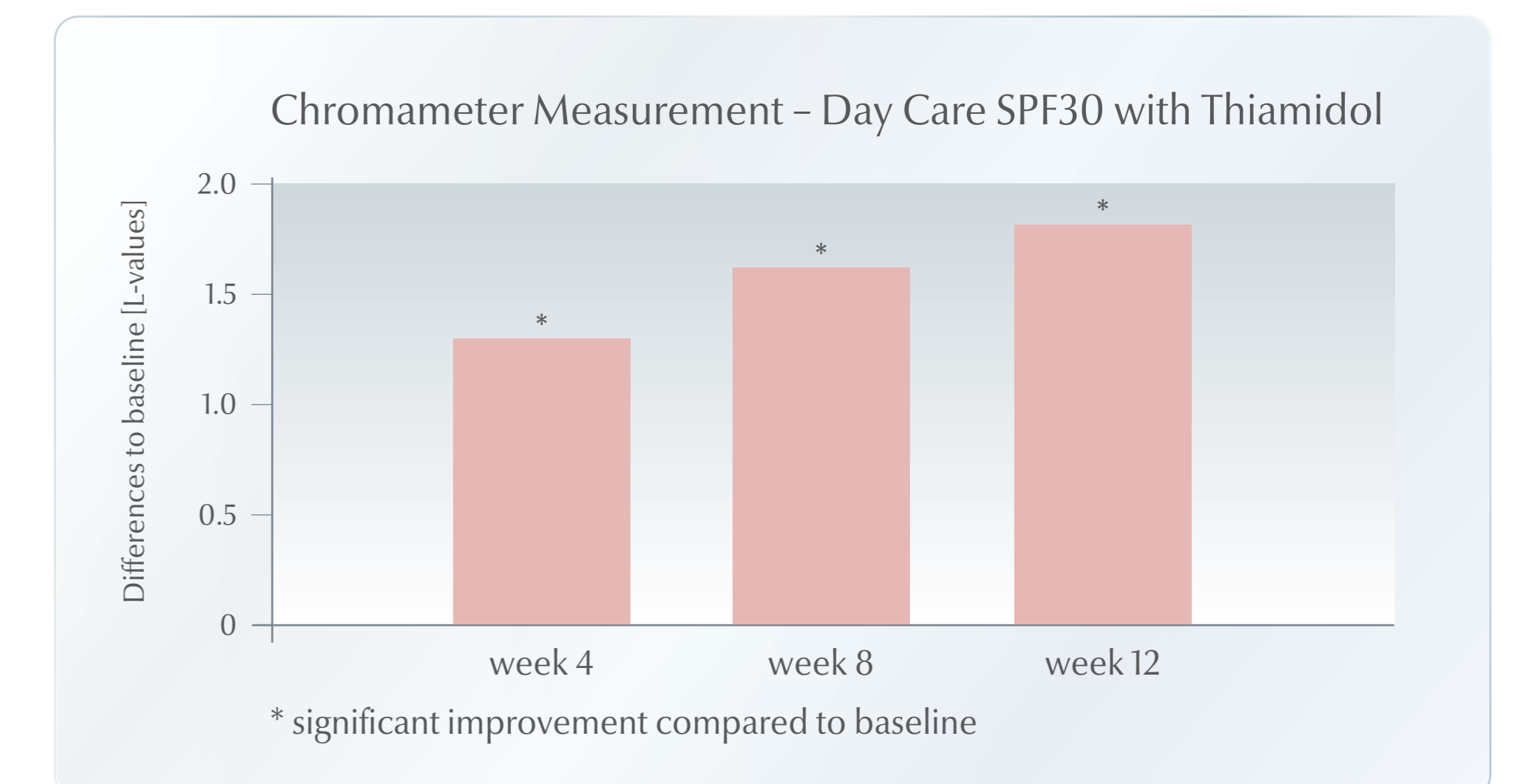


Figure 2: Chromameter measurements on subjects' side of the face treated with day care SPF30 with Thiamidol for 12 weeks.

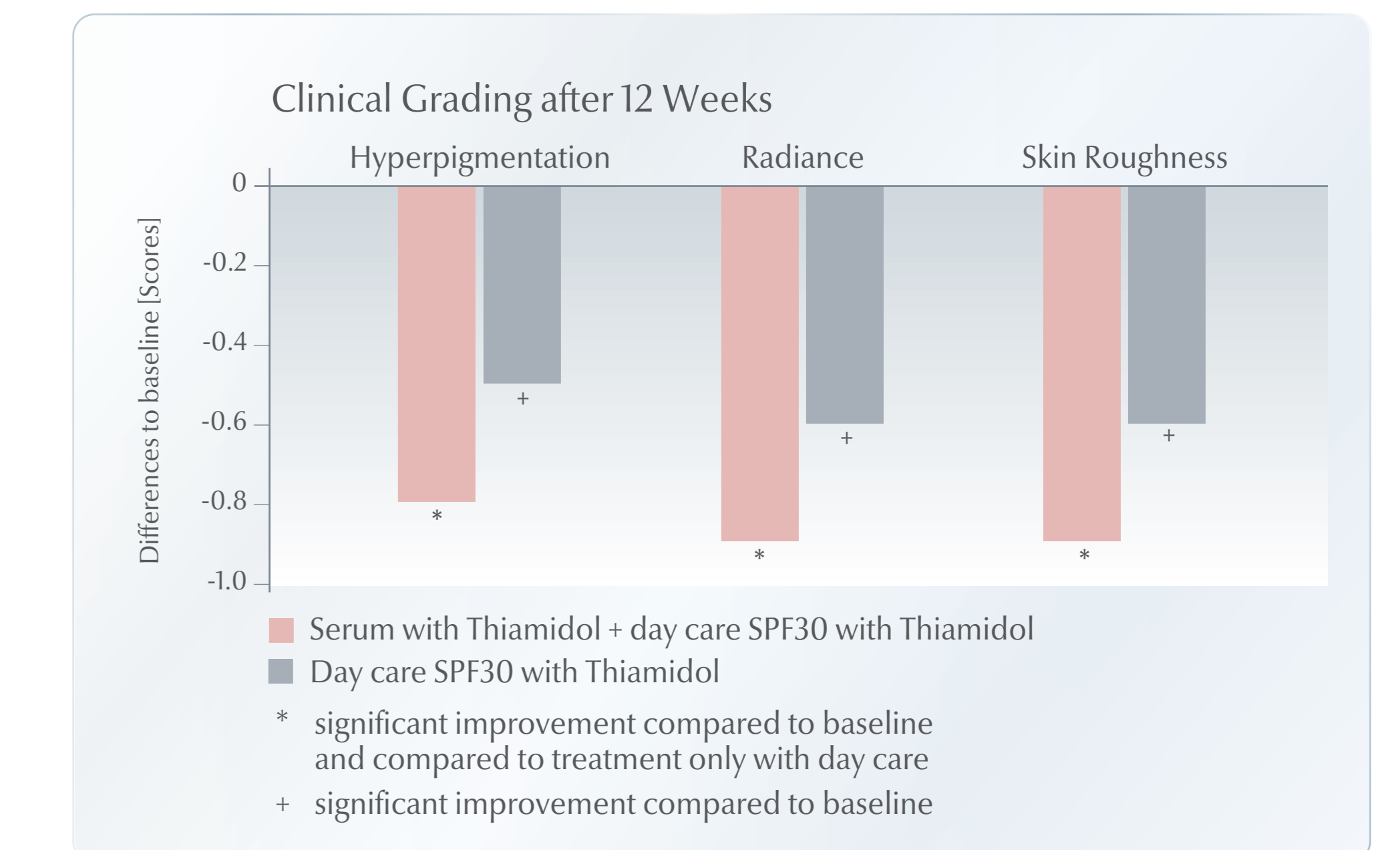


Figure 4: Clinical grading of efficacy parameters by investigator. Split-face application of either day care or combination of day care and serum (all containing Thiamidol) for 12 weeks.

References

- [1] Chang TS. An updated review of tyrosinase inhibitors. *Int J Mol Sci* 2009; 10:2440-75
- [2] Mann et al., Inhibition of human tyrosinase requires molecular motifs distinctively different from mushroom tyrosinase. *J Invest Dermatol.* (2018) 138: 1601-1608

Endothelial Cells Promote Pigmentation through Endothelin Receptor B Activation

Claire Regazzetti¹, Gian Marco De Donatis¹, Houda Hammami Ghorbel², Nathalie Cardot-Leccia³, Damien Ambrosetti³, Philippe Bahadoran^{2,4}, Bérengère Chignon-Sicard⁵, Jean-Philippe Lacour², Robert Ballotti¹, Andre Mahns⁶ and Thierry Passeron^{1,2}

Findings of increased vascularization in melasma lesions and hyperpigmentation in acquired bilateral telangiectatic macules suggested a link between pigmentation and vascularization. Using high-magnification digital epiluminescence dermatoscopy, laser confocal microscopy, and histological examination, we showed that benign vascular lesions of the skin have restricted but significant hyperpigmentation compared with the surrounding skin. We then studied the role of microvascular endothelial cells in regulating skin pigmentation using an *in vitro* co-culture model using endothelial cells and melanocytes. These experiments showed that endothelin 1 released by microvascular endothelial cells induces increased melanogenesis signaling, characterized by microphthalmia-associated transcription factor phosphorylation, and increased tyrosinase and dopachrome tautomerase levels. Immunostaining for endothelin 1 in vascular lesions confirmed the increased expression on the basal layer of the epidermis above small vessels compared with perilesional skin. Endothelin acts through the activation of endothelin receptor B and the mitogen-activated protein kinase, extracellular signal-regulated kinase (ERK)1/2, and p38, to induce melanogenesis. Finally, culturing of reconstructed skin with microvascular endothelial cells led to increased skin pigmentation that could be prevented by inhibiting EDNRB. Taken together these results demonstrated the role of underlying microvascularization in skin pigmentation, a finding that could open new fields of research for regulating physiological pigmentation and for treating pigmentation disorders such as melasma.

Journal of Investigative Dermatology (2015) **135**, 3096–3104; doi:10.1038/jid.2015.332; published online 24 September 2015

INTRODUCTION

Pigmentation is a complex and a tightly regulated process. Microphthalmia-associated transcription factor (MITF) is the master gene of pigmentation and controls several key mechanisms in melanocytes such as melanogenesis, dendricity, and proliferation in response to environmental factors including UV radiation and to molecules produced by other cells in the skin. Activation of MITF induces expression of the key enzymes of melanogenesis, which are tyrosinase,

dopachrome tautomerase (DCT), and tyrosinase-related protein 1, leading to the production of melanin. Numerous factors additionally provide the finer regulation of melanin pigment production and/or melanocyte growth and differentiation. Alpha-melanocyte-stimulating hormone and ACTH are the most potent activators of melanogenesis, whereas nitric oxide (NO) and some growth factors present in the circulation or secreted by keratinocytes act to varying degrees on melanogenesis and melanocyte growth, including basic fibroblast growth factor, KIT ligand, hepatocyte growth factor, endothelin 1 (Edn1), and some prostaglandins (Hirobe, 2005; Plonka *et al.*, 2009). Fibroblasts also have a key role in melanocytogenesis and melanogenesis. Palmoplantar fibroblasts express high levels of Dickkopf 1, which reduces melanocyte proliferation and differentiation by acting on MITF, explaining (at least partially) the lower pigmentation generally observed on human palms and soles (Yamaguchi *et al.*, 2007 and 2008). Fibroblasts also produce melanogenesis-associated factors that differ according to the skin type of the individual. One of these factors, known as neuregulin-1, is secreted by fibroblasts in black skin (skin type VI) and significantly increases the pigmentation of human melanocytes in culture (Choi *et al.*, 2010). Interestingly, fibroblasts also seem to be involved in melasma pathophysiology via their secretion of Wnt inhibitor factor-1 (Kang *et al.*, 2011; Kim *et al.*, 2013; Park *et al.*, 2014b).

¹C3M, INSERM U1065, team 12, Nice, France; ²Department of Dermatology, University Hospital Center of Nice, Nice, France; ³Department of Pathology, University Hospital Center of Nice, Nice, France; ⁴Centre de Recherche Clinique (CRC), University Hospital of Nice, Nice, France; ⁵Department of Plastic Surgery, University Hospital Center of Nice, Nice, France and ⁶Beiersdorf AG, Front End Innovation, Hamburg, Germany

Correspondence: Thierry Passeron, Department of Dermatology, Hôpital Archet 2, University Hospital Center of Nice, 151, Route de St Antoine de Ginestière, 06200 Nice, France. E-mail: passeron@unice.fr

Abbreviations: DCT, dopachrome tautomerase; Edn1, endothelin 1; ERK, extracellular signal-regulated kinase; HMVEC, human dermal microvascular endothelial cell; MITF, microphthalmia-associated transcription factor; NHK, normal human keratinocyte; NHM, normal human melanocyte; NO, nitric oxide

Received 23 December 2014; revised 22 June 2015; accepted 29 June 2015; accepted article preview online 26 August 2015; published online 24 September 2015

In addition to keratinocytes and fibroblasts, growing evidence also implicates endothelial cells in pigmentation (Plonka *et al.*, 2009). Indeed, melanocytes express receptors that can potentially be regulated by several factors secreted by endothelial cells such as vascular endothelial growth factor (VEGF), Edn1, NO, and leukotrienes (Kim *et al.*, 2005; Yamaguchi and Hearing, 2009). In addition, histological studies have clearly shown a significant increase in vascularization within melasma lesions compared with that in the surrounding healthy skin (Kim *et al.*, 2007). These results were subsequently confirmed by laser confocal microscopy examination (Kang *et al.*, 2010), although the significance of this increased vascularization in melasma remains poorly understood. However, a recent clinical report cited cases presenting with acquired telangiectatic and hyperpigmented macules (Park *et al.*, 2014a), for which the clinical and histological findings of skin hyperpigmentation localized above telangiectasias suggested a close relationship between melanocytes and endothelial cells.

In the current study, we therefore examined the role of dermal microvascular endothelial cells in regulating skin pigmentation.

RESULTS

Vascularization influences skin pigmentation *in vivo*

A total of 100 benign vascular skin lesions were assessed, comprising cherry angiomas, botriomycomas, spider angiomas, involutive infantile hemangiomas, capillaro-venous malformation, acquired bilateral telangiectatic macules, and leg telangiectasias. Using high-magnification digital dermatoscopy, we observed a mild to marked hyperpigmentation within and surrounding the vascular lesions compared with the surrounding skin in 89% of cases (Figure 1; Supplementary table 1 online). The hyperpigmentation was marked in 22% of cases. The association between the vascular lesions and the hyperpigmentation of the overlying skin was significantly more frequent in dark skin types (III to V) compared with light ones (I and II; $P=0.021$) and in photoexposed areas compared with those located in photoprotected areas ($P<0.001$) (Supplementary Tables 1 and 2 online). No correlation was found between the size of vascular lesions and the overlying pigmentation (Supplementary Table 3 online). Analysis of the vascular lesions using laser confocal microscopy confirmed the increased pigmentation of the skin above the vascular proliferation compared with the surrounding skin (Supplementary Figure 1 online). We next analyzed tissue samples of benign vascular lesions of the skin, available in our biobank. Ten samples from cherry angiomas, botriomycomas, capillaro-venous malformation, and acquired bilateral telangiectasia were stained with hematoxylin eosin and Fontana–Masson staining to assess the vascularization and pigmentation, respectively. MITF staining was also performed to identify the melanocytes. For each sample, histological sections were analyzed in the center of the lesion and in the borders on the immediately surrounding, non-affected skin. The lesion sections showed an increased melanin content in the epidermis compared with the surrounding skin. However, there was no significant increase in melanocyte number with a mean ratio of

melanocytes/keratinocytes of 0.128 and 0.122 in lesional and perilesional areas, respectively ($P=0.41$; Figure 2).

Microvascular endothelial cells increase the melanogenesis pathway in melanocytes

To further investigate the role of vascularization in skin pigmentation, we studied the effects of human dermal microvascular endothelial cells (HMVECs) on the melanogenesis pathway in normal human melanocytes (NHMs). In co-culture experiments with HMVECs and NHMs, we observed upregulation of the phosphorylated form of MITF in melanocytes after 30 minutes of co-culture (Figure 3a). After 3 days of co-culture, the expression level of tyrosinase and DCT was increased by approximately twofold (Figure 3b). This effect was also specific to the endothelial cells, because co-culturing of the NHMs with normal human keratinocytes (NHKs) under the same conditions produced no such effect (Supplementary Figure 2 online). We then investigated the potential role of endothelial cells in melanocyte proliferation. After plating the same number of NHMs for 7 days in a co-culture with HMVECs or alone, the melanocytes were counted. After 7 days of co-culture, the HMVECs induced a slight but a significant increase in melanocytes number (Figure 3c). Taken together, these results showed that the microvascular endothelial cells could promote melanogenesis and, to a lesser extent, enhance melanocyte proliferation.

Endothelin released by HMVECs upregulates melanogenesis signaling in NHMs

To understand how endothelial cells upregulate the melanogenesis pathway in melanocytes, we next investigated the factors released by endothelia by incubating NHMs with HMVEC-conditioned medium for 30 minutes and 3 days under the co-culture experiment conditions. The NHM starvation medium conditioned in the presence of endothelial cells (CM. HMVEC) induced similar phosphorylation of MITF after 30 minutes to that observed in the co-culture experiment with HMVECs (Figure 4a) and similarly increased tyrosinase and DCT expression after 3 days (Figure 4b). Many factors are produced and secreted by endothelial cells, but herein we focused on molecules that could potentially act on melanogenesis and melanocyte proliferation such as NO, VEGF, endothelin, and leukotriene. In our co-culture experiments, inhibition of NO with L-N^G-Nitroarginine methyl ester and 2-Phenyl-4,4,5,5-tetramethylimidazole-1-oxyl 3-oxide (PTIO; Supplementary Figure 3a online), VEGF receptor with VEGF receptor inhibitor IV and CBO-P11 (Supplementary Figure 3b online), and leukotriene with baicalein (Supplementary Figure 3c online) did not impair the phosphorylation of MITF. In contrast, inhibition of endothelin receptor with PD142893 inhibited the phosphorylation of MITF under our co-culture conditions (Figure 4c). Furthermore, we observed the same effects, with the same kinetics, on the phosphorylation of MITF and the levels of DCT and tyrosinase in melanocytes stimulated with Edn1 (Supplementary Figure 4 online). Analyses of Edn1 secretion also showed that the HMVECs cultured in NHM starvation medium secreted fourfold more Edn1 than NHK, and no secretion was detected

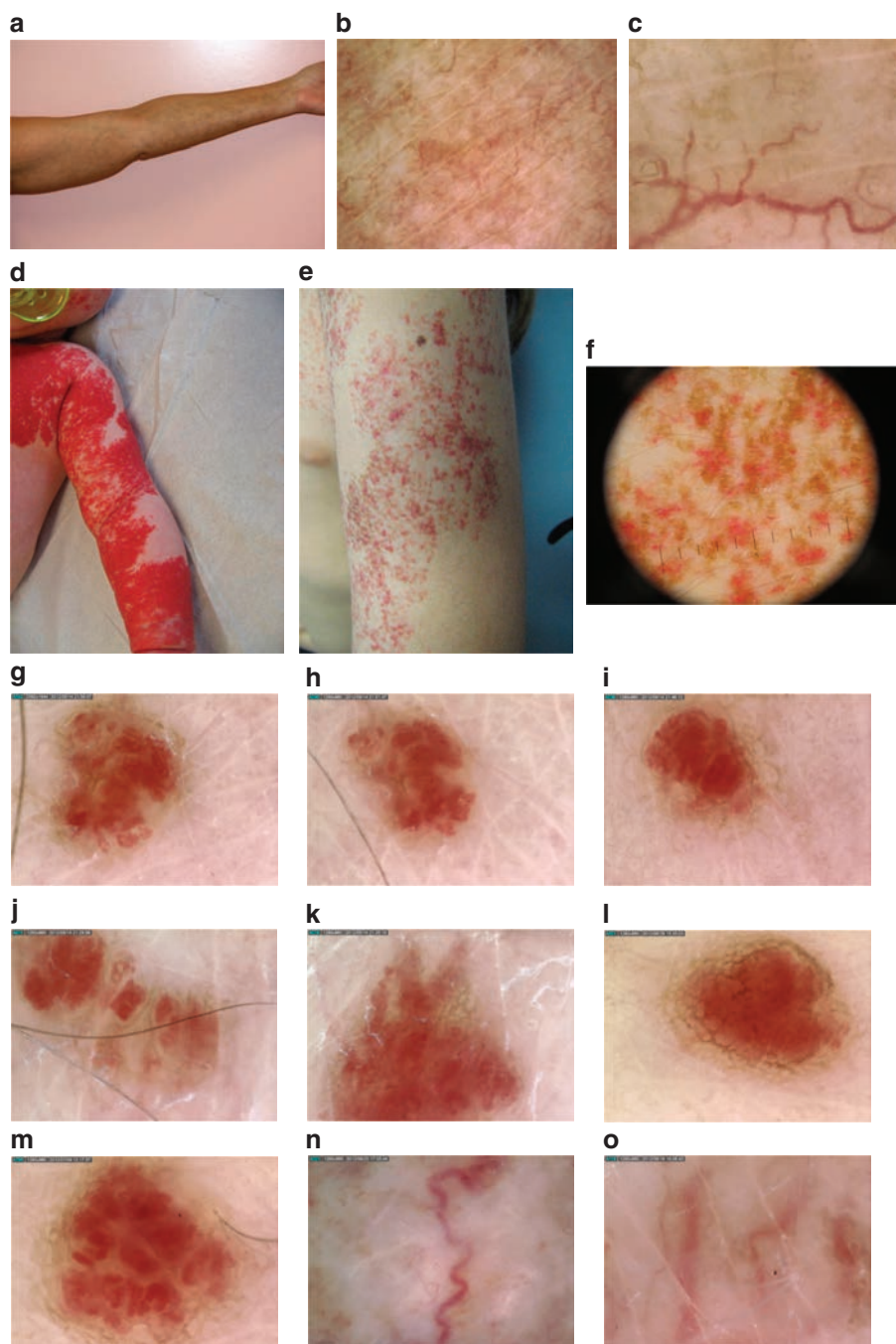


Figure 1. Clinical and epiluminescence dermatoscopy pattern of hyperpigmentation associated with vascularization. (a) Acquired bilateral telangiectatic macules. (b) Digital epiluminescence dermatoscopy of the lesions (x50). (c) Digital epiluminescence dermatoscopy of the lesions (x200). (d) Superficial congenital hemangioma in an infant of 2 months of age. (e) Clinical presentation at the age of 5 years with regression of the vascular component and hyperpigmentation localized only on the area of the hemangioma. (f) Digital epiluminescence dermatoscopy of the lesions (x10). Digital epiluminescence dermatoscopy (x200) of cherry angiomas (g–m) and leg telangiectasias (n and o).

for NHM (Figure 4d). Finally, to correlate these results *in vivo*, we assessed the expression of Edn1 in skin samples of vascular lesions compared with the perilesional skin and found increased Edn1 at the basal layers of the epidermis above vascular lesions (Figure 4e and h).

HMVECs induce melanogenesis via the activation of endothelin receptor B and the MAPK pathway via ERK1/2 and p38 in melanocytes

There are two subtypes of the endothelin receptor: EDNRA and EDNRB. In order to identify the receptor involved in this

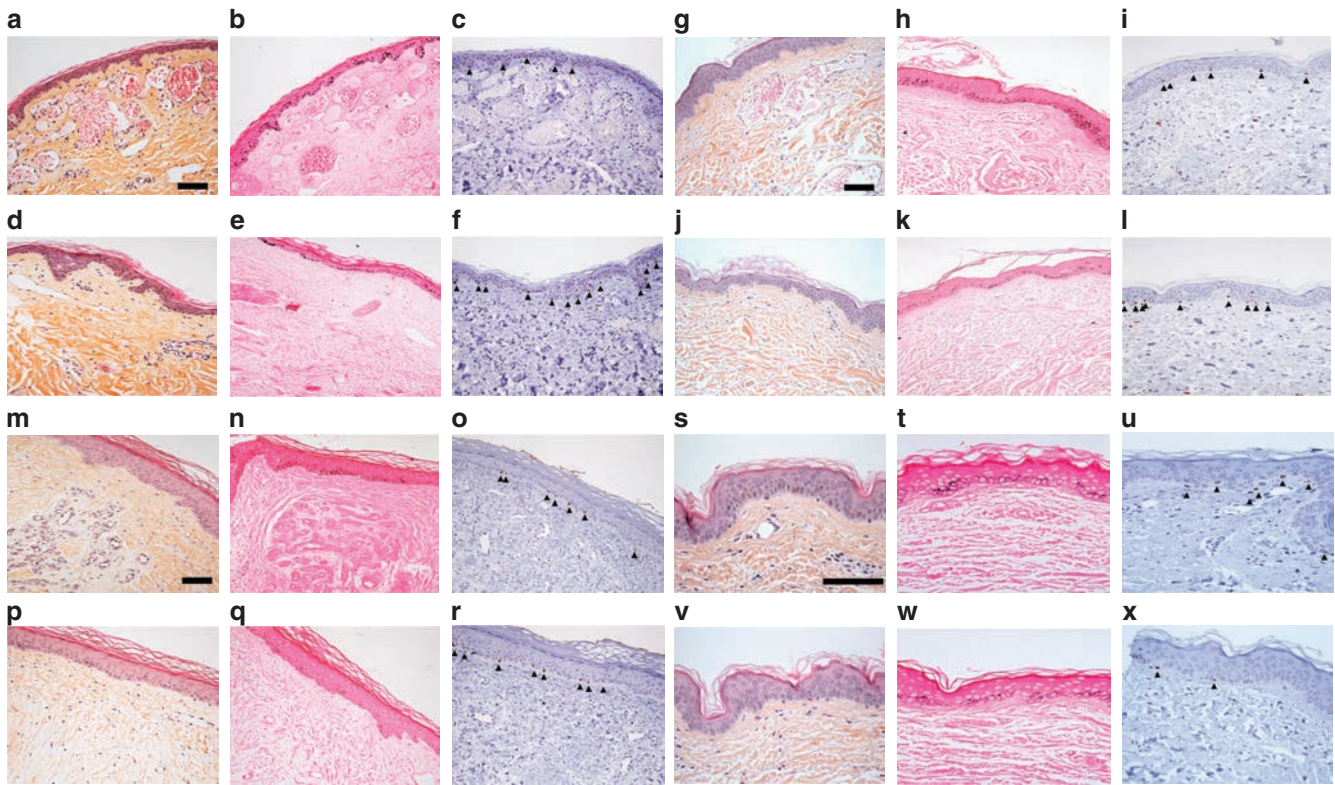


Figure 2. Histological analysis of vascular lesions. Cherry angioma with hematoxylin and eosin (HE) (a), Fontana–Masson (b) and microphthalmia-associated transcription factor (MITF) (c) staining. Perilesional normal skin of the same cherry angioma with HE (d), Fontana–Masson, (e) and MITF (f) staining. Capillary venous malformation with HE (g), Fontana–Masson, (h) and MITF (i) staining. Perilesional normal skin of the same capillary venous malformation with HE (j), Fontana–Masson, (k) and MITF (l) staining. Botriomycoma with HE (m), Fontana–Masson, (n) and MITF (o) staining. Perilesional normal skin of the same botriomycoma with HE (p), Fontana–Masson, (q) and MITF (r) staining. Acquired bilateral telangiectatic macules with HE (s), Fontana–Masson, (t) and MITF (u) stainings. Perilesional normal skin of the same lesion with HES (v), Fontana–Masson, (w) and MITF (x) staining. All the pictures were taken with $\times 200$ magnification. Arrows designate MITF-positive cells. Scale bar = 50 μm .

process, we used specific inhibitors of EDNRA (BQ123) and EDNRB (BQ788). The inhibition of EDNRA showed no effect on MITF phosphorylation induced by endothelial cells, whereas the inhibition of EDNRB inhibited the effects of HMVECs on NHMs (Figure 5a). To determine whether Edn1 directly stimulates the melanocytes, we repeated the experiment using conditioned medium of HMVECs with or without BQ788. Treatment with BQ788 inhibited the phosphorylation of MITF induced by HMVEC-conditioned medium as observed for NHMs and HMVECs co-cultured in the presence of BQ788, showing that Edn1 released by HMVECs directly stimulates NHM (Figure 5b). The effect of EDNRB in this mechanism was further confirmed using siRNA knockdown of EDNRA and EDNRB expression. Specifically, decreasing EDNRB expression in NHMs inhibited the phosphorylation of MITF, but also the upregulation of tyrosinase induced by HMVECs, whereas silencing EDNRA had no effect on these processes (Figure 5c and d, Supplementary Figure 5 online).

In melanocytes, the stimulation of EDNRB activates protein kinase C, which, in turn, stimulates extracellular signal-regulated kinase (ERK)1/2 and p38, mitogen-activated protein kinases that are implicated in the phosphorylation of MITF and the upregulation of tyrosinase, respectively. We therefore

also investigated the status of ERK1/2 and p38 in NHMs in co-culture with HMVECs and found that, after 30 minutes, ERK1/2 and p38 were phosphorylated (Figure 5e), with the phosphorylation of ERK also inhibited by siRNA EDNRB (Supplementary Figure 5 online). Furthermore, inhibition of the ERK pathway with U0126 inhibited the phosphorylation of MITF in NHMs co-cultured with HMVECs (Figure 5f), whereas the inhibition of p38 with SB203580 did not prevent this phosphorylation (Figure 5g). The increased tyrosinase and DCT after 3 days of co-culture was inhibited by U0126 and partially inhibited by SB203580, suggesting a role for both ERK and p38 activation in this mechanism (Figure 5h and i).

Taken together these results show that the microvascular endothelial cells secrete endothelin, which activates EDNRB on melanocytes and stimulates the ERK and p38 pathways. Activation of ERK leads first to the phosphorylation of MITF, whereas the activation of both ERK and p38 induces the subsequent upregulation of tyrosinase and DCT.

Microvascular endothelial cells increase the pigmentation of reconstructed epidermis through endothelin secretion

On the basis of the stimulation of melanogenesis by endothelial cells under co-culture conditions, we then assessed

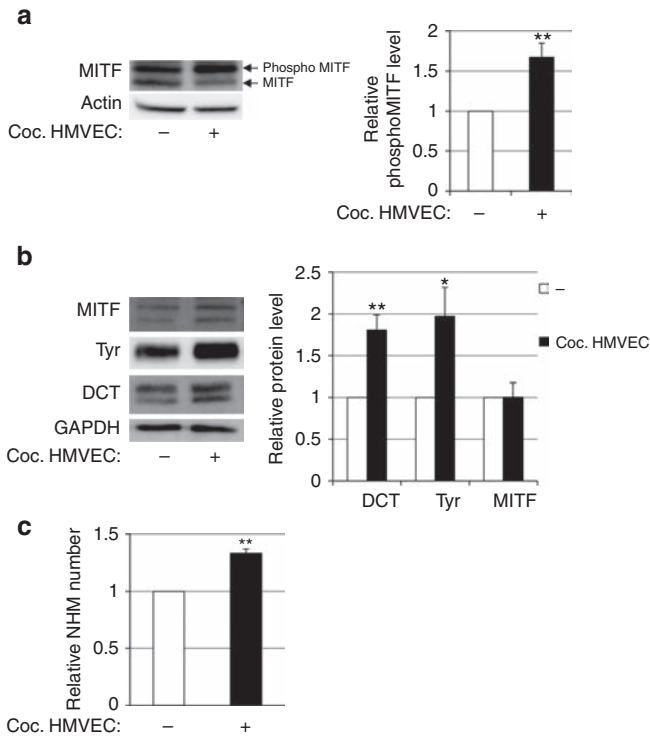


Figure 3. Microvascular endothelial cells increase the melanogenesis pathway in melanocytes. Normal human melanocytes (NHMs) are incubated with human dermal microvascular endothelial cells (HMVECs) in the transwell chamber during 30 minutes (a) or 3 days (b). The lysate of NHMs is analyzed by western blot with indicated antibodies and the relative protein level quantified ($n=6$ and 8 , respectively). The same number of NHMs is plated and incubated with HMVECs in the transwell chamber for 7 days (c). The HMVECs are changed every second day. After 7 days of co-culture, the NHMs are trypsinized and counted on Malassez cell ($n=3$). * $P \leq 0.05$; ** $P \leq 0.005$.

their effect on melanin synthesis in reconstructed epidermis composed of human keratinocytes and melanocytes cultured with or without HMVECs. After 3 weeks, the co-culture with HMVECs induced an increased pigmentation of the reconstructed epidermis that could be observed clinically (Figure 6a and b) and using Fontana–Masson staining (Figure 6c). This HMVEC-induced hyperpigmentation of the epidermis was prevented by the inhibition of EDNBRB with BQ788 (Figure 6c).

DISCUSSION

In 1963 Fitzpatrick and Breathnach formulated the concept of the epidermal melanin unit, with melanocytes and keratinocytes working together to produce skin color. Forty years later, Jim Nordlund expanded this concept to a cutaneous troika involving keratinocytes, Langerhans cells, and melanocytes (Nordlund, 2007), with fibroblasts also recently implicated in regulating skin pigmentation (Yamaguchi *et al.*, 2007 and 2008; Choi *et al.*, 2010). Here, we demonstrated that the dermal microvascular endothelial cells also have a role in the complex regulation of skin pigmentation. In our experiments, endothelial cells, but not keratinocytes, could stimulate melanogenesis in melanocytes

without UV stimulation. The absence or low stimulation of melanogenesis in our co-cultures with keratinocytes is not so surprising, and indeed all studies demonstrating a stimulating effect of keratinocytes on melanogenesis were conducted in the presence of UV stimulation (Duval *et al.*, 2001) or another pigmentation inducer such as Alpha-melanocyte-stimulating hormone (Lei *et al.*, 2002). We now show that endothelial cells have a role, through the secretion of endothelin, in upregulating key gene regulators of melanogenesis, MITF, tyrosinase, and DCT, without any UV stimulation. Activation of melanogenesis through activation of the MAPK pathway and phosphorylation of MITF is in accordance with previous reports (Sato-Jin *et al.*, 2008). However, the increased contrast in pigmentation between photo-exposed areas of the epidermis above vascular skin lesions and the perilesional skin led us to hypothesize that the stimulation of melanogenesis by endothelial cells might be even stronger after UV radiation. Further studies are warranted to confirm this hypothesis. Interestingly, in samples of the benign vascular lesions, the melanin content was increased in the epidermis located above the microvascularization along with an increased expression of Edn1 in the basal layers of the epidermis, further confirming that Edn1 is produced *in vivo* by endothelial cells, reaches the basal layers of the epidermis, and is capable of stimulating melanogenesis. We additionally observed *in vitro* a slight increase in melanocyte proliferation when co-cultured with endothelial cells, although the number of melanocytes was not significantly increased in either reconstructed epidermis experiments or skin samples of benign vascular lesions. Thus, the proliferative effect of Edn1 appears limited, at least *in vivo*. Interestingly, it was recently reported that choroidal melanocytes could regulate uveal vascularization through the secretion of fibromodulin (Adini *et al.*, 2014), emphasizing the constant cross-talk between melanocytes and endothelial cells. Edn1 is also produced by proliferating endothelial cells or by cells involved in inflammatory processes. Thus, on the basis of the current study, it could be hypothesized that Edn1 also has a role in post-inflammatory hyperpigmentation. Although more pronounced in darker skin types and in photo-exposed area, our clinical and histological data show that the vascular component of the dermis influences the pigmentation of the skin *in vivo*. Clearly, the physiological function that endothelial cells have in skin pigmentation, beyond their role in pigmentation disorders, warrants further investigations. Indeed, the potential impact of vascularization on hyperpigmented lesions observed in acquired bilateral telangiectatic macules was suspected by the authors who reported this entity (Park *et al.*, 2014a). Now, our results confirm a role for endothelial cells but also rule out the implicated role of VEGF as initially hypothesized and show instead the key role of the released endothelin. The vascular component may also have a key role in melasma. Histological studies and confocal laser microscopy studies have clearly shown a significant increase in vascularization within melasma lesions compared with that in the surrounding healthy skin (Kim *et al.*, 2007; Kang *et al.*, 2010). Although the significance of this increased vascularization was unknown, studies using different therapeutic

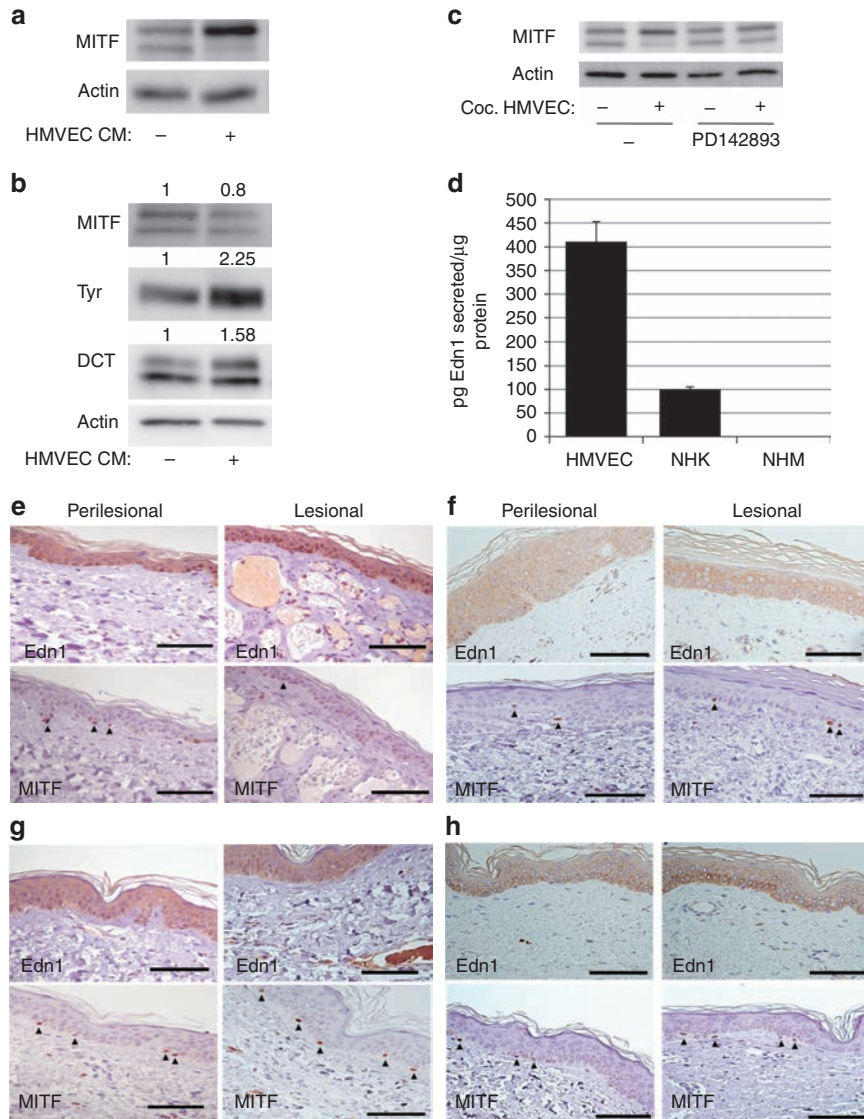


Figure 4. Endothelial cells secrete endothelin 1 implicated in the upregulation of the melanogenesis pathway in melanocytes. Human dermal microvascular endothelial cells (HMVECs) are incubated 24 hours with the normal human melanocytes (NHMs) starvation medium. NHMs are incubated with HMVEC-conditioned medium (HMVEC CM.) for 30 minutes (a) or 3 days and changed every day with new HMVEC CM. (b). NHMs and HMVECs are treated with the endothelin receptor antagonist PD142893 (5 µM) (c), 2 hours before the start of the co-culture with HMVECs for 30 minutes. The lysate of NHMs is analyzed by western blot with indicated antibodies. Numbers above the gels indicate levels of intensity compared with actin. The secretion of endothelin 1 by HMVECs, normal human keratinocytes (NHKs), and NHM in NHM starvation medium is measured using the ELISA method (d). The expression of endothelin 1 and microphthalmia-associated transcription factor (MITF) is analyzed in microvascular lesional skin sections compared with perilesional skin (e) (cherry angioma), (f) (botriomycoma), (g) (capillary venous malformation), (h) (acquired bilateral telangiectatic macules). Arrows designate MITF-positive cells. Scale bar = 50 µm.

approaches, but sharing the same aim of targeting the vascular component of melasma, have been recently reported. A prospective comparative split face randomized study showed that the combination of stabilized Kligman's trio and pulsed dye laser (PDL) was significantly more effective than the stabilized Kligman's trio alone (Passeron *et al.*, 2011). Interestingly, the combination approach prevented, at least partially, the typical relapses after the summer period, whereas the cream alone did not. In support of these findings, additional data suggest a preventive role of targeting vessels in the relapses of melasma (Passeron,

2013). A different kind of approach also assessed the effect on melasma of tranexamic acid, an anti-fibrinolytic used to prevent and to treat some hemorrhagic events. The combined use of this agent topically and orally during 8 weeks decreased hyperpigmentation in melasma lesions, whereas histological examinations confirmed a decrease in melanin content and in vascularization (Na *et al.*, 2013). These pilot studies underline the potential interest in targeting the vascular component for treating melasma. However, using laser approaches to remove the vessels may promote post-inflammatory hyperpigmentation, especially in darker skin

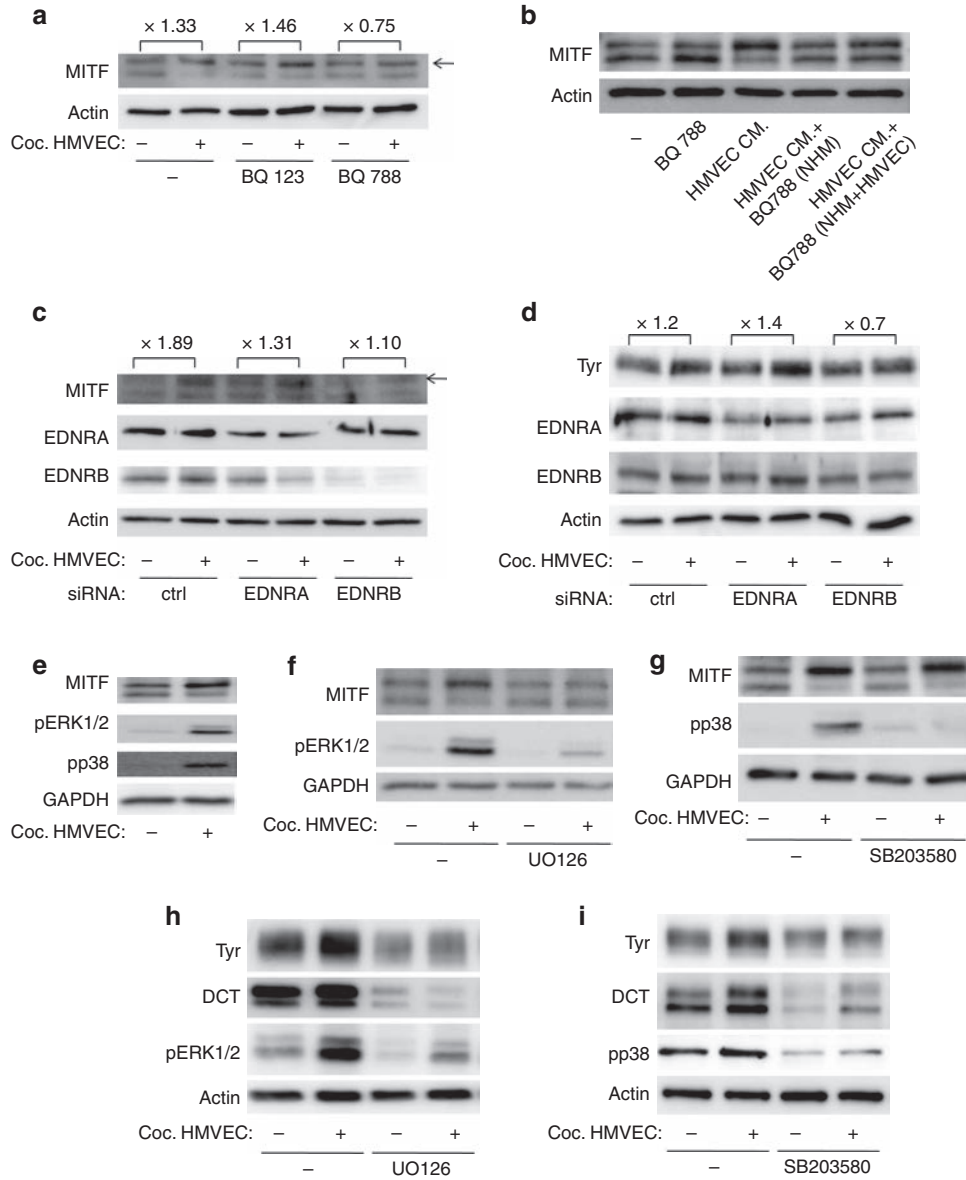


Figure 5. Endothelin acts through endothelin receptor B and mitogen-activated protein kinase (MAPK) extracellular signal-regulated kinase (ERK)1/2 and p38 to increase the melanogenesis pathway in melanocytes. Normal human melanocytes (NHMs) and human dermal microvascular endothelial cells (HMVECs) are pre-treated 2 hours with EDNRA and EDNRB inhibitors, respectively, BQ123 and BQ788 (2 μ M), and put in co-culture for 30 minutes (a). NHMs are pre-treated 2 hours with EDNRB inhibitor (2 μ M) and incubated with HMVECs treated or not with BQ788-conditioned medium for 30 minutes (b). NHMs are transfected with siRNA directed against EDNRA, EDNRB, or siRNA-negative control. One (c) or 4 (d) days later, NHMs are incubated with HMVECs during 30 minutes (c) or 3 days (d). NHMs are incubated with HMVECs in the transwell chamber during 30 minutes (e). NHMs and HMVECs are stimulated with ERK1/2 inhibitor UO126 (10 μ M) or p38 inhibitor SB203580 (10 μ M) 2 hours before the addition of the HMVEC transwell chamber in the well for 30 minutes (f and g) or 3 days (h and i). The lysate of NHM is analyzed by western blot with indicated antibodies. Numbers above the gels indicate the levels of intensity compared with actin.

types (Passeron *et al.*, 2011), and the efficacy of tranexamic acid has still to be confirmed in a prospective comparative trial. Moreover, its effects are nonspecific and may induce side effects. By dissecting the pathway involved in the pigmentation associated with vascularization, we demonstrate here the key role of the EDNRB. Thus, developing topical agents to inhibit EDNRB activation on melanocytes may limit the impact of the underlying vascularization and provide, in combination with classic

depigmenting agents, a powerful approach to treat melasma and prevent relapses.

MATERIALS AND METHODS

Patients

Consecutive patients presenting at least one benign vascular proliferation on the skin were included. Exclusion criteria were inflammatory skin disorders, photodermatoses, melasma, acquired brachial cutaneous dyschromia, post-inflammatory hyperpigmentation,

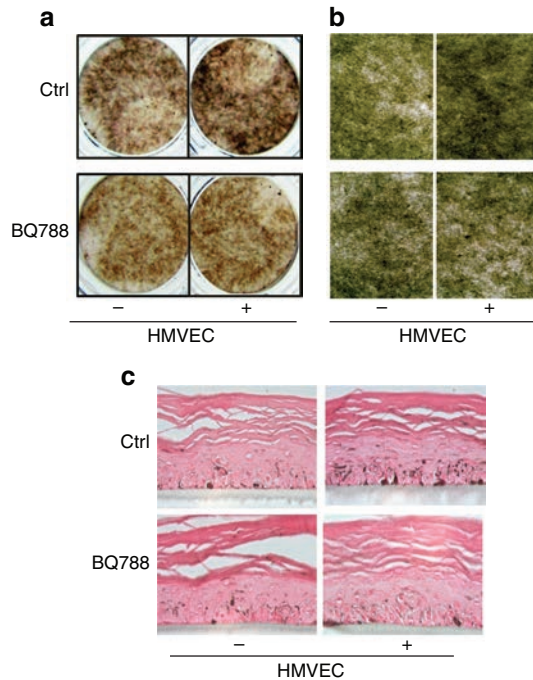


Figure 6. Endothelin released by endothelial cells increases the pigmentation in reconstructed epidermis. Reconstructed human pigmented epidermis in a transwell chamber is stimulated with EDNRb inhibitor BQ788 (2 μM) and incubated with human dermal microvascular endothelial cells (HMVECs) at the bottom of the well for 3 weeks. HMVECs are changed every other days, and BQ788 added every day. Reconstructed human pigmented epidermis is photographed in full size (a) or in $\times 20$ magnification (b). Melanin quantity is determined by Fontana–Masson staining and observed at $\times 40$ (c).

and concomitant medication with photosensitizing drugs. Cherry angiomas, botriomycomas, spider angiomas, involutive infantile hemangiomas, capillaro-venous malformation, acquired bilateral telangiectatic macules, and leg telangiectasias were included after written informed consent was granted. The patient age, gender, and skin type were noted together with the localization and size of involved lesions. As only noninvasive examination (epiluminescence dermatoscopy) was performed and all the data were definitively anonymized, institutional review board approval was waived.

Assessment of pigmentation

A digital epiluminescence dermatoscope at $\times 200$ magnification (Dinolite, Naarden, The Netherlands) was used for evaluating the vascular lesions and the pigmentation above the lesions. The same physician performed (HHG) all the evaluations. Pigmentation was assessed using a physician global assessment score that grades the difference in pigmentation within and in the infra millimeter border of vascular lesions compared with that in the surrounding skin. The contrast in pigmentation was scored as none, mild, moderate, or marked.

Vascular lesions were also assessed using laser confocal microscopy (Vivascope 1500, Caliber ID, Rochester, NY). Optical sections (Vivablock) of 4-mm width were acquired every 20 microns depth from the *stratum corneum* up to the superficial dermis. Confocal images were exported from the VivaScan Database to analyze using Confoscan to discern high- (bright) or low- (dark) intensity objects

against circular and fixed-shape models. We thus detected optically hyperreflective keratinocytes surrounding an angioma cavity and less-pigmented keratinocytes located on the perilesional skin for the quantification of pigmentation.

Reagent and antibodies

We obtained antibodies against MITF and β -actin from Abcam (Cambridge, MA), pERK, and pp38 from Cell Signaling Technology (Beverly, MA), EDNRA, EDNAB, and GAPDH from Santa Cruz Biotechnology (Santa Cruz, CA), and tyrosinase and DCT from V. Hearing.

U0126 and SB203580, baicalein, VEGF receptor inhibitor IV, CBO-P11, and PTIO were purchased from Millipore (Billerica, MA), PD142893 from Enzo Life Science (Farmingdale, NY), and LNAME, endothelin 1, BQ123, and BQ788 from Sigma Aldrich (Saint Quentin Fallavier, France).

Cell culture

NHMs and NHKs were obtained from the foreskin of skin type IV children as described previously. Briefly, epidermal cells are obtained by overnight digestion of the skin in a dispase solution at 4°C followed by incubation of the epidermis in a trypsin/EDTA solution for 20 minutes at 37°C . NHMs were isolated in MCDB 153 medium (Sigma Aldrich) supplemented with 2% FBS (Perbio; Helsingborg, Sweden), $5 \mu\text{g ml}^{-1}$ insulin (Sigma Aldrich), $0.5 \mu\text{g ml}^{-1}$ hydrocortisone (Sigma Aldrich), 16 nM TPA (Sigma Aldrich), 1 ng ml^{-1} FGF (Promega; Madison, WI), $15 \mu\text{g ml}^{-1}$ bovine pituitary extract (Invitrogen; Carlsbad, CA), $10 \mu\text{M}$ forskolin (Sigma Aldrich), and $20 \mu\text{g ml}^{-1}$ geneticin (Invitrogen) over 2 weeks. NHKs were isolated in KGM 2 medium (Promocell, Heidelberg, Germany). HMVECs were obtained from Invitrogen and grown in Cascade 131 medium supplemented with microvascular growth supplement on attachment factor-coated plates (Invitrogen). All cells were maintained at 37°C in a 5% CO_2 atmosphere.

Co-culture experiments

For the co-culture experiments, NHMs were seeded in six-well plates, whereas HMVECs and NHKs were seeded separately on $0.4 \mu\text{m}$ Transwell inserts (Becton Dickinson; East Rutherford, NJ).

Two days before experiments, NHMs were starved in MCDB 153 medium supplemented with $5 \mu\text{g ml}^{-1}$ insulin, $15 \mu\text{g ml}^{-1}$ bovine pituitary extract, and 2% fetal bovine serum to remove propigmenting agents. HMVECs and NHKs were also incubated for 2 days in the NHM starvation medium to avoid medium-dependent effects on pigmentation. The co-cultures were initiated when a Transwell coated with HMVECs or NHKs was placed in a well containing cultured NHM.

Reconstructed human pigmented epidermis (RHPE) experiment

RHPE (skin type IV), obtained from SkinEthic (Lyon, France), is characterized by keratinocytes and melanocytes 3-D culture from foreskin disposed on a $0.4 \mu\text{m}$ transwell chamber that allows an air–liquid interface. According to SkinEthic procedure, RHPE are incubated 24 hours in RHPE growth medium before experiment.

For the HMVEC/RHPE co-culture experiment, HMVECs are seeded in 24-well plates and incubated 24 hours with RHPE growth factor before incubation with the RHPE. HMVECs are changed every second or third days during the 3 weeks of co-culture.

Histopathology

Each biopsy was fixed in 4% formalin and paraffin embedded. Morphological examination was carried out on sections (2- μ m thickness) stained by hematoxylin and eosin or Fontana–Masson. Sections were heated for 20 minutes at 97 °C in low pH buffer solution for antigen retrieval (PT-link Dako device, Glostrup, Denmark). MITF immunolabeling (mouse mAb product code: M3621, Clone:D5, dilution 1/100, immunogen: Histidine fusion protein of the amino-terminal Taq-Sac fragment of human MITF cDNA, Dako France SAS, les Ulis,) and endothelin immunolabeling (goat polyclonal antibody, product code: ET-1 (N-8) sc-21625, dilution 1/200, Santa Cruz Biotechnology) were performed using a Dako autostainer according to the manufacturer's recommendations. After washing with phosphate-buffered saline, the sections were incubated with Envision FLEX+mouse (Linker)/HRP (DAKO) for 15 minutes at room temperature. After washing with phosphate-buffered saline, the sections were incubated with Envision FLEX/HRP (DAKO) for 20 minutes at room temperature, followed by revelation using the Envision System according to the manufacturer's recommendations, with DAB (diaminobenzidine) for 8 minutes as chromogen. Finally, the sections were counterstained in Mayer's hematoxylin and mounted in glycergel mounting medium (Dako). Melanocytes, identified by Mitf immunohistochemical staining, and basal keratinocytes were counted along the basement membrane, beside and away from the vascular lesion, within the entire length of each biopsy. We then set the ratio of keratinocytes/melanocytes. For each sample, at least 10 fields at $\times 400$ magnification were studied.

Transient siRNA transfection

A total of 500,000 NHMs are used for reverse transfection. NHMs are trypsinized, resuspended in starvation medium, and transfected using INTERFER in (Polyplus Transfection; Illkirch, France) according to the manufacturer instructions. Briefly, siRNA-negative control, EDNRA and EDNRB (50 pmol) (#1-Thermo Fisher Scientific; Waltham, MA), (#2-Ambion; Foster City, CA) are incubated with INTERFER in 15 minutes and lay into the well before the addition of the cells. The experiments of 30 minutes of co-culture were conducted 4 days after the transfection, and the experiments of 3 days of co-culture were performed 1 day avec the transfection.

Statistical analysis

Statistical differences between groups were analyzed by Student's *t*-test. They were considered significant at $P < 0.05$.

CONFLICT OF INTEREST

AM is an employee of Beiersdorf. The remaining authors state no conflict of interest.

ACKNOWLEDGMENTS

Light microscopy was performed on the C3M Imaging Core Facility (part of Microscopy and Imaging platform Côte d'Azur, MICA).

SUPPLEMENTARY MATERIAL

Supplementary material is linked to the online version of the paper at <http://www.nature.com/jid>

REFERENCES

- Adini I, Ghosh K, Adini A *et al.* (2014) Melanocyte-secreted fibro-modulin promotes an angiogenic microenvironment. *J Clin Invest* 124: 425–36
- Choi W, Wolber R, Gerwat W *et al.* (2010) The fibroblast-derived paracrine factor neuregulin-1 has a novel role in regulating the constitutive color and melanocyte function in human skin. *J Cell Sci* 123:3102–11
- Duval C, Regnier M, Schmidt R (2001) Distinct melanogenic response of human melanocytes in mono-culture, in co-culture with keratinocytes and in reconstructed epidermis, to UV exposure. *Pigment Cell Res* 14:348–55
- Fitzpatrick TB, Breathnach AS (1963) The epidermal melanin unit system. *Dermatologische Wochenschrift* 147:481–9
- Hirobe T (2005) Role of keratinocyte-derived factors involved in regulating the proliferation and differentiation of mammalian epidermal melanocytes. *Pigment Cell Res* 18:2–12
- Kang HY, Bahadoran P, Suzuki I *et al.* (2010) *In vivo* reflectance confocal microscopy detects pigmentary changes in melasma at a cellular level resolution. *Exp Dermatol* 19:e228–33
- Kang HY, Suzuki I, Lee DJ *et al.* (2011) Transcriptional profiling shows altered expression of wnt pathway- and lipid metabolism-related genes as well as melanogenesis-related genes in melasma. *J Invest Dermatol Symp Proc* 131:1692–700
- Kim EH, Kim YC, Lee ES *et al.* (2007) The vascular characteristics of melasma. *J Dermatol Sci* 46:111–6
- Kim EJ, Park HY, Yaar M *et al.* (2005) Modulation of vascular endothelial growth factor receptors in melanocytes. *Exp Dermatol* 14:625–33
- Kim JY, Lee TR, Lee AY (2013) Reduced WIF-1 expression stimulates skin hyperpigmentation in patients with melasma. *J Invest Dermatol Symp Proc* 133:191–200
- Lei TC, Virador VM, Vieira WD *et al.* (2002) A melanocyte-keratinocyte coculture model to assess regulators of pigmentation in vitro. *Anal Biochem* 305:260–8
- Na JI, Choi SY, Yang SH *et al.* (2013) Effect of tranexamic acid on melasma: a clinical trial with histological evaluation. *J Eur Acad Dermatol Venereol* 27: 1035–9
- Nordlund JJ (2007) The melanocyte and the epidermal melanin unit: an expanded concept. *Dermatol Clin* 25:271–81
- Park JH, Lee DJ, Lee YJ *et al.* (2014a) Acquired bilateral telangiectatic macules: a distinct clinical entity. *JAMA Dermatol* 150:974–7
- Park TJ, Kim M, Kim H *et al.* (2014b) Wnt inhibitory factor (WIF)-1 promotes melanogenesis in normal human melanocytes. *Pigment Cell Melanoma Res* 27:72–81
- Passeron T (2013) Long-lasting effect of vascular targeted therapy of melasma. *J Am Acad Dermatol* 69:e141–2
- Passeron T, Fontas E, Kang HY *et al.* (2011) Melasma treatment with pulsed-dye laser and triple combination cream: a prospective, randomized, single-blind, split-face study. *Arch Dermatol* 147:1106–8
- Plonka PM, Passeron T, Brenner M *et al.* (2009) What are melanocytes really doing all day long...? *Exp Dermatol* 18:799–819
- Sato-Jin K, Nishimura EK, Akasaka E *et al.* (2008) Epistatic connections between microphthalmia-associated transcription factor and endothelin signaling in Waardenburg syndrome and other pigmentary disorders. *FASEB J* 22: 1155–68
- Yamaguchi Y, Hearing VJ (2009) Physiological factors that regulate skin pigmentation. *Biofactors* 35:193–9
- Yamaguchi Y, Passeron T, Hoashi T *et al.* (2008) Dickkopf 1 (DKK1) regulates skin pigmentation and thickness by affecting Wnt/beta-catenin signaling in keratinocytes. *FASEB J* 22:1009–20
- Yamaguchi Y, Passeron T, Watabe H *et al.* (2007) The effects of dickkopf 1 on gene expression and Wnt signaling by melanocytes: mechanisms underlying its suppression of melanocyte function and proliferation. *J Invest Dermatol Symp Proc* 127:1217–25

Inhibition of Human Tyrosinase Requires Molecular Motifs Distinctively Different from Mushroom Tyrosinase

Tobias Mann¹, Wolfram Gerwat¹, Jan Batzer¹, Kerstin Eggers¹, Cathrin Scherner¹, Horst Wenck¹, Franz Stäb¹, Vincent J. Hearing², Klaus-Heinrich Röhm³ and Ludger Kolbe¹

Tyrosinase is the rate-limiting enzyme of melanin production and, accordingly, is the most prominent target for inhibiting hyperpigmentation. Numerous tyrosinase inhibitors have been identified, but most of those lack clinical efficacy because they were identified using mushroom tyrosinase as the target. Therefore, we used recombinant human tyrosinase to screen a library of 50,000 compounds and compared the active screening hits with well-known whitening ingredients. Hydroquinone and its derivative arbutin only weakly inhibited human tyrosinase with a half-maximal inhibitory concentration (IC₅₀) in the millimolar range, and kojic acid showed a weak efficacy (IC₅₀ > 500 μmol/L). The most potent inhibitors of human tyrosinase identified in this screen were resorciny-thiazole derivatives, especially the newly identified Thiamidol (Beiersdorf AG, Hamburg, Germany) (isobutylamido thiazolyl resorcinol), which had an IC₅₀ of 1.1 μmol/L. In contrast, Thiamidol only weakly inhibited mushroom tyrosinase (IC₅₀ = 108 μmol/L). In melanocyte cultures, Thiamidol strongly but reversibly inhibited melanin production (IC₅₀ = 0.9 μmol/L), whereas hydroquinone irreversibly inhibited melanogenesis (IC₅₀ = 16.3 μmol/L). Clinically, Thiamidol visibly reduced the appearance of age spots within 4 weeks, and after 12 weeks some age spots were indistinguishable from the normal adjacent skin. The full potential of Thiamidol to reduce hyperpigmentation of human skin needs to be explored in future studies.

Journal of Investigative Dermatology (2018) ■, ■-■; doi:10.1016/j.jid.2018.01.019

INTRODUCTION

Melasma, actinic and senile lentiginos, and postinflammatory hyperpigmentation are major cosmetic problems for which many patients seek medical advice. Generally, those disorders affect populations with darker skin complexions with a greater frequency and severity (Stratigos and Katsambas, 2004). Many topical products are available to treat hyperpigmentary disorders, and they contain diverse active ingredients to reduce melanin production and/or distribution. Although skin hyperpigmentation can be reduced by various mechanisms (Briganti et al., 2003), tyrosinase, the rate-limiting enzyme of melanin production, is the obvious target for inhibitors of hyperpigmentation (Kanteev et al., 2015; Lee et al., 2014; Ramsden and Riley, 2014). Many substances have been described in the literature as inhibitors of tyrosinase, but most of them lack clinical efficacy, and only a few compounds are currently used in topical dermatological products (Chang, 2009; Kim and Uyama, 2005; Rescigno

et al., 2002). Among those, kojic acid, hydroquinone, and arbutin are the most common (Solano et al., 2006).

The unsatisfactory clinical efficacy of currently used tyrosinase inhibitors is largely due to the fact that those compounds were tested using only tyrosinase isolated from the mushroom *Agaricus bisporus* (mTyr) (Espin et al., 2000; Garcia-Molina et al., 2005), which is the only active tyrosinase readily commercially available. The catalytic activities and substrate specificities of mTyr have been shown to be significantly different from the mammalian enzyme (Hearing et al., 1980). The three-dimensional structures of several tyrosinases were recently solved, among them the structures of mTyr (Ismaya et al., 2011) and of two bacterial enzymes from *Streptomyces castaneoglobisporus* (Matoba et al., 2006) and *Bacillus megaterium* (Sendovski et al., 2011). By contrast, very little kinetic or structural information is available for human tyrosinase (hTyr), mainly because of substantial difficulties in obtaining sufficient amounts of hTyr from natural sources or by heterologous expression. hTyr has been transiently expressed in various animal cell lines (Olivares et al., 2002; Schweikardt et al., 2007; Tripathi et al., 1992; Wendt, 2006), but yields were always too low for a detailed characterization of the resulting hTyr preparations. More recently, several groups have developed more efficient expression systems for hTyr (Cordes et al., 2013; Fogal et al., 2015; Lai et al., 2016), but data on the three-dimensional structure of hTyr or kinetic data of hTyr inhibitors were still missing.

In this study, we used a recombinant hTyr construct (Cordes et al., 2013) to conduct a high-throughput screen (HTS) of a large compound library to identify structural motifs in small-molecule compounds that efficiently inhibit

¹Front End Innovation, Beiersdorf AG, Hamburg, Germany; ²DASS Manuscript, Haymarket, Virginia, USA; and ³Institute of Physiological Chemistry, Philipps University, Marburg, Germany

Correspondence: Ludger Kolbe, Front End Innovation, Beiersdorf AG, Unnastrasse 48, BF519, 20245 Hamburg, Germany. E-mail: Ludger.Kolbe@Beiersdorf.com

Abbreviations: HTS, high-throughput screen; hTyr, human tyrosinase; IC₅₀, half maximal inhibitory concentration; K_i, inhibitor constant; mTyr, mushroom (*Agaricus bisporus*) tyrosinase

Received 9 December 2017; revised 3 January 2018; accepted 15 January 2018; accepted manuscript published online 7 February 2018; corrected proof published online XXX

hTyr. We also evaluated the effects of well-known whitening compounds, such as hydroquinone, arbutin, kojic acid, rhododendrol and 4-butylresorcinol, on hTyr activity and compared their efficacies with the new compounds identified by the HTS screen. Among the screening hits, we identified Thiamidol (Beiersdorf AG, Hamburg, Germany) (International Nomenclature of Cosmetic Ingredients name, isobutylamido thiazolyl resorcinol; International Union of Pure and Applied Chemistry name, *N*-(4-(2,4-dihydroxyphenyl)thiazol-2-yl)isobutyramide) as an especially potent inhibitor of hTyr, and we show that it is an effective and safe inhibitor of human hyperpigmentation in vivo.

RESULTS

Inhibition of hTyr

A screen of 50,000 compounds in the library, which spans a wide chemical space, yielded several hit series of active and effective hTyr inhibitors. Among them, derivatives of thiazolyl-resorcinol were the most promising group. This lead compound was then optimized to develop derivatives with high activity and physico-chemical properties compatible with topical formulations. Thiamidol (isobutylamido thiazolyl resorcinol, compound 1) (Figure 1) was identified as one of the most potent derivatives. In addition to Thiamidol, 4-butylresorcinol (compound 2) and the classical tyrosinase inhibitors kojic acid (compound 5), hydroquinone (compound 6), and arbutin (compound 7), as well as rhododendrol (compound 9), were also tested as inhibitors of the diphenolase (L-dopa oxidase) activity of hTyr over a wide range of concentrations (up to 4 orders of magnitude). The results are summarized in Figure 2a and Table 1. Among these actives, Thiamidol was by far the most efficient inhibitor of hTyr, with a half-maximal inhibitory concentration (IC_{50}) of 1.1 $\mu\text{mol/L}$, with almost complete enzyme inhibition of hTyr occurring at concentrations above 10 $\mu\text{mol/L}$. The resorcinol derivatives 4-butylresorcinol, 4-hexylresorcinol, and 4-phenylethylresorcinol had IC_{50} values of 21 $\mu\text{mol/L}$, 94 $\mu\text{mol/L}$, and 131 $\mu\text{mol/L}$, respectively (Table 1). With an IC_{50} of about 500 $\mu\text{mol/L}$, kojic acid was 500 times less potent than Thiamidol. Hydroquinone and arbutin were both very poor inhibitors of hTyr, with IC_{50} values in the millimolar range. Kojic acid, arbutin, and hydroquinone were not able to completely inhibit hTyr in the concentration range tested. Racemic rhododendrol was also rather ineffective as an inhibitor of L-dopa oxidation, with an $IC_{50} > 1,200 \mu\text{mol/L}$ (Figure 2a).

A detailed kinetic analysis of the inhibition of hTyr by Thiamidol yielded a strictly competitive type of inhibition with an inhibitor constant (K_i) of 0.25 $\mu\text{mol/L}$ (Figure 2b, Table 1). This value is in agreement with the IC_{50} value estimated from dose-response curves (1.1 $\mu\text{mol/L}$) (cf. Figure 2a) which, for competitive inhibition, should be about 3 times higher than the K_i . The K_i values for 4-butylresorcinol (9 $\mu\text{mol/L}$), 4-hexylresorcinol (39 $\mu\text{mol/L}$), and 4-phenylethylresorcinol (24 $\mu\text{mol/L}$) were also markedly higher than the K_i value of Thiamidol (Table 1). These data illustrate that the thiazolylamide moiety of Thiamidol conveys a much better inhibition of hTyr than do the hydrocarbon side chains present in three other derivatives of resorcinol (4-butyl-, 4-hexyl-, and 4-phenyl ethylresorcinol). As noted, the efficacy is distinctively different in mTyr,

where 4-butylresorcinol, 4-hexylresorcinol, and 4-phenylethylresorcinol, and even kojic acid, are superior to Thiamidol in inhibiting the enzyme (Table 1). Thus, Thiamidol would not have been identified as positive in a screening using mTyr, and the efficacy of 4-phenylethylresorcinol would have been grossly overestimated.

Garcia-Jimenez et al. (2016) recently reported that mTyr slowly oxidizes certain resorcinols, provided that the prevailing met- form of the enzyme is previously converted to either the oxy- or deoxy- form by additives like H_2O_2 and ascorbate and that the reaction is sustained by *o*-diphenols. Therefore, we used quantitative high-performance liquid chromatography analysis (Ito and Wakamatsu, 2015) to ascertain whether Thiamidol might also be a substrate of hTyr. In our normal assay conditions (i.e., in the absence of the additives mentioned by Garcia-Jimenez et al., 2016), no detectable oxidation of Thiamidol took place within several hours of incubation with hTyr, whereas rhododendrol was readily oxidized within that time frame (see Supplementary Figure S1 online). Thus, we assume that the reaction described by Garcia-Jimenez et al. is not relevant for Thiamidol and hTyr in physiological conditions.

Inhibition of melanin production

We then tested the potential inhibitory effects of these compounds using a three-dimensional model for human skin. As observed with purified hTyr, arbutin showed only a negligible efficacy at inhibiting melanin production in MelanoDerm (MatTek Corporation, Ashland, MA) skin models ($IC_{50} > 4,000 \mu\text{mol/L}$) (Figure 2c). Kojic acid inhibited melanin production with an IC_{50} of $\sim 400 \mu\text{mol/L}$, showing a surprisingly steep dose-response curve, with concentrations below 200 $\mu\text{mol/L}$ only slightly inhibiting melanin production (i.e., by 5% at 150 $\mu\text{mol/L}$). Rhododendrol showed only marginal effects on melanogenesis, with an apparent IC_{50} for inhibition of $\sim 1,200 \mu\text{mol/L}$. Hydroquinone inhibited melanin production in MelanoDerm skin models with an IC_{50} of 15 $\mu\text{mol/L}$, suggesting that it has a mechanism other than tyrosinase inhibition. 4-Butylresorcinol inhibited melanin synthesis with an IC_{50} of 13.5 $\mu\text{mol/L}$. Again, Thiamidol was, by far, the most potent inhibitor of melanin production in MelanoDerm skin models, with an IC_{50} of 0.9 $\mu\text{mol/L}$, and in monolayer cultures, Thiamidol visibly reduced melanin formation (Figure 3a).

Hydroquinone and Thiamidol were then tested in long-term melanocyte monolayer cultures to check the potential reversibility of inhibition. Although 1 $\mu\text{mol/L}$ Thiamidol reduced melanin production to less than 60% after 2 weeks, 1 $\mu\text{mol/L}$ hydroquinone reduced melanin production only to approximately 85% (Figure 3b). However, upon further cultivation without the active compounds, melanocytes that had been inhibited by Thiamidol rapidly restarted their melanin production, reaching pretreatment levels within 1 week. In contrast, hydroquinone-treated cells did not recover their full capacity for melanin production within the 2-week culture period, and melanin production continued at 85% of pretreatment levels.

Molecular modeling

Possible binding modes of Thiamidol to hTyr were examined by virtual docking studies. Figure 4a shows the active site of

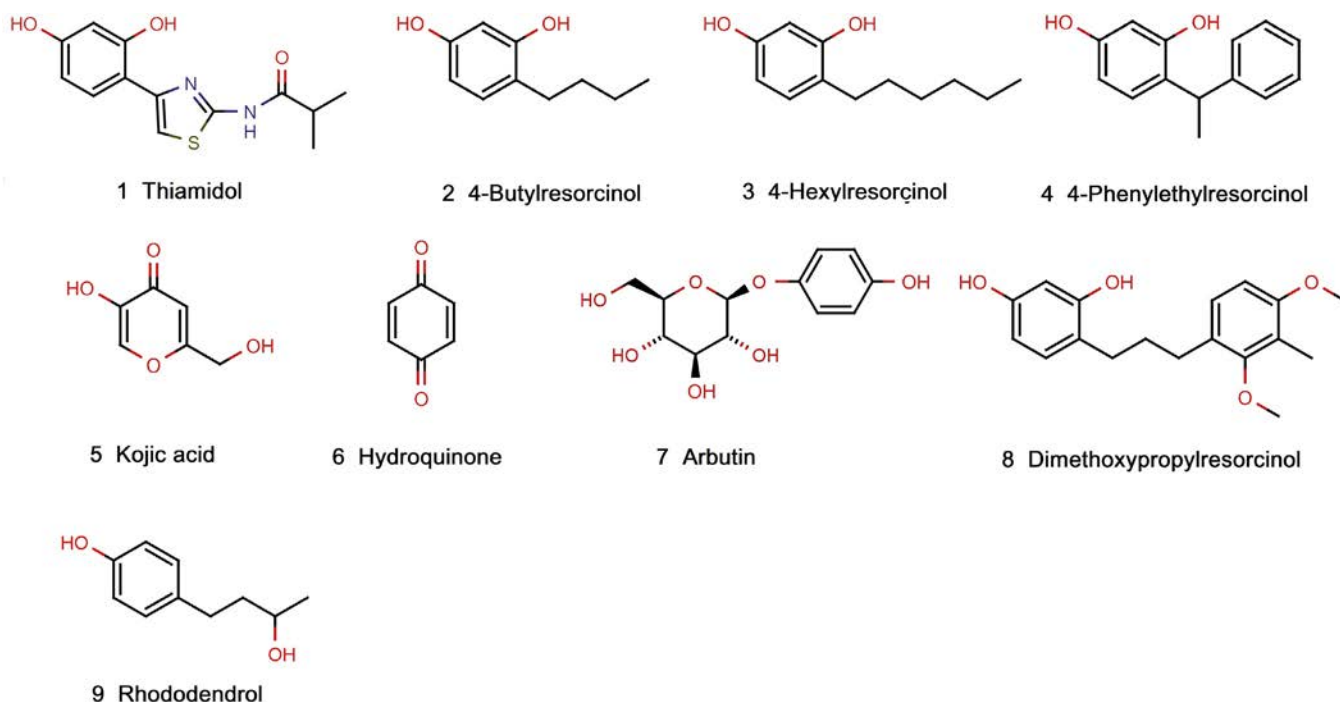


Figure 1. Chemical structure of inhibitory compounds evaluated in this study. Compound 1, Thiamidol (Beiersdorf AG, Hamburg, Germany) (isobutylamido thiazolyl resorcinol); compound 2, 4-butylresorcinol; compound 3, 4-hexylresorcinol; compound 4, 4-phenylethylresorcinol; compound 5, kojic acid; compound 6, hydroquinone; compound 7, arbutin; compound 8, dimethoxytolylpropyl resorcinol; and compound 9, rhododendrol.

the homology model of hTyr in the met- form, with a docked Thiamidol ligand in a lowest-energy conformation. The di-copper center with the bridging oxygen is visible on the left. Only amino acid residues immediately adjacent to the bound inhibitor are shown. (Residue numbering includes the signal peptide). The inner surface of the binding pocket is colored according to hydrophobicity on a scale from blue for hydrophilic to brown for hydrophobic. Although the environment of the di-copper center is distinctly hydrophilic, a strongly hydrophobic subpocket is formed mainly by the side chains of I368, V377, and F347. In the spatial orientation shown, the 1-hydroxy group of the aromatic ring of the ligand makes extensive contacts with the di-copper center, and the 3-hydroxy group is involved in hydrogen bonds with the side chain of S380 and the backbone carbonyl of M374. The thiazolyl ring is held in place by hydrophobic interactions with the nonpolar pocket (Figure 4b), formed by side chains of amino acids, most of which differ between mTyr and hTyr (Figure 4c).

Comparable results were obtained when Thiamidol was docked to the recently published x-ray structure of the structurally similar TRP1, a Zn²⁺-containing melanogenic enzyme of yet unknown function in humans (Ghanem and Fabrice, 2011; Lai et al., 2017), suggesting that the TYRP1 enzyme is inhibited by Thiamidol as well (see Supplementary Figure S2 online).

Clinical studies

The in vivo efficacy of Thiamidol was then examined in clinical studies where elderly subjects treated age spots on their skin twice daily with a formula containing 0.2% Thiamidol or with the vehicle only as a control. Already after 4 weeks of treatment, the treated age spots were significantly

lighter than the untreated control age spots (Figure 5a). Improvement continued over the entire treatment period, and after 12 weeks some of the age spots were indistinguishable from the surrounding normally pigmented skin (Figure 5b). EpiFlash (Canfield Scientific Inc., Parsippany, NJ) photographs showed visible improvement in the appearance of age spots, and the untreated control age spots remained unchanged (not shown). A follow-up study showed that concentrations of Thiamidol as low as 0.1% effectively reduced the visibility of age spots (see Supplementary Figure S3 online).

DISCUSSION

The safest and most effective way to treat cutaneous hyperpigmentation is to reduce melanin production by inhibiting tyrosinase activity. However, most tyrosinase inhibitors described in the literature lack clinical efficacy when incorporated into topical products. Almost all of them were tested only against mTyr (Espin et al., 2000; Garcia-Molina et al., 2005) and thus, although being effective against mTyr, turned out to be poor inhibitors of hTyr. Commercially available mTyr is not a homogeneous preparation but rather is a mixture of several tyrosinase isoenzymes and small amounts of additional enzyme activities that may affect inhibition studies in unpredictable ways (Pretzler et al., 2017). Isoenzymes AbPPO3 and AbPPO4, the main components of commercially available mTyr, have amino acid sequences in the region of the active site that significantly differ from hTyr (Figure 4c). Both mTyr isoenzymes contain extra loops between Asn371 (one of the glycosylation sites of hTyr) and Gly372. Several of the residues interacting with Thiamidol in hTyr (cf. Figure 4b) are not conserved in mTyr, for example,

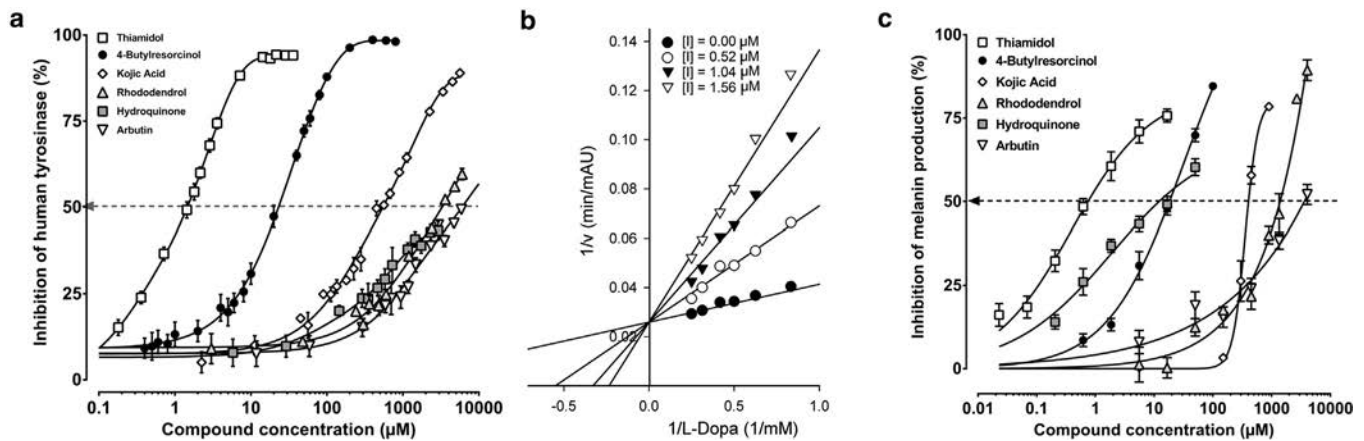


Figure 2. Inhibition of melanin production by Thiamidol, 4-butylresorcinol, kojic acid, rhododendrol, hydroquinone, and arbutin. (a) In vitro assays using purified hTyr in 50 mmol/L sodium phosphate buffer, pH 7.0, at a substrate (L-dopa) concentration of 1 mmol/L and various concentrations of inhibitors as noted. Data represent mean \pm standard deviation of three independent experiments. (b) Kinetics of inhibition of hTyr by Thiamidol (Beiersdorf AG, Hamburg, Germany) at the concentrations noted. The experiment was performed in triplicate at pH 7.0. The data are plotted according to Lineweaver-Burk. (c) Inhibition of melanin production in MelanoDerm (MatTek Corporation, Ashland, MA) skin models. The melanin content of each MelanoDerm skin model was determined after 13 days of cultivation in the presence of various inhibitors at the concentrations noted. Data represent mean \pm standard deviation of five independent experiments. AU, arbitrary unit; hTyr, human tyrosinase; M, mol/L.

Ile368, Ser375, and Ser380. Phe207 is structurally conserved in mTyr, whereas Phe347 is not. Because even small changes in enzyme-ligand interactions may have dramatic effects on binding affinities, the diverse inhibition profiles of hTyr and mTyr (summarized in Table 1) did not come as a surprise.

The main objective of this study was to compare the effects of arbutin, hydroquinone, and kojic acid with various resorcinol derivatives on the catalytic function of hTyr and on melanin production in vivo. Except for Thiamidol, all of the tested substances have been described as tyrosinase inhibitors (Kim et al., 2012); however, their reported inhibitory activities are extremely divergent. In the medical literature, hydroquinone is considered the criterion standard for the treatment of skin hyperpigmentation, although there are severe concerns

regarding its safety. Hydroquinone is banned in the European Union from use in cosmetics, but it is still sold in the United States as an over-the-counter drug in formulations containing up to 2% hydroquinone. Recently, the US Food and Drug Administration (2006) expressed concern about hydroquinone; however, a final ruling is still pending. The published IC₅₀ values for hydroquinone inhibition of mTyr cover a range from 1.1 μmol/L (Kang et al., 2003) to 680 μmol/L (Abu Ubeid et al., 2009). In our analysis, hydroquinone was remarkably ineffective against hTyr, inhibiting it only slightly, reaching just 50% inhibition at approximately 4,000 μmol/L. Although hydroquinone has been considered as a tyrosinase inhibitor since the early 1990s (Palumbo et al., 1991), our results suggest that its cytotoxic properties are actually more important, not only for its adverse effects on melanocytes but also

Table 1. Kinetic data for inhibitors of hTyr and/or mTyr and inhibition of melanin production

Number	Compound	K _i (μmol/L)		IC ₅₀ (μmol/L)		MelanoDerm Skin Model
		hTyr	mTyr	hTyr	mTyr	
1	Thiamidol	0.25	1.1	108	0.9	
2	4-Butylresorcinol	9.1	21	0.6	13.5	
3	4-Hexylresorcinol	39	94	1.2 ¹	n.d.	
4	4-Phenylethylresorcinol	24	131	0.3 ²	n.d.	
5	Kojic acid	145	500	6.0 ³	400	
6	Hydroquinone	n.d.	>4,000	1.1 ⁴	16.3	
7	Arbutin	n.d.	>4,000	40 ⁵	>4,000	
8	Dimethoxytolylpropyl resorcinol	n.d.	No inh.	0.24 ⁶	n.d.	

Abbreviations: hTyr, human tyrosinase; IC₅₀, half maximal inhibitory concentration; K_i, inhibitor constant; M, mol/L; mTyr, mushroom tyrosinase; n.d., not determined; no inh., no inhibition.

¹IC₅₀ value from Chen et al., 2004.

²IC₅₀ value calculated from Vielhaber et al., 2007.

³IC₅₀ value from Curto et al., 1999.

⁴IC₅₀ value from Kang et al., 2003.

⁵IC₅₀ value from Ying et al., 1999.

⁶IC₅₀ value from Nesterov et al., 2008.

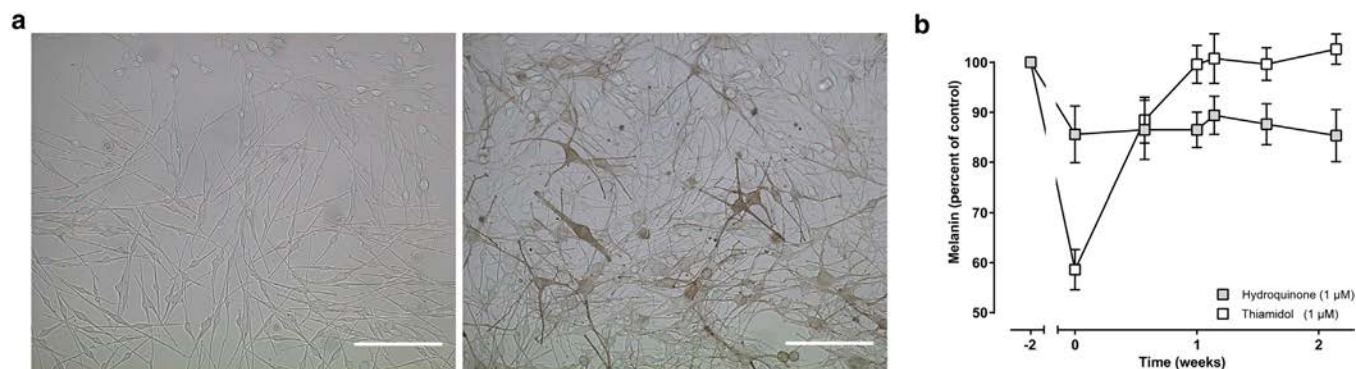


Figure 3. Characteristics of hTyr inhibition by Thiamidol or hydroquinone. (a) Melanocytes from African donors were cultivated for 2 weeks (left) with or (right) without 5 $\mu\text{mol/L}$ Thiamidol (Beiersdorf AG, Hamburg, Germany) in microplate dishes; photographs were taken in bright field mode. Scale bars = 200 μm . (b) Melanocytes from Caucasian donors were cultivated with 1 $\mu\text{mol/L}$ hydroquinone or 1 $\mu\text{mol/L}$ Thiamidol for 2 weeks to reduce melanin production and then were cultured for 2 more weeks without those active compounds to monitor the recovery of melanin production. Melanin content was measured at the times noted using a microplate reader, and data are reported as % control. Mean \pm standard error of the mean, $n = 5$. M, mol/L.

for its efficacy as an inhibitor of melanogenesis (Jimbow et al., 1974; Penney et al., 1984; Smith et al., 1988). This view is substantiated not only by our results with hTyr and the fact that hydroquinone significantly reduced melanin production in skin models but also by our experiments with melanocyte cultures. Here, hydroquinone reduced melanin production, but the treated cells did not regain the full capacity to produce melanin after removal of the active.

Although arbutin is generally considered an effective tyrosinase inhibitor, the published IC_{50} values of arbutin for mTyr range from 40 $\mu\text{mol/L}$ (Ying et al., 1999) to more than 30,000 $\mu\text{mol/L}$ (Sugimoto et al., 2005). In our test system, we found very high IC_{50} values ($>4,000$ $\mu\text{mol/L}$)

for arbutin with both purified hTyr and the MelanoDerm skin model. Data on the efficacy of both α -arbutin and β -arbutin have been published (Garcia-Jimenez et al., 2017). However, both compounds are actually hydroquinone pro-drugs, with their biological activity dependent on the release of hydroquinone from the molecule (Briganti et al., 2003). The European Union Scientific Committee on Consumer Products (2008) published a critical opinion on arbutin. In view of the release of hydroquinone from the molecule, it regards the use of arbutin in cosmetic products as unsafe.

The published IC_{50} values for tyrosinase inhibition by kojic acid range from 6 $\mu\text{mol/L}$ (Curto et al., 1999) to more

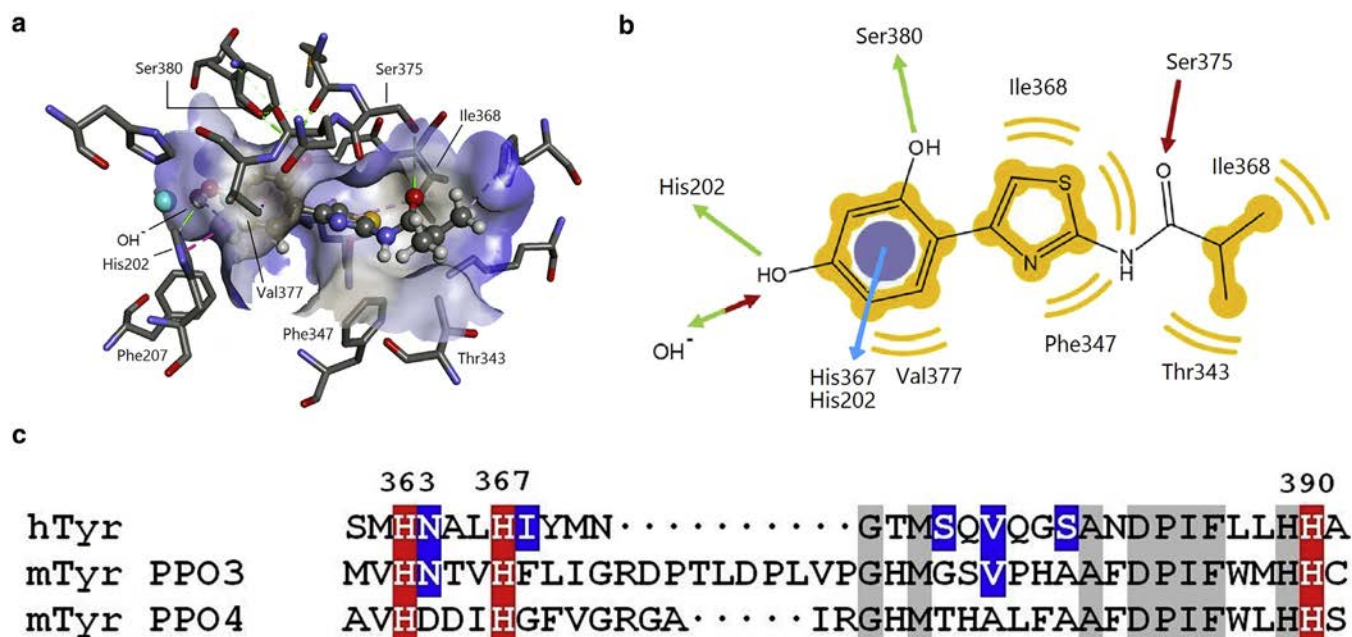


Figure 4. Structural aspects of hTyr and mTyr. (a) Thiamidol (Beiersdorf AG, Hamburg, Germany) docked into a homology model of hTyr as detailed in the text. The inner surface of the substrate binding pocket is colored according to hydrophobicity: gray, hydrophobic; blue, hydrophilic. (b) Schematic view of interactions stabilizing the modeled enzyme-ligand complex. Hydrophobic interactions are depicted by yellow arcs, hydrogen bonding interactions by red and green arrows, and π - π bonding by a blue arrow. (c) Comparison of the amino acid sequences of hTyr with mTyr isoenzymes PPO3 and PPO4 in the CuB region. Cu-coordinating histidines are highlighted in red, residues probably interacting with Thiamidol are in blue. hTyr, human tyrosinase; mTyr, mushroom tyrosinase.

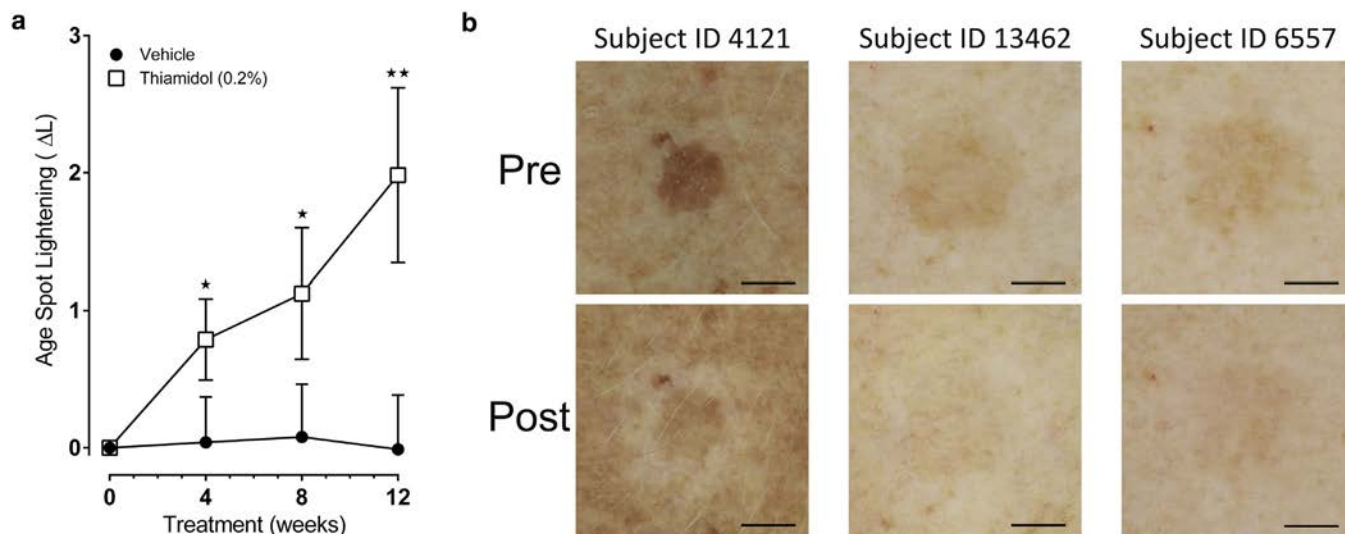


Figure 5. Effects of Thiamidol on age spots in clinical studies. (a) Age spots on the volar forearms of each subject were treated twice daily for 12 weeks with 0.2% Thiamidol (Beiersdorf AG, Hamburg, Germany) or with the vehicle only as a control using a spot applicator. Efficacy was evaluated after 4, 8, and 12 weeks. Data represent the mean \pm standard error of the mean of 17 subjects. * $P < 0.05$, ** $P < 0.01$; statistically significant versus the control. (b) Visual monitoring of the lightening of age spots during treatment. Photographs were taken (top) before and (bottom) after 12 weeks of treatment. Images show three representative age spots. Scale bar = 5 mm. Pre, before treatment; Post, after 12 weeks of treatment.

than 100 $\mu\text{mol/L}$ (Jeon et al., 2005). As an inhibitor of hTyr, kojic acid is much less efficient, with an IC_{50} of about 500 $\mu\text{mol/L}$. Kojic acid exhibits a mixed type of inhibition, with a K_i of 145 $\mu\text{mol/L}$, indicating that it binds to the deoxy-form of tyrosinase (Sun et al., 2014). When used to treat the MelanoDerm model, kojic acid shows an exceptionally steep dose-response curve, with relative inhibition increasing from 5% at 150 $\mu\text{mol/L}$ to more than 75% inhibition at 900 $\mu\text{mol/L}$ (see Figure 2c). This fact may be the main reason for the very limited efficacy of kojic acid in vivo. Concerning the safety of kojic acid, the European Scientific Committee on Consumer Safety (2012) now considers kojic acid at concentrations up to 1.0% to be safe for cosmetic products when applied to healthy skin, a view shared by the Cosmetic Ingredient Review Expert Panel (Burnett et al., 2010).

Rhododendrol was granted quasi-drug status in Japan in 2008 and was used as a whitening ingredient in cosmetic products. It was assumed to be a competitive inhibitor of tyrosinase. However, in 2013, rhododendrol-containing products were recalled in 10 Asian countries when close to 20,000 consumers developed leukoderma after using the products. It was shown that rhododendrol is not only an inhibitor but is also a substrate of both hTyr (Ito et al., 2014a) and mTyr (Ito et al., 2014b). The tyrosinase-dependent accumulation of endoplasmic reticulum stress and/or activation of the apoptotic pathway may contribute to the melanocyte cytotoxicity of rhododendrol (Sasaki et al., 2014).

The 4-substituted resorcinol motif has been known for some time as an efficient chemical moiety that inhibits tyrosinase (Khatib et al., 2005). Many natural compounds that have been identified as whitening agents, mainly flavonoids, contain this motif (Shimizu et al., 2000, 2011). Because the bioavailability of flavonoids is generally low, our goal was to identify resorcinol derivatives with better

effectiveness and bioavailability. 4-Butylresorcinol had already been identified as an inhibitor of mouse and human tyrosinase (Kim et al., 2005; Kolbe et al., 2013) and of the dihydroxyindole carboxylic acid oxidase activity of mouse TYRP1 (Katagiri et al., 2001), and it is commercially available for the medical and cosmetic treatment of hyperpigmentation (Bohnsack et al., 2012; Jimenez and Garcia-Carmona, 1997; Kim et al., 2005). Nevertheless, detailed kinetic data of 4-butylresorcinol were still missing. In the hTyr assay, we found a strictly competitive type of inhibition by 4-butylresorcinol with a K_i of 9.1 $\mu\text{mol/L}$, which is in excellent agreement with the IC_{50} value determined (Table 1).

In our in vitro experiments, Thiamidol, with an IC_{50} of 1.1 $\mu\text{mol/L}$ in the hTyr enzyme assay and 0.9 $\mu\text{mol/L}$ in the MelanoDerm skin model, was by far the most effective of all substances tested. Further experiments confirmed that Thiamidol is a strictly competitive inhibitor (Figure 2b) and not a substrate for tyrosinase (see Supplementary Figure S1), and, thus, Thiamidol is not converted to a toxic and potentially leukoderma-inducing quinone. Therefore, Thiamidol was selected for clinical studies to assess its efficacy in vivo. A study of Thiamidol using a spot applicator showed continuous improvement in the appearance of age spots over the entire 12-week treatment period, reaching statistical significance as early as 4 weeks. These results show a strong pigment-reducing efficacy of the Thiamidol test product and a clear clinical benefit in the management of skin hyperpigmentation.

In conclusion, our study shows that the structural differences between hTyr and mTyr are reflected in the molecular features of effective inhibitors. Highly effective inhibitors of hTyr are distinctively different from inhibitors of mTyr and vice versa. Thiamidol (isobutylamido thiazolyl resorcinol) was identified as a potent inhibitor of hTyr with a remarkable efficacy in vitro and in vivo. However, the full potential of this compound needs to be explored in further studies.

MATERIALS AND METHODS

Human tyrosinase

A truncated, His-tagged form of hTyr (hTyr-D_{His}) comprising the catalytic domain of hTyr was expressed in HEK 293 cells and purified by metal affinity chromatography on Ni²⁺-Sephacel (GE Healthcare, Munich, Germany) as described elsewhere (Cordes et al., 2013). The resulting preparation had the same catalytic properties as wild-type hTyr.

Sources of inhibitors

From the Evotec compound library (Evotec, Hamburg, Germany), 50,000 compounds, covering a wide chemical space, were selected to conduct an HTS for hTyr inhibitors, assessed using the Tyr assay described in the next section. Derivatives of promising lead compounds were then synthesized for further optimization. The other inhibitors were purchased from various suppliers (see [Supplementary Materials](#) online for details).

Tyrosine assay and HTS procedure

Full details of the L-dopa oxidase activity and the HTS screening procedures used can be found in the [Supplementary Materials](#).

Molecular modeling

In silico docking was based on a new homology model of hTyr, described elsewhere (Mann et al., 2017). The simulations were performed using Molegro Virtual Docker (Molegro, Aarhus, Denmark). Discovery Studio Visualizer 4.0 (Accelrys, San Diego, CA) was used for visual data analysis and presentation. The sequences were taken from the UniProt database (UniProt Consortium, 2017).

Skin model assays

Full details of MelanoDerm tissues used as a skin model and quantitation of their melanin content can be found in the [Supplementary Materials](#).

Melanocyte cultures

Full details of melanocyte cultures and quantitation of their melanin content can be found in the [Supplementary Materials](#).

Clinical studies

Two randomized in vivo studies (blinded for the test products, open for the untreated control) were conducted. One study enrolled 18 female subjects (56–71 years of age), with 17 subjects completing the study. The second study was performed with 19 subjects (18 females, 1 male; 58–70 years of age), with all 19 subjects completing the study. Each subject applied two different formulations twice daily to age spots on their volar forearms using a spot applicator. The formulations differed only in the active ingredient: 0.2% Thiamidol versus vehicle in the first study, 0.1% Thiamidol versus vehicle in the second study. One age spot per subject was treated with a formula containing the active ingredient, and a control spot was treated with the vehicle only. Pigmentation of the age spots was analyzed as described in the [Supplementary Materials](#). The in vivo studies were conducted according to the recommendations of the current version of the Declaration of Helsinki and the guidelines of the International Conference on Harmonization Good Clinical Practice. All participants in these studies provided written informed consent. In addition, the studies were approved and cleared by the institutional review board of Beiersdorf AG (Hamburg, Germany).

CONFLICT OF INTEREST

TM, WG, JB, KE, CS, HW, FS, and LK are employees of Beiersdorf AG. Thiamidol is patented by Beiersdorf AG. None of the other authors has a conflict of interest to declare.

SUPPLEMENTARY MATERIAL

Supplementary material is linked to the online version of the paper at www.jidonline.org, and at <https://doi.org/10.1016/j.jid.2018.01.019>.

REFERENCES

- Abu Ubeid A, Zhao L, Wang Y, Hantash BM. Short-sequence oligopeptides with inhibitory activity against mushroom and human tyrosinase. *J Invest Dermatol* 2009;129:2242–9.
- Bohnsack K, Koop U, Hiddemann S, Kolbe L, Rippke F. Pigmentation reducing efficacy and tolerability of six new face care formulations containing 4-n-butylresorcinol, poster no. P864. Poster presented at: 21st EADV Congress, September 27-30, 2012; Prague, Czech Republic.
- Briganti S, Camera E, Picardo M. Chemical and instrumental approaches to treat hyperpigmentation. *Pigment Cell Res* 2003;16:101–10.
- Burnett CL, Bergfeld WF, Belsito DV, Hill RA, Klaassen CD, Liebler DC, et al. Final report of the safety assessment of Kojic acid as used in cosmetics. *Int J Toxicol* 2010;29(6 Suppl.). 244S–73.
- Chang TS. An updated review of tyrosinase inhibitors. *Int J Mol Sci* 2009;10:2440–75.
- Chen QX, Ke LN, Song KK, Huang H, Liu XD. Inhibitory effects of hexyl-resorcinol and dodecylresorcinol on mushroom (*Agaricus bisporus*) tyrosinase. *Protein J* 2004;23:135–41.
- Cordes P, Sun W, Wolber R, Kolbe L, Klebe G, Röhm KH. Expression in non-melanogenic systems and purification of soluble variants of human tyrosinase. *Biol Chem* 2013;394:685–93.
- Curto EV, Kwong C, Hermersdörfer H, Glatt H, Santis C, Virador V, et al. Inhibitors of mammalian melanocyte tyrosinase: in vitro comparisons of alkyl esters of gentisic acid with other putative inhibitors. *Biochem Pharmacol* 1999;57:663–72.
- Espin JC, Varon R, Fenoll LG, Gilabert MA, Garcia-Ruiz PA, Tudela J, et al. Kinetic characterization of the substrate specificity and mechanism of mushroom tyrosinase. *Eur J Biochem* 2000;267:1270–9.
- Fogal S, Carotti M, Giaretta L, Lanciari F, Nogara L, Bubacco L, Bergantino E. Human tyrosinase produced in insect cells: a landmark for the screening of new drugs addressing its activity. *Mol Biotechnol* 2015;57:45–57.
- Garcia-Jimenez A, Teruel-Puche JA, Berna J, Rodriguez-Lopez JN, Tudela J, Garcia-Canovas F. Action of tyrosinase on alpha and beta-arbutin: A kinetic study. *PLoS One* 2017;12:e0177330.
- Garcia-Jimenez A, Teruel-Puche JA, Berna J, Rodriguez-Lopez JN, Tudela J, Garcia-Ruiz PA, Garcia-Canovas F. Characterization of the action of tyrosinase on resorcinols. *Bioorg Med Chem* 2016;24:4434–43.
- Garcia-Molina F, Hiner AN, Fenoll LG, Rodriguez-Lopez JN, Garcia-Ruiz PA, Garcia-Canovas F, et al. Mushroom tyrosinase: catalase activity, inhibition, and suicide inactivation. *J Agric Food Chem* 2005;53:3702–9.
- Ghanem G, Fabrice J. Tyrosinase related protein 1 (tyrp1/gp75) in human cutaneous melanoma. *Mol Oncol* 2011;5:150–5.
- Hearing VJ Jr, Ekel TM, Montague PM, Nicholson JM. Mammalian tyrosinase. Stoichiometry and measurement of reaction products. *Biochim Biophys Acta* 1980;611:251–68.
- Ismaya WT, Rozeboom HJ, Weijn A, Mes JJ, Fusetti F, Wichers HJ, Dijkstra BW. Crystal structure of *Agaricus bisporus* mushroom tyrosinase: identity of the tetramer subunits and interaction with tropolone. *Biochemistry* 2011;50:5477–86.
- Ito S, Gerwat W, Kolbe L, Yamashita T, Ojika M, Wakamatsu K. Human tyrosinase is able to oxidize both enantiomers of rhododendrol. *Pigment Cell Melanoma Res* 2014a;27:1149–53.
- Ito S, Ojika M, Yamashita T, Wakamatsu K. Tyrosinase-catalyzed oxidation of rhododendrol produces 2-methylchromane-6,7-dione, the putative ultimate toxic metabolite: implications for melanocyte toxicity. *Pigment Cell Melanoma Res* 2014b;27:744–53.
- Ito S, Wakamatsu K. A convenient screening method to differentiate phenolic skin whitening tyrosinase inhibitors from leukoderma-inducing phenols. *J Dermatol Sci* 2015;80:18–24.

- Jeon SH, Kim KH, Koh JU, Kong KH. Inhibitory effects of L-Dopa oxidation of tyrosinase by skin whitening agents. *Bull Korean Chem Soc* 2005;26:1135–7.
- Jimbow K, Obata H, Pathak MA, Fitzpatrick TB. Mechanism of depigmentation by hydroquinone. *J Invest Dermatol* 1974;62:436–49.
- Jimenez M, Garcia-Carmona F. 4-substituted resorcinols (sulfite alternatives) as slow-binding inhibitors of tyrosinase catecholase activity. *J Agric Food Chem* 1997;45:2061–5.
- Kang HH, Rho HS, Hwang JS, Oh SG. Depigmenting activity and low cytotoxicity of alkoxy benzoates or alkoxy cinnamate in cultured melanocytes. *Chem Pharm Bull (Tokyo)* 2003;51:1085–8.
- Kanteev M, Goldfeder M, Fishman A. Structure-function correlations in tyrosinases. *Prot Sci* 2015;24:1360–9.
- Katagiri T, Okubo T, Oyobikawa M, Futaki K, Shaku M, Kawai M, et al. Inhibitory action of 4-n-butylresorcinol on melanogenesis and its skin whitening effect. *J Soc Cosmet Chem Jpn* 2001;35:42–9.
- Khatib S, Nerya O, Musa R, Shmuel M, Tamir S, Vaya J. Chalcones as potent tyrosinase inhibitors: the importance of a 2,4-substituted resorcinol moiety. *Bioorg Med Chem* 2005;13:433–41.
- Kim DS, Kim SY, Park SH, Choi YG, Kwon SB, Kim MK, et al. Inhibitory effects of 4-n-butylresorcinol on tyrosinase activity and melanin synthesis. *Biol Pharm Bull* 2005;28:2216–9.
- Kim H, Choi HR, Kim DS, Park KC. Topical hypopigmenting agents for pigmentary disorders and their mechanisms of action. *Ann Dermatol* 2012;24:1–6.
- Kim YJ, Uyama H. Tyrosinase inhibitors from natural and synthetic sources, structure, inhibition mechanism and perspective for the future. *Cell Mol Life Sci* 2005;62:1707–23.
- Kolbe L, Mann T, Gerwat W, Batzer J, Ahlheit S, Scherner C, et al. 4-n-butylresorcinol, a highly effective tyrosinase inhibitor for the topical treatment of hyperpigmentation. *J Eur Acad Dermatol Venereol* 2013;27:19–23.
- Lai X, Soler-Lopez M, Wichers HJ, Dijkstra BW. Large-scale recombinant expression and purification of human tyrosinase suitable for structural studies. *PLoS One* 2016;11:e0161697.
- Lai X, Wichers HJ, Soler-Lopez M, Dijkstra BW. Structure of human tyrosinase related protein 1 reveals a binuclear zinc active site important for melanogenesis. *Angew Chem Int Ed Engl* 2017;56:9812–5.
- Lee SY, Baek N, Nam TG. Natural, semisynthetic and synthetic tyrosinase inhibitors. *J Enzyme Inhib Med Chem* 2014;31:1–13.
- Mann T, Gerwat W, Wenck H, Röhm KH, Kolbe L. Isobutylamido thiazolyl resorcinol a new powerful inhibitor of human tyrosinase. *Pigment Cell Melanoma Res* 2017:e85.
- Matoba Y, Kumagai T, Yamamoto A, Yoshitsu H, Sugiyama M. Crystallographic evidence that the dinuclear copper center of tyrosinase is flexible during catalysis. *J Biol Chem* 2006;281:8981–90.
- Nesterov A, Zhao J, Minter D, Hertel C, Ma W, Abeyasinghe P, et al. 1-(2,4-dihydroxyphenyl)-3-(2,4-dimethoxy-3-methylphenyl)propane, a novel tyrosinase inhibitor with strong depigmenting effects. *Chem Pharm Bull (Tokyo)* 2008;56:1292–6.
- Olivares C, Garcia-Borrón JC, Solano F. Identification of active site residues involved in metal cofactor binding and stereospecific substrate recognition in mammalian tyrosinase. Implications to the catalytic cycle. *Biochemistry* 2002;41:679–86.
- Palumbo A, d'Ischia M, Misuraca G, Prota G. Mechanism of inhibition of melanogenesis by hydroquinone. *Biochim Biophys Acta* 1991;1073:85–90.
- Penney KB, Smith CJ, Allen JC. Depigmenting action of hydroquinone depends on disruption of fundamental cell processes. *J Invest Dermatol* 1984;82:308–10.
- Pretzler M, Bijelic A, Rompel A. Heterologous expression and characterization of functional mushroom tyrosinase (AbPPO4). *Sci Rep* 2017;7:1810.
- Ramsden CA, Riley PA. Tyrosinase: the four oxidation states of the active site and their relevance to enzymatic activation, oxidation and inactivation. *Bioorg Med Chem* 2014;22:2388–95.
- Rescigno A, Sollai F, Pisu B, Rinaldi A, Sanjust E. Tyrosinase inhibition, general and applied aspects. *J Enzyme Inhib Med Chem* 2002;17:207–18.
- Sasaki M, Kondo M, Sato K, Umeda M, Kawabata K, Takahashi Y, et al. Rhododendrol, a depigmentation-inducing phenolic compound, exerts melanocyte cytotoxicity via a tyrosinase-dependent mechanism. *Pigment Cell Melanoma Res* 2014;27:754–63.
- Schweikardt T, Olivares C, Solano F, Jaenicke E, Garcia-Borrón JC, Decker H. A three-dimensional model of mammalian tyrosinase active site accounting for loss of function mutations. *Pigment Cell Res* 2007;20:394–401.
- Scientific Committee on Consumer Products. Opinion on β -arbutin, http://ec.europa.eu/health/archive/ph_risk/committees/04_sccp/docs/sccp_o_134.pdf; 2008 (accessed November 21, 2017).
- Scientific Committee on Consumer Safety. Opinion on kojic acid, http://ec.europa.eu/health/scientific_committees/consumer_safety/docs/sccs_o_098.pdf; 2012 (accessed November 21, 2017).
- Sendovski M, Kanteev M, Ben-Yosef VS, Adir N, Fishman A. First structures of an active bacterial tyrosinase reveal copper plasticity. *J Mol Biol* 2011;405:227–37.
- Shimizu K, Kondo R, Sakai K. Inhibition of tyrosinase by flavonoids, stilbenes and related 4-substituted resorcinols: structure-activity investigations. *Planta Med* 2000;66:11–5.
- Shimizu MM, Melo GA, Brombini Dos Santos A, Bottcher A, Cesarino I, Araújo P, et al. Enzyme characterisation, isolation and cDNA cloning of polyphenol oxidase in the hearts of palm of three commercially important species. *Plant Physiol Biochem* 2011;49:970–7.
- Smith CJ, O'Hare KB, Allen JC. Selective cytotoxicity of hydroquinone for melanocyte-derived cells is mediated by tyrosinase activity but independent of melanin content. *Pigment Cell Res* 1988;1:386–9.
- Solano F, Briganti S, Picardo M, Ghanem G. Hypopigmenting agents: an updated review on biological, chemical and clinical aspects. *Pigment Cell Res* 2006;19:550–71.
- Stratigos AJ, Katsambas AD. Optimal management of recalcitrant disorders of hyperpigmentation in dark-skinned patients. *Am J Clin Derm* 2004;5:161–8.
- Sugimoto K, Nomura K, Nishimura T, Kiso T, Sugimoto K, Kuriki T. Syntheses of α -arbutin- α -glycosides and their inhibitory effects on human tyrosinase. *J Biosci Bioeng* 2005;99:272–6.
- Sun W, Wendt M, Klebe G, Röhm KH. On the interpretation of tyrosinase inhibition kinetics. *J Enzyme Inhib Med Chem* 2014;29:92–9.
- Tripathi RK, Hearing VJ, Urabe K, Aroca P, Spritz RA. Mutational mapping of the catalytic activities of human tyrosinase. *J Biol Chem* 1992;267:23707–12.
- UniProt Consortium. UniProt: the universal protein knowledgebase. *Nucleic Acids Res* 2017;45:D158–69.
- US Food and Drug Administration, Department of Health and Human Services. Skin bleaching drug products for over-the-counter human use; proposed rule. 71 Federal Register 51146-511521 (codified at 21 CFR Part 310); 2006.
- Vielhaber G, Schmaus G, Jacobs K, Franke H, Lange S, Herrmann M, et al. 4-(1-phenylethyl)1,3-benzenediol: a new, highly efficient lightening agent. *Int J Cosmet Sci* 2007;29:65–6.
- Wendt M. Rationales design neuer tyrosinase-inhibitoren. PhD thesis. Marburg, Germany: University of Marburg Medical School; 2006.
- Ying YH, Lee SJ, Chung MH, Ying HJ, Suk JL, Myung HC, et al. Aloesin and arbutin inhibit tyrosinase activity in a synergistic manner via a different action mechanism. *Arch Pharm Res* 1999;22:232–6.



This work is licensed under a Creative Commons Attribution-NonCommercial-NoDerivatives 4.0 International License. To view a copy of this license, visit <http://creativecommons.org/licenses/by-nc-nd/4.0/>

Isobutylamido thiazolyl resorcinol a highly effective inhibitor of human tyrosinase

Mann T¹, Gerwat W¹, Wenck H¹, Roehm KH², Kolbe L¹ | ¹Research & Development, Beiersdorf AG, Hamburg, Germany, ²Institute of Physiological Chemistry, Philipps University, Marburg, Germany

INTRODUCTION

Melasma, actinic lentigines and post-inflammatory hyperpigmentation are major cosmetic concerns. Various strategies have been proposed to reduce unwanted melanin production in human skin. Tyrosinase is the rate-limiting enzyme of melanin production and the obvious target for inhibitors of hyperpigmentation. Due to their immediate and reversible mode of action, selective tyrosinase inhibitors are considered not only most effective but also very safe reducers of hyperpigmentation.

However, most known tyrosinase inhibitors lack clinical efficacy because they were selected based on their ability to inhibit mushroom tyrosinase. To overcome this problem, we expressed human tyrosinase in a mammalian cell system and used the recombinant enzyme to screen a library of 50,000 chemically diverse compounds for inhibition of human tyrosinase. Screening hits were developed to the final active ingredient by classical hit-to-lead-to candidate chemistry [1].

MATERIAL AND METHODS

The L-Dopa oxidase activity of human Tyrosinase was assayed by a modification of the method of Winder and Harris. In this assay, the reaction product, L-dopaquinone, is trapped by MBTH (3-methyl-2-benzothiazoline hydrazone) to yield a stable pink dye that can be quantified at 490 nm. Dose-response curves were obtained by testing various concentrations of each inhibitor at a fixed substrate (L-Dopa) concentration. Inhibitor concentrations at 50% inhibition (IC₅₀ values) were estimated by fitting a four-parameter logistic equation to the profiles.

For *in vivo* efficacy, pigmentation of age spots was measured by spectrometry and digital photography. Significance of results was tested using the Wilcoxon's signed rank test.

RESULTS

Isobutylamido thiazolyl resorcinol (Thiamidol) was identified as a very powerful inhibitor of human tyrosinase [2]. Compared to other well-known inhibitors of human skin pigmentation, Thiamidol was by far the most active compound. Further analysis of the mode of action revealed that Thiamidol is a strictly competitive inhibitor of the human enzyme and only marginally inhibits mushroom tyrosinase. *In vivo* studies showed a strong reduction in age spot visibility after treatment with topical formulations containing Thiamidol.

CONCLUSION

Thiamidol is a very effective inhibitor of human tyrosinase (*in vitro*) and a highly effective inhibitor of hyperpigmentation (*in vivo*). In comparison to well-known ingredients like Hydroquinone, Arbutin, Kojic Acid and Rucinol, Thiamidol is much more effective. However, the full potential of this compound needs to be explored in further studies.

References

- [1] Mann T, Scherner C, Röhm KH, Kolbe L. Structure-Activity Relationships of Thiazolyl Resorcinols, Potent and Selective Inhibitors of Human Tyrosinase. *Int J Mol Sci*. 2018 Feb 28;19(3). pii: E690. doi: 10.3390/ijms19030690
- [2] Mann T, Gerwat W, Batzer J, Eggers K, Scherner C, Wenck H, Stäb F, Hearing VJ, Röhm KH, Kolbe L. Inhibition of Human Tyrosinase Requires Molecular Motifs Distinctively Different from Mushroom Tyrosinase. *J Invest Dermatol*. 2018 Jul;138(7):1601-1608. doi: 10.1016/j.jid.2018.01.019

THIAMIDOL IS BY FAR THE MOST POTENT TYROSINASE INHIBITOR

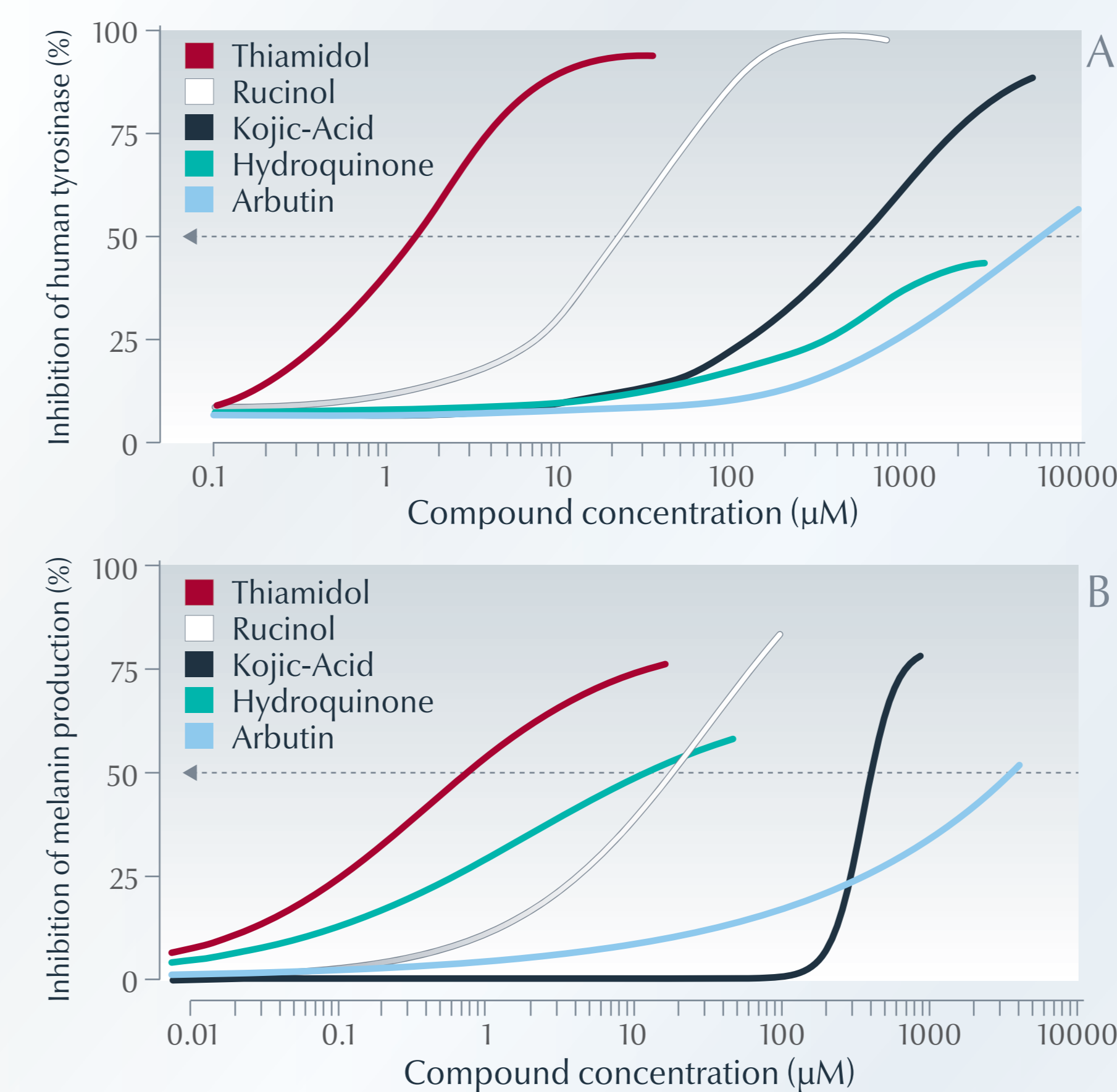


Figure 1(A): Inhibition of human tyrosinase activity. Thiamidol, Rucinol, Kojic Acid, Hydroquinone and Arbutin were tested using purified human tyrosinase and various concentrations of inhibitors as noted. Data represent means of 3 independent experiments. (B) Inhibition of melanin production in MelanoDerm skin models. The melanin content of each skin model was determined after 13 days of cultivation in the presence of various inhibitors at the concentrations noted. Data represent means of 5 independent experiments.

THIAMIDOL PERFECTLY FITS INTO THE ACTIVE SITE OF HUMAN TYROSINASE

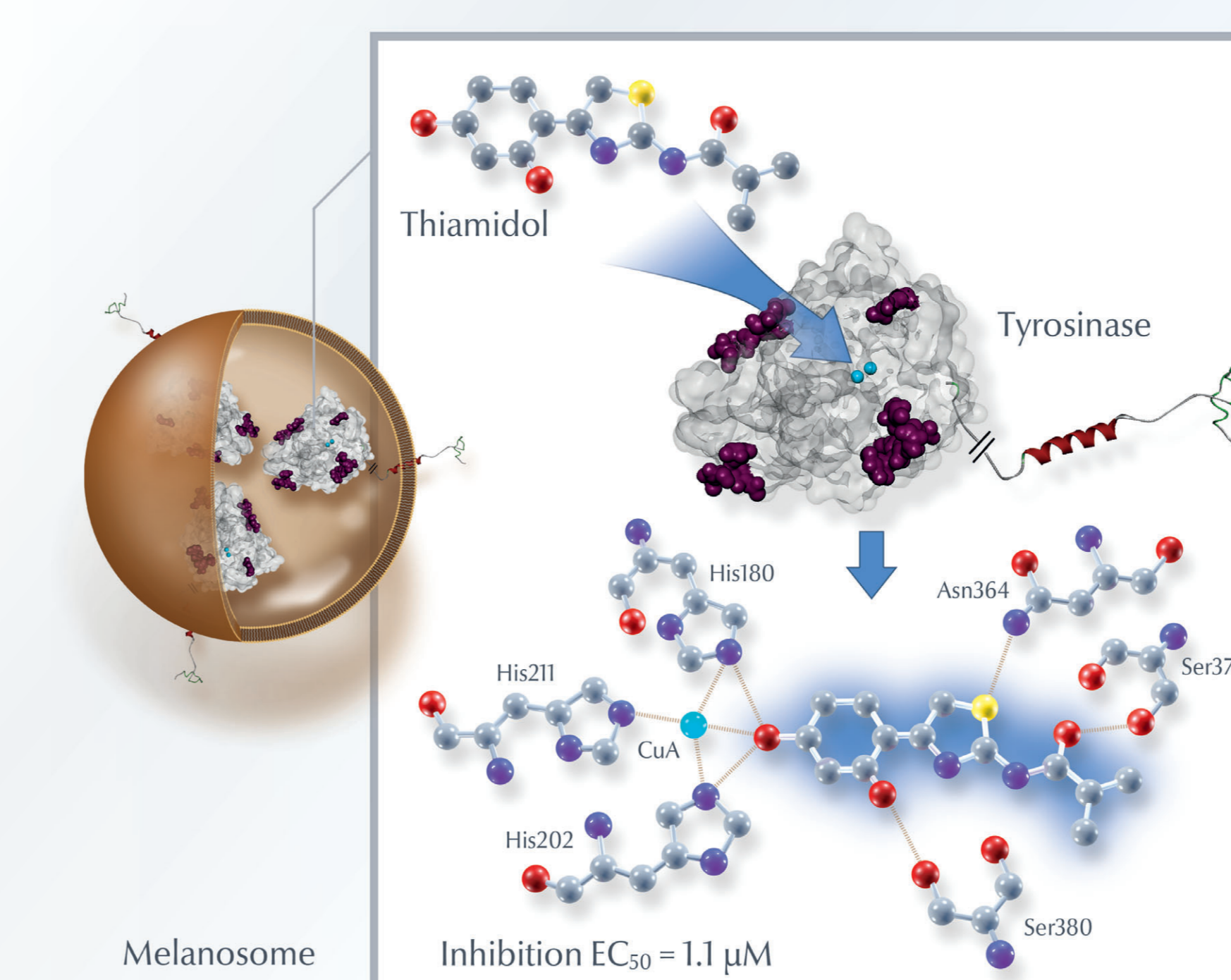


Figure 2: Thiamidol is a competitive inhibitor of human tyrosinase. Almost all parts of the molecule interact with amino acid residues in the binding pocket of the active site and, consequently, blocking the enzyme activity.

THIAMIDOL IS A HIGHLY SELECTIVE INHIBITOR OF HUMAN TYROSINASE

Active ingredient	IC ₅₀ inhibition of Mushroom Tyrosinase	IC ₅₀ inhibition of Human Tyrosinase
Dimethoxytolyl Propylresorcinol	0.2 μM#	No inhibition!*
Phenylethyl resorcinol	0.5 μM#	131 μM*
Hexylresorcinol	1.2 μM#	94 μM*
Rucinol	0.6 μM*	21 μM*
Thiamidol	108.1 μM*	1 μM*

Figure 3: Inhibition of human versus mushroom tyrosinase by various resorcinol derivatives. Thiamidol is a potent inhibitor of human tyrosinase but only a weak inhibitor of mushroom tyrosinase. Other resorcinol derivatives are more selective for mushroom tyrosinase. (*BDF data on file, #published data)

THIAMIDOL VISIBLY INHIBITS MELANIN PRODUCTION

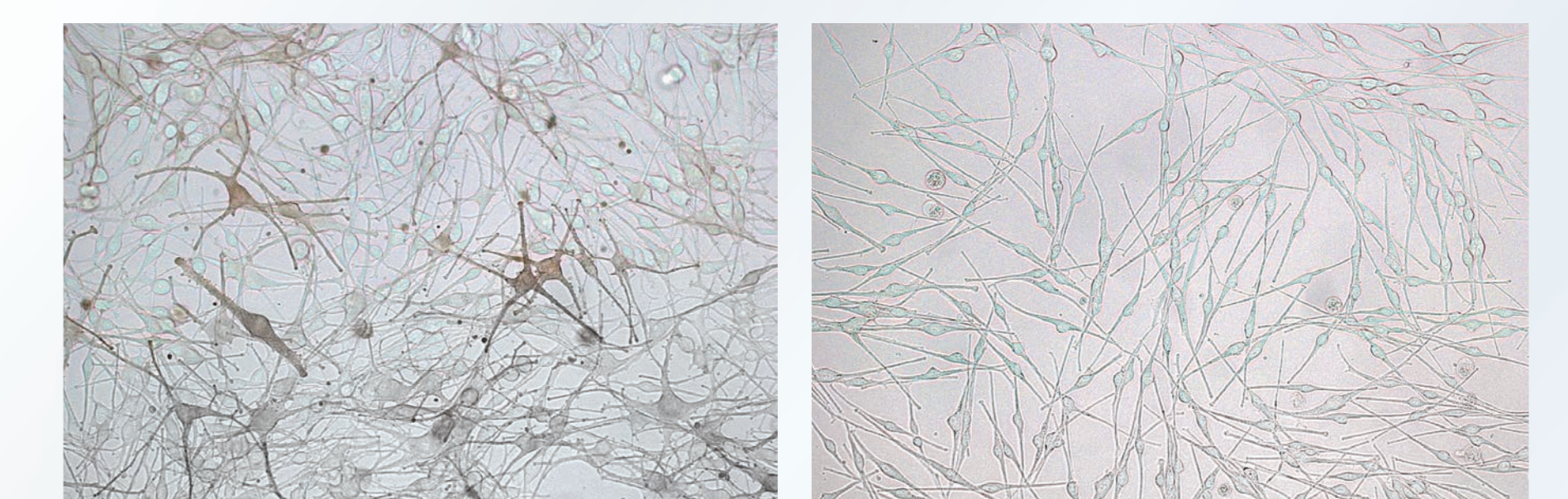


Figure 4: Impact of human tyrosinase inhibition by thiamidol on cultured primary human melanocytes. Melanocytes from African donors were cultivated for 2 weeks without (left) or with 5 μM thiamidol (right) in microplate dishes; photographs were taken in bright field mode (scale bar = 200 μm).

THIAMIDOL SIGNIFICANTLY LIGHTENS AGE SPOTS

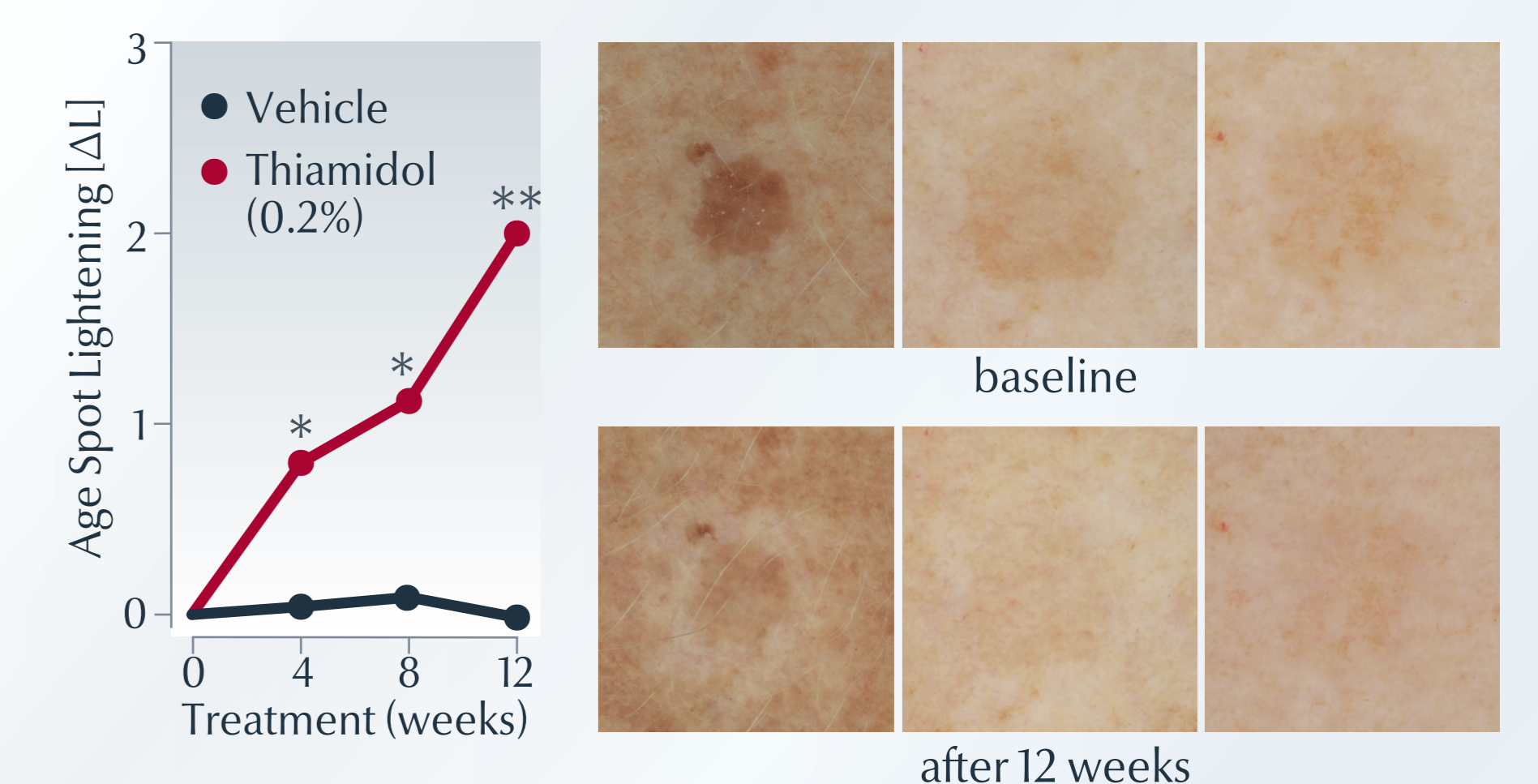


Figure 5: Effects of thiamidol on age spots in clinical studies. (A) Age spots on the volar forearms of each subject were treated twice daily for 12 weeks with 0.2% thiamidol (●) or with the vehicle only (●) using a spot applicator. Efficacy was evaluated after 4, 8 and 12 weeks. Data represent means ± SEM of 17 subjects. *p < 0.05, **p < 0.01; statistically significant versus the control. (B) Visual monitoring of the lightening of age spots during treatment. Photographs were taken prior to (top row) and after 12 weeks (bottom row) of treatment. Images show 3 representative age spots (scale bar = 5 mm).

Licochalcone A activates Nrf2 *in vitro* and contributes to licorice extract-induced lowered cutaneous oxidative stress *in vivo*

Jochen Kühnl, Dennis Roggenkamp, Sandra A. Gehrke, Franz Stäb, Horst Wenck, Ludger Kolbe and Gitta Neufang

Beiersdorf AG, Research Skin Care, Hamburg, Germany

Correspondence: Gitta Neufang, PhD, Beiersdorf AG, Germany, Tel.: +49-40-4909-6676, Fax: +49-40-4909-186676, e-mail: gitta.neufang@beiersdorf.com

Abstract: The retrochalcone licochalcone A (LicA) has previously been shown to possess antimicrobial and anti-inflammatory properties. In this study, we focused on pathways responsible for the antioxidative properties of LicA. *In vitro*, LicA protected from oxidative stress mediated by reactive oxygen species (ROS) by activating the expression of cytoprotective phase II enzymes. LicA induced nuclear translocation of NF-E2-related factor 2 (Nrf2) in primary human fibroblasts and elevated the expression of the cytoprotective and anti-inflammatory enzymes heme oxygenase 1 and glutamate–cysteine ligase modifier subunit. LicA-treated cells displayed a higher ratio of reduced to oxidized glutathione and decreased concentrations of ROS in UVA-irradiated human dermal fibroblasts, as well as in activated neutrophils. *In vivo*, ultraweak photon emission analysis of skin treated with LicA-rich

licorice extract revealed a significantly lowered UVA-induced luminescence, indicative for a decrease in oxidative processes. We conclude from these data that topical application of licorice extract is a promising approach to induce Nrf2-dependent cytoprotection in human skin.

Abbreviations: fMLP, N-formyl-MET-LEU-PHE; HO-1, heme oxygenase 1; GCLM, glutamate–cysteine ligase regulatory subunit; LicA, licochalcone A; Nrf2, NF-E2-related factor 2; ROS, reactive oxygen species; UPE, ultraweak photon emission.

Key words: anti-inflammatory – cytoprotection – heme oxygenase 1 – licochalcone A – Nrf2

Accepted for publication 31 October 2014

Introduction

Human skin is an efficient permeability barrier, protecting the organism from constant exposure to environmental stressors, such as UV radiation and harmful chemicals (1,2). To cope with UV radiation and electrophilic chemicals, skin cells have evolved cytoprotective antioxidant defense systems and detoxifying enzymes, scavenging harmful reactive oxygen species (ROS) and electrophiles (3,4). A key player in orchestrating the cytoprotective response is the NF-E2-related factor 2 (Nrf2) (5). Several studies demonstrated that Nrf2 activation efficiently protects cells from ROS-induced damage, such as lipid peroxidation, as well as DNA and protein damage *in vitro* and *in vivo* by inducing the expression of numerous detoxifying enzymes and antioxidant proteins. Conversely, knockout of the transcription factor in mice results in enhanced susceptibility to hyperoxic injury and ROS-mediated inflammation (6–8).

Important downstream effector proteins of Nrf2 are heme oxygenase 1 (HO-1) and glutamate–cysteine ligase (GCLM). The HO-1-catalysed degradation of heme results in the formation of the antioxidative and anti-inflammatory mediators biliverdin and carbon monoxide (CO), mediating anti-inflammatory effects by suppressing pro-inflammatory cytokines and inducing tolerogenic actions in adaptive immune responses (9). HO-1 was referred to as a ‘therapeutic amplification funnel’, attributing beneficial effects of anti-inflammatory molecules, such as IL-10, 15-PGJ2 and acetylsalicylic acid to HO-1 activation (10).

Another important downstream effector of Nrf2-signalling is the glutamate–cysteine ligase modifier subunit (GCLM), an integral part of the rate-limiting enzyme for glutathione synthesis

(11,12). The scavenging capacity of GSH provides a major line of defense against oxidative stress and electrophilic chemicals. In skin, Nrf2 activation can be triggered by UV radiation or phytochemicals such as sulforaphane (SF) and quercetin in keratinocytes, fibroblasts and melanocytes *in vitro* (4,13–18) Nrf2 activation was frequently associated with protective effects against UVA irradiation. Topical application of SF exerts beneficial effects on UV-caused erythema and preventive effects against UV-induced or chemically induced skin cancer *in vivo*.

We report here that the retrochalcone licochalcone A (LicA) and the LicA-rich root extract from *Glycyrrhiza inflata*, protect skin cells from oxidative stress *in vitro* and *in vivo* by activating Nrf2, resulting in elevated HO-1 and GCLM expression that translate into decreased intracellular ROS concentration. The relevance of the *in vitro* data is substantiated by *in vivo* ultraweak photon emission (UPE) data, displaying that topical application of LicA-rich lotion significantly decrease the UVA-induced UPE signal as an indicator for oxidative processes in the skin. This study provides mechanistic insights into the protective effects of LicA against various oxidative stresses (19–21). Moreover, they link *in vitro* results with *in vivo* efficacy, showing that topical application of phytochemicals, such as LicA, is able to protect skin from subsequent UV radiation.

Material and methods

Cell culture

Primary human fibroblasts were isolated from plastic surgery-derived skin biopsies of healthy donors as described by Roggenkamp et al. (22). Dermal fibroblasts were cultivated in Dulbecco’s modified Eagle’s medium (Invitrogen, Darmstadt, Germany)

supplemented with 10% foetal calf serum (FCS) (PAA, Linz, Austria), penicillin/streptomycin (50 µg/ml) and 1% L-glutamine (all from Invitrogen, Darmstadt, Germany) at 37°C and 7% CO₂. Human granulocytes were isolated from buffy coats as stated in Kolbe et al. (20).

Cells were treated with licochalcone A (LicA) purchased from Calbiochem-Novabiochem (CAS 58749-22-7, Bad Soden, Germany) or sulforaphane (SF) (Sigma-Aldrich, Munich, Germany) as described in figure legends.

Neutral red assay

To determine suitable substance concentrations, we performed Neutral Red viability experiments according to manufacturer's instructions. Briefly, cells were incubated with licochalcone A and sulforaphane for 24 h, washed with PBS and treated with 0.05 mg/ml neutral red solution for 2.5 h. Cellular neutral red uptake was measured at 540 nm using a SAFIRE spectrometer (Tecan, Crailsheim, Germany). Highest applicable concentrations were 9 µM for LicA and 10 µM for sulforaphane corresponding to ~90% cell viability.

Real-time quantitative PCR (RT-PCR)

Total RNA was isolated from dermal fibroblasts using the RNeasy Mini Kit (Qiagen, Hilden, Germany) according to the manufacturer's instructions. cDNA synthesis was performed with the High Capacity cDNA Reverse Transcription Kit (Applied Biosystems, Darmstadt, Germany) according to the manufacturer's instructions. Real-time quantitative PCR was performed on a 7900HT fast real-time PCR system using the TaqMan master mix reagent kit and the following primers: HO-1: Hs01110250_m1; GCLM: Hs00978073_m1; HSPA1A: Hs00271229_s; HSPA4: Hs00382884_m1; HSP90: Hs00743767_sH. Ct values were calculated by the RQ Manager Software v.1.2 (all from Applied Biosystems). 18S RNA expression was used as endogenous control. Fold change values were calculated using the comparative Ct method (23).

Quantification of heme oxygenase 1 (HO-1) protein concentration

Heme oxygenase 1 protein concentration was assessed using an ELISA specific for human HO-1 (R&D Systems, Abington, UK) according to the manufacturer's instructions.

Following incubation for 24 h with LicA- or SF-containing medium, cells were washed with PBS and lysed with cell lysis buffer supplemented with protease inhibitors (Biorad, Munich, Germany). Lysates were subjected to the HO-1 ELISA, and absorption was measured using the Spectra Max 250 (Molecular Devices, Ismaning, Germany).

Immunofluorescence

Primary human fibroblasts were seeded on either Lab-Tek™ chambered coverglasses (Nunc, Langensfeld, Germany) or 96-well optical plates (BD Bioscience, San Diego, USA). Cells were fixed with BD Cytofix (BD Bioscience, San Diego, USA) at room temperature for 15 min and washed with PBS, and free aldehyde groups were subsequently blocked with 0.1 M glycine (Sigma-Aldrich) for 10 min at RT. Cells were permeabilized with 0.1% Triton X-100 in 5% normal goat serum (NGS) for 20 min and blocked with 5% NGS for additional 60 min (all from Sigma-Aldrich). Cells were incubated with primary antibodies (α-Nrf2, H-300, rabbit polyclonal IgG, Santa Cruz, Dallas, TX, USA) over night at 4°C. Afterwards, cells were stained with Alexa594-conju-

gated goat anti-rabbit IgG antibodies (Invitrogen, Darmstadt, Germany). Nuclear counterstaining was performed with 4',6-diamidino-2-phenylindole (DAPI) (Sigma-Aldrich). Cells were analysed using a Zeiss Axiovert S100 fluorescence microscope (Zeiss, Göttingen, Germany).

Analysis of intracellular thiol concentration

To analyse intracellular thiol level, GSH/ GSSG-Glo™ assay (Promega, Madison, WI, USA) was performed according to the manufacturer's instructions. Briefly, cells were incubated with LicA or SF for 24 h, subsequently lysed and subjected to the assay procedure. Two different reaction schemes were used to determine both the amount of total glutathione (GSH + GSSG) as well as oxidized glutathione (GSSG) in the same sample to calculate the ratio of reduced to oxidized glutathione (GSH/ GSSG).

Analysis of reactive oxygen species

Generation of ROS was assessed by quantifying dichlorodihydrofluorescein diacetate (DCF) fluorescence as described previously (24). Briefly, cells were irradiated with solar simulated light (SSR) using an Oriol 1600W (Newport Corporation, Stratford, CT, USA) at a dose of 80 mJ/cm², which was determined and expressed as the dose of UVB light. UV doses were determined with an IL1700 Research Radiometer (International light, Newburyport, MA, USA). After irradiation, cells were immediately treated for 30 min with 150 ng/ml DCFH-DA. Fluorescence intensity was quantified at 530 nm using a SAFIRE spectrometer (Tecan, Crailsheim, Germany).

Oxidative burst of fMLP-stimulated human granulocytes

Human granulocytes were incubated at a cell density of 5 × 10⁶ cells/ml in a total volume of 250 µl with different concentrations of LicA or SF in lumina strips (Labsystems, Helsinki, Finland) for 15 min. Cells were stimulated by the addition of fMLP (Sigma-Aldrich) at a final concentration of 10 µM. Total photon count of chemiluminescence was measured within a period of 6 min utilizing a single photon camera (Hamamatsu Photonics GmbH, Herrsching am Ammersee, Germany).

Inhibition of NFκB activation

The inhibition of TNF-α-induced NFκB signalling was measured using the A549-NFκB reporter cell line (Evotec, Hamburg, Germany) expressing secreted embryonic alkaline phosphatase (SEAP) upon NFκB activation. Cells were incubated with LicA, SF or NFκB inhibitor Ro 106-9920 (10 µg/ml) for 6 h and subsequently stimulated with 10 ng/ml TNF-α. After 18 h, the expression of SEAP was measured in culture medium using CSPD® as substrate. The chemiluminescent product was detected by plate luminometer (PheraStar, BMG, Ortenberg, Germany).

In vivo study: detection of ultraweak photon emission after UVA irradiation

The *in vivo* study was conducted according to the Declaration of Helsinki and the guideline of the International Conference on Harmonization Good Clinical Practice (ICH GCP). All volunteers gave written informed consent. Twenty two female volunteers, ranging from 28 to 65 years of age (mean age 50.3 ± 12.1) and with healthy skin (Fitzpatrick types I-III), followed a 3-day preconditioning period prior to the first visit (no moisturizing products, sun exposure). Defined oil-in-water lotions containing LicA-rich licorice extract from Maruzen Chemicals (Osaka, Japan) were used for the clinical study. The test formulation and the respective vehicle without licorice extract were applied on the

inner forearm twice daily for 2 weeks. The amount of applied test formulation was subjected to the custom habit of the volunteers to apply skin lotion. UVA-induced bioluminescence was detected by UPE, quantified *in vivo* by utilizing a photomultiplier system (25). Experiments were performed using the following parameters: UVA irradiation: 8.0 s (source: Oriel 300W X2-lamp, filter: WG335/UG11, intensity: 4.5 mW/cm²), delay: 0.5 s and emission: 25 s. The total number of photons was counted and normalized to the corresponding measurements of the first visit. Data were analysed using Wilcoxon's signed rank test for original data.

Statistical analysis

The arithmetic mean and the standard error of the mean (SEM) were represented graphically for description of the data. Analysis of the data was conducted with GraphPad Prism 5 (San Diego, CA, USA). The Shapiro–Wilk test was used to test the normality of the data. If the null hypothesis was rejected, nonparametric methods were used. With regard to the structure of the data, ade-

quate test methods were used for detecting differences (see legends of the corresponding figures).

Results

Licochalcone A induces the nuclear translocation of Nrf2

The anti-inflammatory and antioxidative properties of licochalcone A (LicA) (cf. Fig. 1a) partially result from LicA's NfκB inhibitory effect (Figure S1). Another important anti-inflammatory mechanism is mediated by Nrf2. Nrf2 activation is associated with its dissociation from the Keap1–Cul3 complex that sequesters Nrf2 to the actin cytoskeleton (26,27). Following activation, Nrf2 translocates to the nucleus and binds to antioxidative response elements/electrophile response elements (AREs/EpRes) (28) associated with the expression of a battery of cytoprotective genes. Utilizing fluorescence microscopy, we examined the effect of LicA on the subcellular localization of Nrf2. Both, LicA and SF, induced a significant increase in Nrf2-positive nuclei in primary human fibroblasts compared to DMSO-treated control cells (Fig. 1).

Licochalcone A triggers Nrf2-dependent induction of heme oxygenase 1 expression levels in primary human fibroblasts

To characterize the effect of LicA on heme oxygenase 1 (HO-1) expression, primary human fibroblasts were incubated in medium containing 9 μM LicA. HO-1 mRNA concentrations were determined by real-time quantitative PCR after 6 h, 12 h and 24 h of incubation. We compared LicA's effect on HO-1 expression with the known HO-1 inducer SF (29). LicA induced elevated concentrations of HO-1 mRNA at all points in time. HO-1 concentration was highest at 12 h (10-fold induction, Fig. 2a). SF treatment (10 μM) resulted in a comparable induction of HO-1 expression after 6 and 12 h of cultivation. However, in contrast to the LicA-treated cells, the HO-1 mRNA concentration of SF-treated cells declined to baseline levels after 24 h of incubation. To examine whether SF- and LicA-induced mRNA expression levels translate into protein concentrations, HO-1-specific ELISAs were conducted. Treatment with LicA and SF dose-dependently increased the protein concentration of HO-1 (Fig. 2b). LicA induced an even stronger increase in HO-1 protein than SF at concentrations above 3 μM (Fig. 2b).

To test whether the Nrf2-dependent cellular responses towards SF and LicA were due to a general electrophilic stress response, we analysed the expression of several ARE-containing heat shock proteins. Interestingly, while SF treatment induced several heat shock proteins, especially HSP1A1, LicA treatment activated HO-1 rather specifically (Table S1).

Licochalcone A induces the expression of the glutamate–cysteine ligase regulatory subunit and increases the ratio of reduced to oxidized intracellular glutathione

Previous studies demonstrated that Nrf2 partly regulates the homeostasis of the important cytoprotective molecule glutathione (GSH) by affecting its *de novo* synthesis. Thus, we determined whether LicA treatment increased the expression of GCLM. At all points in time analysed (6, 12 and 24 h), LicA treatment resulted in an approximately twofold increase in GCLM mRNA concentration in dermal fibroblasts (Fig. 3a). Comparable with the HO-1 expression data, SF treatment induced a more pronounced increase in GCLM concentration at early points in time (6 and 12 h, 2.5-fold and threefold, respectively) but no induction after 24 h. In contrast, LicA-induced GCLM expression kept stable over this period.

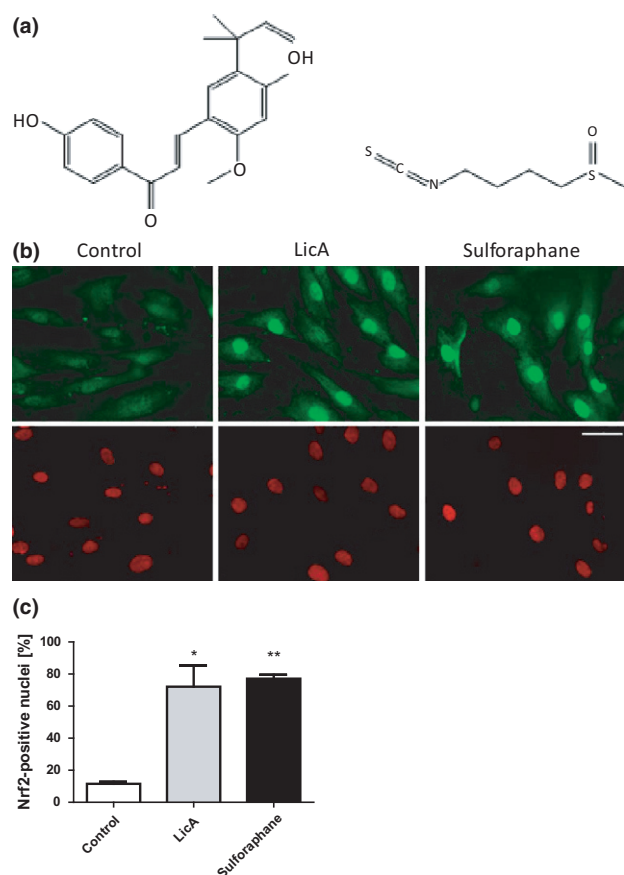


Figure 1. Influence of licochalcone A and sulforaphane on the intracellular localization of Nrf2. (a) Chemical structures of licochalcone A (LicA) and sulforaphane. (b) Primary human fibroblasts were incubated either with LicA (9 μM) or sulforaphane (10 μM) for 5 h. DMSO-treated cells served as control. Fixed cells were stained with Nrf2-specific antibody (Green; H-300, Santa Cruz). Nuclei were counterstained with DAPI (Red). Fluorescence intensity and localization were assessed by fluorescence microscopy. Results were obtained from one representative of four independently performed experiments. (c) Quantification of Nrf2-positive nuclei ($n = 3$; * $P < 0.05$; ** $P < 0.01$, t -test).

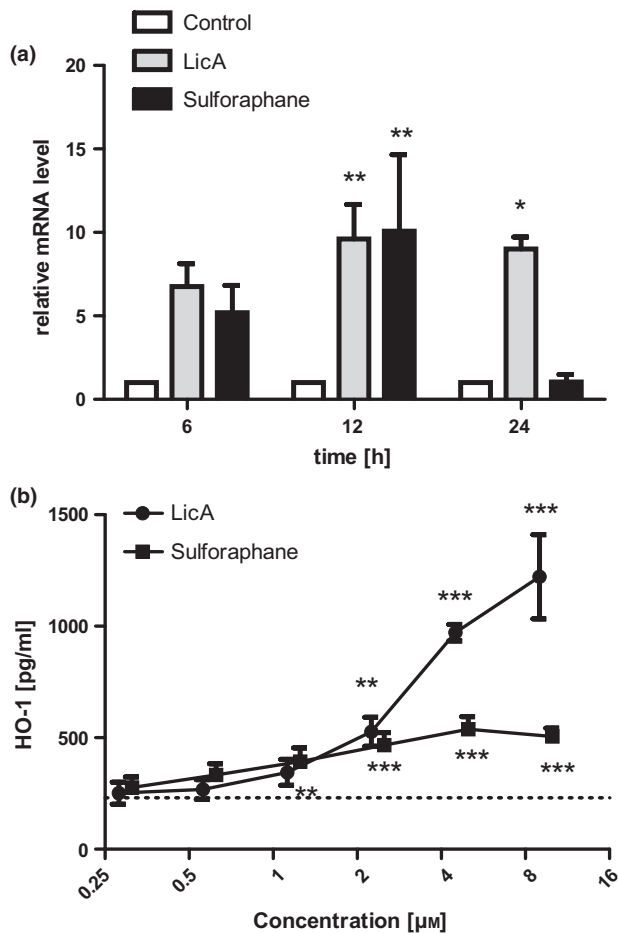


Figure 2. Effect of licochalcone A and sulforaphane on the expression of heme oxygenase 1 in primary human fibroblasts. (a) Heme oxygenase 1 (HO-1) mRNA level of licochalcone A (LicA)- or sulforaphane-treated cells at different points in time. Primary human fibroblasts ($n = 4$) were cultured in presence of either LicA ($9 \mu\text{M}$) or sulforaphane ($10 \mu\text{M}$) for the indicated times. Expression level of the DMSO-treated control is indicated as dotted line. (b) HO-1 protein concentration of primary human fibroblasts cultured in the presence of the indicated concentrations of LicA or sulforaphane for 24 h ($n = 4$). DMSO-treated cells served as control ($*P < 0.05$; $**P < 0.01$; $***P < 0.001$, t -test).

We hypothesized that a higher expression level of this enzyme translates into a higher intracellular glutathione concentration. To test this presumption, we determined the ratio of reduced to oxidized glutathione (GSH/ GSSG ratio) of LicA- and SF-treated cells after 24 h of substance exposure. The data showed that the increased GCLM transcription in LicA-treated cells correlated with a significantly elevated GSH/ GSSG ratio due to a disproportionate increase in GSH in comparison to GSSG (Fig. 3a,b).

Licochalcone A prevents the formation of free radicals *in vitro*

LicA-induced activation of Nrf2 and concomitant expression of antioxidative enzymes such as HO-1 and GCLM suggest an increased antioxidative capacity of LicA-treated cells. To explore the effect of LicA treatment on two different types of free radical formation, we analysed (i) UV-irradiation-dependent generation of ROS in dermal fibroblasts; and (ii) fMLP-triggered oxidative burst reaction in neutrophils.

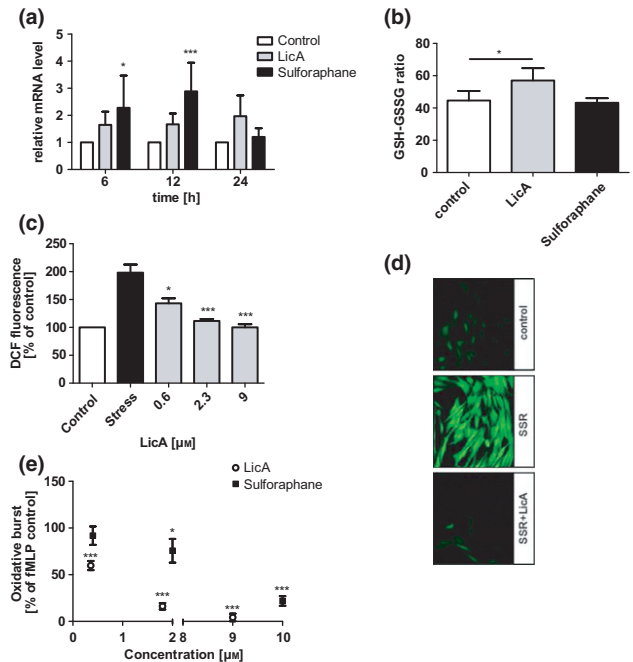


Figure 3. Effects of licochalcone A and sulforaphane on glutamate-cysteine ligase regulatory subunit expression, intracellular thiol concentrations and formation of free radicals. (a) Glutamate-cysteine ligase regulatory subunit (GCLM) mRNA level of licochalcone A (LicA)- or sulforaphane-treated fibroblasts ($n = 4$) at different points in time. Primary human fibroblasts were incubated in medium containing either LicA ($9 \mu\text{M}$) or sulforaphane ($10 \mu\text{M}$) for the indicated times. GCLM mRNA concentrations were determined by quantitative real-time PCR. (b) Quantification of the ratio of reduced to oxidized glutathione (GSH/GSSG ratio) in dermal fibroblasts incubated with $2 \mu\text{M}$ LicA or sulforaphane for 24 h. (c) Dose-dependent reduction of solar simulated light (SSR)-induced reactive oxygen species (ROS) concentration in fibroblasts by LicA. (d) Fluorescence microscopy images of corresponding quantifying dichlorodihydrofluorescein diacetate (DCF) staining of fibroblasts. (e) Effect of different concentrations of LicA and sulforaphane on fMLP-induced oxidative burst of human neutrophilic granulocytes ($*P < 0.05$; $**P < 0.01$; $***P < 0.001$, t -test).

Fibroblasts were cultivated in LicA-containing medium for 24 h and subsequently exposed to sun simulated solar radiation (SSR). The fluorescence intensity of DCFH-DA stainings were analysed as an indication of the amount of ROS generated by irradiation. Pretreatment with LicA for 24 h dose-dependently decreased the irradiation-induced DCF fluorescence (Fig. 3d). The ROS concentration of irradiated fibroblasts pretreated with a LicA concentration of $9 \mu\text{M}$ was indistinguishable from the ROS level of non-irradiated control cells (Fig. 3c,d).

To assess the effect of LicA and SF treatment on the oxidative burst reaction of neutrophil granulocytes, we pre-incubated the cells with LicA and SF for 24 h. Both substances significantly and dose-dependently decreased the fMLP-triggered formation or release of ROS, LicA being more potent (Fig. 3e). Therefore, pre-incubation with LicA reduced both, UV- and NADPH-oxidase-dependent intracellular ROS concentration.

Licochalcone A prevents UVA-induced oxidative processes *in vivo*

To investigate whether the effect of LicA treatment on ROS production *in vitro* translates to the inhibition of oxidative processes *in vivo*, we performed UPE experiments. The UPE method detects photons generated mainly by oxidative processes (e.g. the forma-

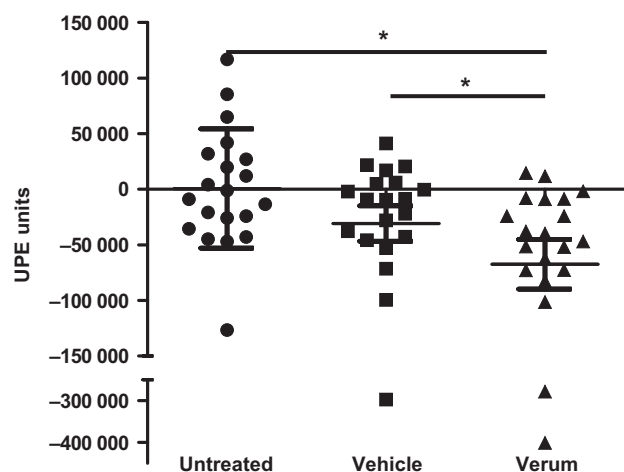


Figure 4. Effect of topically applied licochalcone A on UVA-induced photon emission of the skin. In a study with 22 healthy volunteers, a test formulation containing licochalcone A (LicA) rich licorice extract and a corresponding vehicle without licorice extract were applied on the inner forearm for 2 weeks. The UVA-induced photon emission of untreated, verum and vehicle areas was quantified *in vivo* by utilizing a photomultiplier system. The total number of photons was counted and normalized to the corresponding measurements before the application of products. Data were analysed using Wilcoxon's signed rank test for original data, * $P < 0.05$.

tion and reaction of free radicals) in the skin (25,30). We compared the effects of a topically applied LicA-containing ointment with a LicA-free vehicle in a study with 22 healthy volunteers. Two weeks of treatment with LicA-rich licorice extract lotion significantly lowered the amount of skin-derived photons induced by a short stimulus of UVA light compared to untreated- and vehicle-treated areas (Fig. 4).

Discussion

Solar UV radiation is an important exogenous stressor for the skin, and the attendant formation of free radicals may directly result in damage to cellular proteins, lipids and DNA (31) associated with sunburn. In this study, we provide evidence that the anti-inflammatory and antioxidative compound licochalcone A (LicA) has the potential to increase the robustness of skin cells against harmful effects of UV radiation. Anti-inflammatory and antioxidative properties of LicA have mainly been attributed to its inhibitory activity on NF κ B signalling (32–34). Here, we show that activation of the transcription factor Nrf2 is another important mechanism, as LicA treatment resulted in i) nuclear translocation of the redox-sensitive transcription factor Nrf2, ii) increased expression of antioxidative enzymes such as HO-1 and GCLM and iii) higher ratio of reduced to oxidized glutathione and concomitant decrease of intracellular ROS concentration. These consecutive events, resulting in cytoprotection, are likely to mediate LicA's capability to fortify cells against UV-triggered free radical formation.

LicA dose-dependently prevented the formation of free radicals as indicated by lowered DCF fluorescence intensity in SSR-irradiated primary fibroblasts. Significant effects were observed at nanomolar concentrations (600 nM), while high concentrations of LicA (9 μ M) inhibited the accumulation of free radicals nearly completely.

Similar results for UV-induced erythema reduction and preventive effects against UV-induced or chemically induced skin cancer were reported for other Nrf2-activating phytochemicals, among

them sulforaphane (SF) (4,13,14,35), supporting the concept of beneficial Nrf2 stimulation in the skin. Our UPE results display that the cytoprotective effects *in vitro* correlate with beneficial effects *in vivo*. Topical application of a LicA-rich licorice extract containing formula significantly lowered UVA-induced luminescence *in vivo*. UVA-evoked photon emission is a by-product of oxidative reactions caused by UV irradiation of endogenous chromophores (e.g. porphyrins, quinones and NADH/NADPH), yielding ROS via the transfer of radiation energy to $^3\text{O}_2$ (especially $^1\text{O}_2$) (36,37). Hence, our UPE results are likely indicative of a decreased ROS formation *in vivo*. This effect may be linked to LicA's ameliorating effect on UV-induced erythema formation (20).

In addition to UV-induced ROS formation, LicA prevented the intracellular formation of ROS during the fMLP-triggered oxidative burst of granulocytes. Because of the short incubation time, this effect may be explained by LicA's inhibitory effect on NF κ B activation rather than by Nrf2-dependent ROS scavenging. Connections between Nrf2 and NF κ B signalling exist through Keap1-dependent IKK β degradation (38), and some phytochemicals, such as quercetin and lucidone, were reported to activate Nrf2 and to block NF κ B signalling in neurons and keratinocytes (39–41). Mechanistically, a synergistic effect of NF κ B inhibition and Nrf2 activation is conceivable: LicA's inhibitory effect on NF κ B activation is likely to reduce the expression of NADPH oxidase components (42,43), thereby diminishing the intracellular formation of ROS, which in turn would sustain high concentrations of cytoprotective intracellular thiols. From another perspective, by stimulating Nrf2-dependent antioxidative capacity of skin cells, LicA may prevent cutaneous inflammatory responses by lowering NF κ B activation level, as H_2O_2 activates NF κ B (44). Hence, inhibition of NF κ B and activation of Nrf2 may be a common theme of many beneficial phytochemicals.

The Nrf2 sequestering protein Keap1 contains several intramolecular sensors for distinct stress signals (45). Notably, it has been demonstrated that neither UV irradiation nor ROS directly activate Nrf2 in keratinocytes *in vitro* (46). Cytoprotective responses were rather triggered by electrophilic compounds, releasing Nrf2 from Keap1. *In vivo*, the UV-dependent formation of oxidized lipids may activate Nrf2 in Keratinocytes (47,48). Electrophilic compounds stimulate Nrf2 signalling by covalent modification of intramolecular thiol groups of Keap1 (49,50). LicA contains an electrophilic α , β -unsaturated ketone structure, which is important for the induction of Nrf2, because dihydrochalcone – devoid of this motif – did not induce HO-1 (data not shown). Interestingly, the α , β -unsaturated motif of LicA is also essential for its NF κ B inhibitory activity (51). Other UV-activated, Nrf2-interacting signalling pathways [e.g. PKC, MAPKs and PI3K (52,53)] are likely to modify the outcome.

In addition to the direct cytoprotective effects on suprabasal keratinocytes, topical application of Nrf2 activators may also exert indirect beneficial effects for neighbouring cells, as activation of Nrf2 in suprabasal keratinocytes results in a GSH-secretion-dependent paracrine protection of keratinocytes in deeper layers of the skin, protecting them from UV-induced apoptosis (54).

Several phytochemicals have been reported to activate Nrf2 in skin cells, among them the prototypical Nrf2 activator SF. However, in contrast to SF, LicA did not induce a multitude of heat shock proteins, but rather specifically induced the small heat

shock protein heme oxygenase 1. HO-1 may be an important mediator of LicA-dependent prevention of sunburn, as its induction by suberythemal UVA exposure is linked to the UVA-induced protection of skin against the immunosuppressive effect of ultraviolet B radiation (55,56). This effect was attributed to the generation of anti-inflammatory carbon monoxide by HO-1 (57).

Taken together, topically applied, Nrf2-activating small molecules such as LicA may improve skin's ability to cope with exoge-

nous stressors. We speculate that the activation of Nrf2 and inhibition of NFκB may act in concert to reduce the formation of free radicals and inflammatory responses in the skin.

Acknowledgement

We thank Jeannine Immeyer for excellent technical assistance and Ralf Hagens for UPE technology support.

Conflict of interest

The authors have declared no conflicting interests.

References

- Proksch E, Brandner J M, Jensen J M. *Exp Dermatol* 2008; **17**: 1063–1072.
- Elias P M. *J Invest Dermatol* 2005; **125**: 183–200.
- Saw C L, Huang M T, Liu Y *et al.* *Mol Carcinog* 2011; **50**: 479–486.
- Talalay P, Fahey J W, Healy Z R *et al.* *Proc Natl Acad Sci USA* 2007; **104**: 17500–17505.
- Schafer M, Farwanah H, Willrodt A H *et al.* *EMBO Mol Med* 2012; **4**: 364–379.
- Cho H Y, Jedlicka A E, Reddy S P *et al.* *Am J Respir Cell Mol Biol* 2002; **26**: 175–182.
- Leung L, Kwong M, Hou S *et al.* *J Biol Chem* 2003; **278**: 48021–48029.
- Lee J M, Anderson P C, Padgett J K *et al.* *Biochim Biophys Acta* 2003; **1629**: 92–101.
- Xiang Y, Liu G, Yang L *et al.* *Biosci Trends* 2011; **5**: 239–244.
- Bach F H. *FASEB J* 2005; **19**: 1216–1219.
- Seelig G F, Meister A. *J Biol Chem* 1984; **259**: 3534–3538.
- Dickinson D A, Levenon A L, Moellering D R *et al.* *Free Radic Biol Med* 2004; **37**: 1152–1159.
- Zhang Y, Talalay P, Cho C G *et al.* *Proc Natl Acad Sci USA* 1992; **89**: 2399–2403.
- Tian F F, Zhang F F, Lai X D *et al.* *Biosci Trends* 2011; **5**: 23–29.
- Wagner A E, Ernst I, Iori R *et al.* *Exp Dermatol* 2010; **19**: 137–144.
- Kimura S, Warabi E, Yanagawa T *et al.* *Biochem Biophys Res Commun* 2009; **387**: 109–114.
- Hirota A, Kawachi Y, Itoh K *et al.* *J Invest Dermatol* 2005; **124**: 825–832.
- Marrot L, Jones C, Perez P *et al.* *Pigment Cell Melanoma Res* 2008; **21**: 79–88.
- Haraguchi H. *Bioactive Compounds from Natural Sources: Isolation, Characterization and Biological Properties*. New York, NY: Taylor and Francis, 2001.
- Kolbe L, Immeyer J, Batzer J *et al.* *Arch Dermatol Res* 2006; **298**: 23–30.
- Haraguchi H, Ishikawa H, Mizutani K *et al.* *Bio-org Med Chem* 1998; **6**: 339–347.
- Roggenkamp D, Falkner S, Stab F *et al.* *J Invest Dermatol* 2012; **132**: 1892–1900.
- Livak K J, Schmittgen T D. *Methods* 2001; **25**: 402–408.
- Chen X, Zhong Z, Xu Z *et al.* *Free Radic Res* 2010; **44**: 587–604.
- Khabiri F, Hagens R, Smuda C *et al.* *Skin Res Technol* 2008; **14**: 103–111.
- Kang M I, Kobayashi A, Wakabayashi N *et al.* *Proc Natl Acad Sci USA* 2004; **101**: 2046–2051.
- Furusawa M, Xiong Y. *Mol Cell Biol* 2005; **25**: 162–171.
- Itoh K, Chiba T, Takahashi S *et al.* *Biochem Biophys Res Commun* 1997; **236**: 313–322.
- Keum Y S, Yu S, Chang P P *et al.* *Cancer Res* 2006; **66**: 8804–8813.
- Hagens R, Khabiri F, Schreiner V *et al.* *Skin Res Technol* 2008; **14**: 112–120.
- Svobodova A, Walterova D, Vostalova J. *Biomed Pap Med Fac Univ Palacky Olomouc Czech Repub* 2006; **150**: 25–38.
- Furusawa J, Funakoshi-Tago M, Mashino T *et al.* *Int Immunopharmacol* 2009; **9**: 499–507.
- Furusawa J, Funakoshi-Tago M, Tago K *et al.* *Cell Signal* 2009; **21**: 778–785.
- Funakoshi-Tago M, Tanabe S, Tago K *et al.* *Mol Pharmacol* 2009; **76**: 745–753.
- Wagner A E, Ernst I, Iori R *et al.* *Exp Dermatol* 2010; **19**: 137–144.
- Dalle Carbonare M, Pathak M A. *J Photochem Photobiol, B* 1992; **14**: 105–124.
- Young A R. *Phys Med Biol* 1997; **42**: 789–802.
- Lee D F, Kuo H P, Liu M *et al.* *Mol Cell* 2009; **36**: 131–140.
- Kang C H, Choi Y H, Moon S K *et al.* *Int Immunopharmacol* 2013; **17**: 808–813.
- Shi Y, Liang X C, Zhang H *et al.* *Acta Pharmacol Sin* 2013; **34**: 1140–1148.
- Kumar K J, Yang H L, Tsai Y C *et al.* *Food Chem Toxicol* 2013; **59**: 55–66.
- Anrather J, Racchumi G, Iadecola C. *J Biol Chem* 2006; **281**: 5657–5667.
- Gauss K A, Nelson-Overton L K, Siemsen D W *et al.* *J Leukoc Biol* 2007; **82**: 729–741.
- Gloire G, Legrand-Poels S, Piette J. *Biochem Pharmacol* 2006; **72**: 1493–1505.
- McMahon M, Lamont D J, Beattie K A *et al.* *Proc Natl Acad Sci USA* 2010; **107**: 18838–18843.
- Durchdewald M, Beyer T A, Johnson D A *et al.* *J Invest Dermatol* 2007; **127**: 646–653.
- Gruber F, Oskolkova O, Leitner A *et al.* *J Biol Chem* 2007; **282**: 16934–16941.
- Gruber F, Mayer H, Lengauer B *et al.* *FASEB J* 2010; **24**: 39–48.
- Kensler T W, Wakabayashi N, Biswal S. *Annu Rev Pharmacol Toxicol* 2007; **47**: 89–116.
- Holland R, Hawkins A E, Egger A L *et al.* *Chem Res Toxicol* 2008; **21**: 2051–2060.
- Funakoshi-Tago M, Nakamura K, Tsuruya R *et al.* *Int Immunopharmacol* 2010; **10**: 562–571.
- Yu R, Chen C, Mo Y Y *et al.* *J Biol Chem* 2000; **275**: 39907–39913.
- Lopez-Camarillo C, Ocampo E A, Casamichana M L *et al.* *Int J Mol Sci* 2012; **13**: 142–172.
- Schafer M, Dutsch S, auf dem Keller U *et al.* *Genes Dev* 2010; **24**: 1045–1058.
- Tyrrrell R M, Reeve V E. *Prog Biophys Mol Biol* 2006; **92**: 86–91.
- Reeve V E, Tyrrrell R M. *Proc Natl Acad Sci USA* 1999; **96**: 9317–9321.
- Allanson M, Reeve V E. *J Invest Dermatol* 2005; **124**: 644–650.

Supporting Information

Additional supporting data may be found in the supplementary information of this article.

Figure S1. Licochalcone A and Sulforaphane are potent inhibitors of NFκB.

Table S1. Influence of Licochalcone A and Sulforaphane on expression levels of different heat shock proteins.